UNIVERSITY OF CALIFORNIA, SAN DIEGO

SAN DIEGO STATE UNIVERSITY

Gene Therapy and Cell Fusion Enhances Stem Cell Mediated Cardiac Repair

A dissertation submitted in partial satisfaction of the requirements for the degree

Doctor of Philosophy

in

Biology

by

Pearl Jennine Quijada

Committee in charge:

University of California, San Diego

Professor Asa B. Gustafsson
Professor Deborah L. Yelon

San Diego State University

Professor Mark A. Sussman, Chair
Professor Christopher C. Glembotski
Professor Greg L. Harris

2015

The Dissertation of Pearl Jennine Quijada is approved, and it is acceptable in quality and form for publication on microfilm and electronically:

_____

_____

_____

_____

_____

Chair

University of California, San Diego

San Diego State University

2015

DEDICATION

I want to dedicate this to my family. My father, Jaime, for his kindness and patience, your calm is a perfect balance for our eclectic family. My brother Thomas for teaching me how far you can go when you stop caring about what other people think. My sister Becky, your strength amazes me, mentally and physically. My sister Jessica, your drive and motivation are inspiring. And of course my mother Laura for her unyielding support and unconditional love, you instilled in me drive and an amazing work ethic. But most of all, you guided me towards what I love and I thank you for that. Of course, I would like to dedicate this to Benjamin Knowles, my biggest fan and cheerleader. You carefully challenge as well as support me. Your optimism depletes my pessimistic attitude, and no day is boring when I'm with you. Thank you for being in my life.

EPIGRAPH

“Every day you play with the light of the universe.”

–Pablo Neruda

“Be less curious about people and more curious about ideas.”

-Marie Curie

TABLE OF CONTENTS

LIST OF ABBREVIATIONS

2N	diploid, euploid DNA content
4N	tetraploid, aneuploid DNA content
α-SMA	α-smooth muscle actin
ANOVA	analysis of variance
AWT	anterior wall thickness
B1-AR	B1-adrenergic receptor
B2-AR	B2-adrenergic receptor
BMC	bone marrow cell
BMP4	bone morphogenic factor 4
Ca^{2+}	calcium
CAD	coronary artery disease
CaMKII	calcium/calmodulin kinase II
CC	CardioChimera
CC1	CardioChimera 1
CC2	CardioChimera 2
CPC	cardiac progenitor cell
CPC + MSC	cardiac progenitor cells and mesenchymal stem cells
CPCe	cardiac progenitor cells overexpressing eGFP
CPCeδB	cardiac progenitor cells overexpressing CaMKIIδB
CSC	cardiac stem cell
cTNT	cardiac troponin T
CVD	cardiovascular disease

DAPI	4',6-diamidino-2-phenylindole
Dex	dexamethasone
dP/dT	developed pressure over time
EF	ejection fraction
eGFP	enhanced green fluorescent protein
ESC	embryonic stem cell
FACS	fluorescence activated cell sorting
FBS	fetal bovine serum
FVB/NJ	friend virus B, common mouse strain
GAPDH	glyceraldehyde 3-phosphate dehydrogenase
GATA4	GATA binding protein 4
HDAC4	histone deacetylase 4
HDAC5	histone deacetylase 5
HW/BW	heart weight to body weight ratio
HSC	hematopoietic stem cell
IL-6	interleukin-6
IP3R	inositol 1,4,5-trisphosphate receptor
iPSC	induced pluripotent stem cell
LAD	left anterior descending artery
LVAD	left ventricular assisted device
MEF2	myocyte-specific enhancer factor 2
MH-CC	mouse-human CardioChimera
MI	myocardial infarction

MLHF	Minnesota Living with Heart Failure Questionnaire
MSC	mesenchymal stem cell
Myh6	myosin heavy chain α
Myh7	myosin heavy chain β
NRCM	neonatal rat cardiomyocyte
NS	nucleostemin
NYHA	New York Heart Association
P_2YR	purinergic receptor P_2Y
PBS	phosphate buffered saline, vehicle control group
PECAM (CD31)	platelet endothelial cell adhesion molecule
PGK	phosphoglycerate kinase
pHDAC4	phosphorylated histone deacetylase 4 on serine 632
PKA	phospho-kinase A
PKD	phospho-kinase D
RNA-seq	RNA-sequencing
RyR	ryanodine receptor
SCIPIO	Stem Cell Infusion in Patients with Ischemic cardiOmyopathy
SDF-1	stromal derived factor-1
SERCA	sarco/endoplasmic reticulum Ca^{2+}-ATPase
sh-Ctrl	lentivirus expressing small hairpin control
sh-δB	lentivirus small hairpin targeting CaMKIIδB
SM22	smooth muscle 22
TOPRO	TO-PRO-3 iodide

LIST OF FIGURES

LIST OF TABLES

ACKNOWLEDGMENTS

"The desire to sacrifice an entire lifetime to the noblest of ideals serves no purpose if one works alone." – Ernesto Guevara.

I could not have gotten to this point without the support of several people in my personal and academic career. I am a huge proponent of working as a team, especially in science. Making new friends and keeping in touch with old ones is important for discussion of novel research ideas.

I would like to thank Professor Mark Sussman. You have always defended me, supported me and taught me everything I know. Your curiosity and general love for science inspires me. I would also like to thank my dissertation committee members, Dr. Glembotski, Dr. Harris, Dr. Gustafsson and Dr. Yelon, for their service and the benefits of their scientific acumen. I would also like to thank Dr. Coralie Poizat, although you are far away, your insight and dedication to my research has left an amazing impression on me. I would like to acknowledge the Rees-Stealy Research Foundation and San Diego State University Heart Institute, Achievement Rewards for College Scientists and my sponsors Dr. John and Kathy Hattox for supporting my research. I would like to thank all of the past and current members of the Sussman laboratory. I would also like to extend my thanks to the SDSU Flow Cytometry Core and the vivarium staff.

The Abstract of the Dissertation, Introduction to the Dissertation and the Conclusion of the Dissertation is taken in part as it appears in *Expert Review of Cardiovascular Therapy*, 2014. Making it stick: chasing the optimal stem cells for

cardiac regeneration. Pearl Quijada and Mark Sussman. The dissertation author was the primary author of this review.

Chapter 1, in full, is prepared for submission. Nuclear Calcium/Calmodulin-Dependent Protein Kinase II Signaling Enhances Cardiac Progenitor Cell Survival and Cardiac Lineage Commitment. Pearl Quijada, Nirmala Hariharan, Jonathan Cubillo, Kristin M. Bala, Lucia Ormachea, Donald M. Bers, Mark Sussman and Coralie Poizat. The dissertation author was the primary author and investigator of this manuscript.

Chapter 2, in full, is prepared for submission. Cardiac Stem Cell Hybrids Enhance Myocardial Repair. Pearl Quijada, Hazel T. Salunga, Nirmala Hariharan, Jonathan Cubillo, Farid El-Sayed, Maryam Moshref, Kristin M. Bala, Jaqueline M. Emathinger, Andrea De La Torre, Lucia Ormachea, Roberto Alvarez Jr., Natalie A. Gude, and Mark A. Sussman. The dissertation author was the primary author and investigator of this manuscript.

Chapter 3 is presented in this dissertation as an extension of Chapter 2 to support the creation CardioChimeras with human derived stem cell lines. I would like to acknowledge Megan Monsanto for the isolation of fetal adult stem cells, Sarmistha Ganguly for her part in creating CardioChimeras between mouse and human adult stem cells and Michael McGregor for his initial contribution in identifying senescence markers in stem cells.

VITA

Education

Doctor of Philosophy in Biology
University of California, San Diego and San Diego State University
Received June 2015
Master of Science in Biology (Physiology)
San Diego State University
Received December 2010
Bachelor of Science in Biology
University of California, Riverside
Received June 2006

Publications

Pearl Quijada, Hazel T. Salunga, Nirmala Hariharan, Jonathan Cubillo, Farid El-Sayed, Maryam Moshref, Kristin M. Bala, Jacqueline M. Emathinger, Andrea De La Torre, Lucia Ormachea, Roberto Alvarez Jr., Natalie A. Gude, Mark A. Sussman. (2015) CardioChimeras enhance myocardial repair. *Circulation* (In Review)

Pearl Quijada, Nirmala Hariharan, Jonathan Cubillo, Kristin M. Bala, Lucia Ormachea, Donald M. Bers, Mark A. Sussman, Coralie Poizat. (2015) Nuclear Calcium/Calmodulin-Dependent Protein Kinase II Signaling Enhances Cardiac Progenitor Cell Survival and Cardiac Lineage Commitment. *J Biol Chem*. (In Review)

Kaitlen Samse, NIrmala Hariharan, **Pearl Quijada**, Mirko Völkers, Jacqueline M. Emathinger, Lucia Ormachea, Andrea De La Torre, Shabana Din, Roberto Alvarez, Sadia Mohsin, Walter P. Dembitsky, Megan Monsanto, Kimberlee M. Fischer, Mark A. Sussman. (2015) Functional Effect of Pim1 Depends Upon Intracellular Localization in Human Cardiac Progenitor Cells. *J Biol Chem*. (In Review)

Pearl Quijada, Mark A. Sussman. (2015) Circulating around the tissue: hematopoietic cell based fusion versus transdifferentiation. (Editorial) *Circ Res.* Feb 13;116(4):563-5.

Nirmala Hariharan, **Pearl Quijada**, Sadia Mohsin, Anya Joyo, Kaitlen Samse, Megan Monsanto, Andrea De La Torre, Daniele Avitabile, Lucia Ormachea, Michael McGregor, Emily J. Tsai, Mark A. Sussman. (2015) Nucleostemin rejuvenates cardiac progenitor cells and antagonizes myocardial aging. *J Am Coll Cardiol.* Jan 20; 65(2):133–47.

Salma Awad, Kamar Mohamed Adib Al-Haffar, Qussay Marashly, **Pearl Quijada**, Muhammad Kunhi, Nadya Al-Yacoub, Fallou S. Wade, Shamayel Faheem Mohammed, Fouad Al-Dayel, George Sutherland, Abdullah Assiri A, Mark A. Sussman, Donald M. Bers, Waleed Al-Habeeb, Coralie Poizat. (2014) Control of Histone H3 Phosphorylation by CaMKII in Response to Hemodynamic Cardiac Stress. *J Pathol.* Mar;235(4):606-18.

Pearl Quijada, Mark A. Sussman. (2014) Making it stick: chasing the optimal stem cells for cardiac regeneration. *Expert Rev Cardiovasc Ther*. Nov;12(11):1275-88.

Mirko Völkers, Shirin Doroudgar, Nathalie Nguyen, Mathias H Konstandin, **Pearl Quijada**, Shabana Din, Luis Ornelas, Donna J Thuerauf, Natalie Gude, Kilian Friedrich, Stephan Herzig, Christopher C Glembotski, Mark A Sussman. (2014) PRAS40 prevents development of diabetic cardiomyopathy and improves hepatic insulin sensitivity in obesity. *EMBO Mol Med*. Jan 1;6(1):57-65.

Mirko Völkers, Mathias H. Konstandin, Shirin Doroudgar, Haruhiro Toko, **Pearl Quijada**, Shabana Din, Anya Joyo, Luis Ornelas, Kaitlen Samse, Donna J. Thuerauf, Natalie Gude, Christopher C. Glembotski, Mark A. Sussman. (2013) mTORC2 protects the Heart from Ischemic Damage. *Circulation*. Nov 5;128(19):2132-44.

Mathias H. Konstandin, Mirko Völkers, Brett Collins, **Pearl Quijada**, Mercedes Quintana, Andrea De La Torre, Lucy Ormachea, Shabana Din, Natalie Gude, Haruhiro Toko, Mark A. Sussman. (2013) Fibronectin contributes to pathological cardiac hypertrophy but not physiological growth. *Basic Res Cardiol*. Sep;108(5):375.

Mirko Völkers, Haruhiro Toko, Shirin Doroudgar, Shabana Din, **Pearl Quijada**, Anya Y. Joyo, Luis Ornelas, Eri Joyo, Donna J. Thuerauf, Mathias H. Konstandin, Natalie Gude, Christopher C. Glembotski, and Mark A. Sussman. (2013) Pathological hypertrophy amelioration by PRAS40-mediated inhibition of mTORC1. *Proc Natl Acad Sci U S A*. Jul 30;110(31):12661-6.

Mathias H. Konstandin, Haruhiro Toko, Grady M. Gastelum, **Pearl Quijada**, Andrea De La Torre, Mercedes Quintana, Brett Collins, Shabana Din, Daniele Avitabile, Mirko Völkers, Natalie Gude, Reinhard Fässler, Mark A. Sussman. (2013) Fibronectin is Essential for Reparative Cardiac Progenitor Cell Response Following Myocardial Infarction. *Circ Res*. Jul 5;113(2):115-25.

Shabana Din, Matthew Mason, Mirko Völkers, Bevan Johnson, Christopher T. Cottage, Zeping Wang, Anya Y. Joyo, **Pearl Quijada**, Peter Erhardt, Nancy S. Magnuson, Mathias H. Konstandin, and Mark A. Sussman. (2013) Pim-1

preserves mitochondrial morphology by inhibiting dynamin-related protein 1 translocation. *Proc Natl Acad Sci U S A*. Apr 9;110(15):5969-74.

Mohsin Khan, Sadia Mohsin, Daniele Avitabile, Sailay Siddiqi, Jonathan Nguyen, Kathleen Wallach, **Pearl Quijada**, Michael McGregor, Natalie Gude, Roberto Alvarez, Douglas G. Tilley, Walter J. Koch, Mark A. Sussman. (2013) β-Adrenergic Regulation of Cardiac Progenitor Cell Death Versus Survival and Proliferation. *Circ Res*. Feb 1;112(3):476-86.

Sadia Mohsin, Mohsin Khan, Haruhiro Toko, Brandi Bailey, Christopher T. Cottage, Kathleen Wallach, Divya Nag, Andrew Lee, Sailay Siddiqi, Feng Lan, Kimberlee M. Fischer, Natalie Gude, **Pearl Quijada**, Daniele Avitabile, Silvia Truffa, Brett Collins, Walter Dembitsky, Joseph C. Wu, Mark A. Sussman. (2012) Human Cardiac Progenitor Cells Engineered With Pim-1 Kinase Enhance Myocardial Repair. *J Am Coll Cardiol*. Oct 2;60(14):1278-87.

Pearl Quijada, Haruhiro Toko, Kimberlee M. Fischer, Brandi Bailey, Patrick Reilly, Kristin D. Hunt, Natalie A. Gude, Daniele Avitabile, Mark A. Sussman. (2012) Preservation of myocardial structure is enhanced by pim-1 engineering of bone marrow cells. *Circ Res*. Jun 22;111(1):77-86.

Mark Sussman, Mirko Völkers, Kimberlee Fischer, Brandi Bailey, Christopher C. Cottage, Shabana Din, Natalie Gude, Daniele Avitabile, Roberto Alvarez, Balaji Sundararaman, **Pearl Quijada**, Matthew Mason, Mathias H. Konstandin, Amy Malhowski, Zhaokhang Cheng, Mohsin Khan, Michael McGrego. (2011) Myocardial AKT: the omnipresent nexus. (Review) *Physiol Rev*. Jul;91(3):1023-70.

Kimberlee M. Fischer, Shabana Din, Natalie Gude, Mathias H. Konstandin, Walter Wu, **Pearl Quijada**, Mark A. Sussman. (2011) Cardiac progenitor cell commitment is inhibited by nuclear Akt expression. *Circ Res*. Apr 15;108(8):960-70.

Gwynngelle A. Borillo, Matt Mason, **Pearl Quijada**, Mirko Völkers, Christopher Cottage, Michael McGregor, Shabana Din, Kimberlee Fischer, Natalie Gude, Daniele Avitabile, Steven Barlow, Roberto Alvarez, Silvia Truffa, Ross Whittaker, Matthew S. Glassy, Asa B. Gustafsson, Shigeki Miyamoto, Christopher C. Glembotski, Roberta A. Gottlieb, Joan Heller Brown, Mark A. Sussman. (2010) Pim-1 kinase protects mitochondrial integrity in cardiomyocytes. *Circ Res*. Apr 16;106(7):1265-74.

Christopher T. Cottage, Brandi Bailey, Kimberlee M. Fischer, Daniele Avitable, Brett Collins, Savilla Tuck, **Pearl Quijada**, Natalie Gude, Roberto Alvarez, John Muraski, Mark A. Sussman. (2010) Cardiac progenitor cell cycling stimulated by pim-1 kinase. *Circ Res*. Mar 19;106(5):891-901.

Brandi Bailey, Alberto Izarra, Roberto Alvarez, Kimberlee M. Fischer, Christopher T. Cottage, **Pearl Quijada**, Antonio Díez-Juan, Mark A. Sussman. (2009) Cardiac stem cell engineering using the alphaMHC promoter. *Regen Med*. Nov;4(6):823-33.
Kimberlee M. Fischer, Christopher T. Cottage, Walter Wu, Shabana Din, Natalie A. Gude, Daniele Avitabile, **Pearl Quijada**, Brett L. Collins, Jenna Fransioli, Mark A. Sussman. (2009) Enhancement of myocardial regeneration through genetic engineering of cardiac progenitor cells expressing Pim-1 kinase. *Circulation*. Nov 24;120(21):2077-87.

John A. Muraski, Kimberlee M. Fischer, Weitao Wu, Christopher T. Cottage, **Pearl Quijada**, Matt Mason, Shabana Din, Natalie Gude, Roberto Alvarez Jr, Marcello Rota, Jan Kajstura, Zeping Wang, Erik Schaefer, Xiongen Chen, Scott MacDonnel, Nancy Magnuson, Stephen R. Houser, Piero Anversa, Mark A. Sussman. (2008) Pim-1 kinase antagonizes aspects of myocardial hypertrophy and compensation to pathological pressure overload. *Proc Natl Acad Sci U S A*. Sep 16;105(37):13889-94.

Natalie A. Gude, Gregory Emmanuel, Weitao Wu, Christopher T. Cottage, Kimberlee Fischer, **Pearl Quijada**, John A. Muraski, Roberto Alvarez, Marta Rubio, Eric Schaefer, Mark A. Sussman. (2008) Activation of Notch-mediated protective signaling in the myocardium. *Circ Res*. May 9;102(9):1025-35.

Honors and Awards

2015	BCVS Cardiovascular Outreach Award
2015	ISHR Finalist for the Young Investigator Award
2014	Carl Storm Underrepresented Minority Fellowship
2013	Basic Cardiovascular Sciences Minority Travel Grant
2013	Ruth L. Kirschstein F31 Pre-doctoral Fellowship
2012-2015	Rees-Stealy Research Foundation Fellowship
2012-2013	American Heart Association Pre-doctoral Fellowship
2012	BCVS, AHA, Abstract selected in the top 10%
2012	President's Award, SRS, San Diego State University
2011-2015	ARCS Scholarship
2011	Provost Award, SRS, San Diego State University
2009	NIH/NHLBI Graduate Diversity Supplement

Scientific Presentations

June 2015	International Society of Heart Research, Seattle, WA
January 2015	Fondation Leducq Project Meeting, Université Pierre et Marie Curie. Paris, France

November 2014	American Heart Association Scientific Sessions, Resident Cardiac Stem Cells: The Controversy. Chicago, IL
November 2014	American Heart Association Scientific Sessions, Cardiac Regeneration/Cellular Therapy: Experimental. Chicago, IL
June 2014	Gordon Research Conference: Cardiac Regulatory Mechanisms, New Concepts/Emerging Themes in Cardiovascular Biology, New London, NH
June 2014	Gordon Research Seminar: Cardiac Regulatory Mechanisms, iPS Cells: A Window on Human Myocardial Biology and Disease, New London, NH
November 2013	American Heart Association Scientific Sessions, Late-Breaking Basic Science and Featured Research Presentation, Dallas, TX
March 2012	Student Research Symposium: San Diego State University, San Diego, CA
May 2012	California State University Student Research Competition, Long Beach, CA
July 2012	Basic Cardiovascular Sciences, American Heart Association, New Orleans, LA
November 2012	American Heart Association Scientific Sessions, Los Angeles, CA
March 2011	Student Research Symposium, San Diego State University, San Diego, CA
March 2011	Emerging Molecular and Cellular Insights into Heart Failure and Arrhythmias: The 13th La Jolla-International Cardiovascular Research Conference, La Jolla, CA
April 2011	Graduate Student Symposium, San Diego State University, San Diego, CA

Professional Experience

Doctoral Candidate, San Diego State University	2010-2015
Graduate Teaching Assistant**,** Human Anatomy, SDSU	2008-2012
Masters Candidate, San Diego State University	2007-2010

ABSTRACT OF THE DISSERTATION

Gene Therapy and Cell Fusion Enhances Stem Cell Mediated Cardiac Repair

by

Pearl Jennine Quijada

University of California, San Diego, 2015

San Diego State University, 2015

Professor Mark A. Sussman, Chair

Cardiovascular disease is the leading cause of mortality in the United States. Myocardial infarction (MI) induces massive cellular death and leads to a decline in cardiac function. Cardiomyocytes have limited proliferative capacity sparking interests in molecular and cellular strategies to promote stem cell conversion into new cardiomyocytes.

Cardiac progenitor cells (CPCs) are tissue resident stem cells that give rise to cardiomyogenic structures. Although, CPCs introduced into the heart confer improvements in cardiac function after MI, these effects are not sufficient to support complete heart regeneration and prevent heart failure. Studying molecular pathways that contribute to CPC survival and commitment is essential in advancing CPC based therapeutic approaches. Ca^{2+}/Calmodulin-dependent protein kinase IIδB (CaMKIIδB) regulates survival and growth in cardiomyocytes. However, the role of CaMKIIδ in CPCs has not been previously explored. CPCs increase nuclear CaMKII after MI and *in vitro* differentiation suggesting that CaMKIIδB contributes to the regulation of CPC commitment. Overexpression of CaMKIIδB in CPCs reduces proliferation, enhances resistance to death and increases cardiac specific differentiation. CaMKIIδB may serve as a novel modulatory kinase to promote CPC survival and commitment.

Despite increasing use of stem cells for regenerative-based cardiac therapy, the optimal stem cell population(s) remains uncertain. In the past decade there has been increasing interest and characterization of stem cell populations reported to directly and/or indirectly contributes to cardiac regeneration through processes of cardiomyogenic commitment and / or release of cardioprotective paracrine factors. Future therapies require development of unprecedented concepts to enhance myocardial healing. Combinatorial cell therapy utilizing CPCs and bone marrow derived mesenchymal stem cells (MSCs) promote enhanced reparative functions *in* vivo. However, identifying cell specific mechanisms of cardiac repair are difficult using dual cell systems. Here,

we performed cell fusion between CPCs and MSCs to obtain hybrids with combined cell characteristics called CardioChimeras. Our ideal cell therapy is to combine the beneficial properties of CPCs to undergo cardiac specific commitment as well as MSCs that foster an improved microenvironment with protective paracrine secretion.

INTRODUCTION OF THE DISSERTATION

Cardiovascular Disease

Cardiovascular disease (CVD) is the most common cause of morbidity and mortality in westernized countries due in part to genetics and poor lifestyle behaviors. According the American Heart Association, preventative measures include the maintenance of healthy eating habits and regular exercise to ward off symptoms of CVD. In general, healthy lifestyle practices need to be extended to the youth as 50% of children from 12-19 years of age are obese and have increased chances of developing CVD in early adult years[1]. The socioeconomic burden of CVD estimates in to the billions of dollars making this disease a biomedical priority for millions of Americans currently and into the future[1].

Pharmaceutical and technological advances have lead to improved detection, treatment and prevention of CVD in the past 20 years[2]. Coronary artery disease (CAD), caused by atherosclerosis of the major arteries promotes symptoms of angina pectoris, leads to myocardial infarction (MI) and/or stroke[3]. Implantation of vascular stents and administration of drugs reduces the impact of ischemic events after MI and during chronic remodeling of the heart[2]. Inevitably, global heart remodeling will lead to decreased cardiac function and heart failure[3]. Heart transplantation or left ventricular assisted device (LVAD) implantations are end-stage cardiovascular interventions that modestly extend life span[3]. Unfortunately, early and late stage treatments of CVD do not support regeneration of the heart by direct cardiomyocyte replacement or prevention of collagen deposition. Cardiomyocytes are post-mitotic cells leading to the inability

of the heart to heal. Therefore, the development of novel molecular and cellular strategies to induce regeneration is of strong interest in the biomedical research field.

Cardiomyocyte-based Regeneration

DNA synthesis in cardiomyocytes is highest during the embryonic stage, which drops dramatically in adulthood. The potential for cardiomyocyte division decreases by 20 times in ventricular cardiomyocytes one-day post birth and 4000 times in adult rodent models (0.0005% of total cardiomyocytes) measured by ^{3}H-thymidine incorporation[4-6]. Interestingly, complete heart regeneration is observed after apical resection of the left ventricle or after MI if the damage occurs before 7 days post-birth in the mouse model[7, 8]. Cardiomyocyte cell-cycle withdrawal limits essential regeneration of the heart after damage, yet this discovery has supplied researchers an invaluable tool to investigate novel signaling pathways and microRNAs that regulate cardiomyocyte turnover during this short regenerative window[8, 9]. In contrast, MI induces cardiomyocyte cell-cycle entry observed in 0.0055% to 0.0083% of total myocytes bordering the infarct zone or 11 to 16 fold relative to basal proliferative indices[4-6].

In the adult heart, mature cardiomyocytes respond to damage by undergoing hypertrophy, which impairs cardiac function as early as a few days after MI[10]. Transgenic mouse models over expressing proto-oncogenes c-Myc or nuclear-targeted Akt have been shown to increase cardiomyocyte cell-cycle entry[11-13]. Nuclear Akt accumulation in cardiomyocytes increases the presence of

small myocytes, which corresponds to improved contractility and cardiac performance[11]. Generation of transgenic murine models is important for the elucidation of mechanisms to promote cardiomyocyte-based regeneration, but there remain limitations in applying mouse genetic models towards clinical use.

Stem Cell Therapies: Pluripotent Stem Cells

Not surprisingly given the controversies and inefficiencies of endogenous cardiomyocyte repair, researchers and clinicians have turned their attention towards the isolation and expansion of primary stem cell populations from both embryonic and adult tissue to promote regeneration after adoptive cell transplantation. Pluripotent embryonic stem cells (ESCs) derived from the inner cell mass have been observed to differentiate into cells of the cardiovascular system[14]. The next generation counterpart "induced pluripotent stem cells" (iPSCs) do not cause adverse immune responses after transplantation and differentiation *in vivo* [15, 16]. Cell culture protocols involving the addition of growth factors (BMP4 and activin A), DNA modifiers such as 5-azacytidine and trichostatin A and thyroid hormones enrich for ES/iPSC derived cardiomyocytes (70%-90%) with accumulation of differentiated cell properties reminiscent of young cardiomyocytes including mono-nucleation with the potential to divide [17-21]. Cardiomyocyte purity and efficiency of ESC differentiation is of critical importance as undifferentiated ESCs form teratomas and prevent ESC-cardiomyocyte maturation *in vivo* [19, 22]. Unfortunately, purified ESC derived myocytes are unable to electrically couple with the existing myocardium in both pig and non-human

primates despite suppression of arrhythmias in small animal models[19, 23]. These studies indicate that protocols for the derivation of ESC-cardiomyocytes need to be improved before proceeding to human clinical trials [24].

Stem Cell Therapies: Bone Marrow Derived Cells

Cellular therapy using stem cells derived from the bone marrow and cardiac origin are validated to treat damage after MI in both animal models and human clinical trials[10, 25-29]. Bone marrow derived stem cells are historically the most widely used for clinical therapy[14]. Popularity of bone marrow derived therapy arises from the relative ease and efficiency of isolation, straightforward enrichment of mononuclear bone marrow cells and mesenchymal stem cells (MSCs) from the patient, as well as delivery by both autologous and allogeneic means[30-32]. MSCs are of interest because of ability to secrete an assortment of paracrine factors although they lack marked ability to transdifferentiate into functional cardiac muscle[33-35]. Additionally, MSCs may also provide for immunomodulatory effects *in vivo,* reducing inflammatory responses and stimulating ECM turnover[36]. Reports have highlighted the inconsistencies in clinical trial design, randomization, and statistics to support the efficacy of bone marrow derived cells for use in the United States despite common clinical practice across Europe. These results cast doubts over the value of bone marrow derived cells, which admittedly provide for modest myocardial recovery even under the best of circumstances [37].

Stem Cell Therapies: Cardiac Stem Cells

The coveted cardiac-derived stem cell (CSC) has been traced as early as the developmental stage that defines the mesoderm. Analysis of the early embryonic heart reveals distinct first and second heart fields, housing regulatory niches for multipotent CPCs ($Mef2c^+$ and $Nkx2.5^+$)[38]. In the past decade researchers have come to recognize differential CPCs due to the heterogenic nature of the heart, such as LIM homeodomain transcription factor Islet1 cells, sca-1^+ cells and side population cells[39]. The receptor tyrosine kinase kit is highly expressed in the bone marrow, a marker of hematopoietic stem and progenitor cells and was subsequently used to discover stem and progenitor cell populations in the heart. C-kit lineage transgenic mice, which express the green fluorescent protein under the regulatory control of the c-kit promoter, facilitated the identification of cells of myocardial and vascular lineage[40-43]. Use of c-kit cells in the clinical trial Stem Cell Infusion in Patients with Ischemic cardiOmyopathy (SCIPIO) increased ejection fraction by 12% and and reduced fibrotic scar by 30% based on a one year follow up[10]. Additionally, CSC treatment improved quality of life based on New York Heart Association (NYHA) functional parameters and the Minnesota Living with Heart Failure (MLHF) Questionnaire score, which was downgraded in most patients to NYHA Class I and MLHF score between 20-30 one year following treatment[10]**.** These studies mediate the validation and future use of CPCs for cardiac therapy.

Genetic Engineering Strategies

Optimal cell proliferation and enhanced survival are indispensable traits in an adult stem cell population tailored for cellular therapy. Cardiac ischemia results in cardiomyocyte death, increased inflammation and impaired proteolysis creating a challenging environment for transplanted stem cells[44, 45]. Stem cell populations efficient in DNA replication but susceptible to oxidative stress and inflammatory insults can be augmented by increasing the number of delivered cells to challenge cell death during acute damage. However, limited persistence of stem cells 24-hours after intramyocardial injection reduces the initial population to less than 10% of cells as quantified by sensitive PCR methods [46, 47]. Increased quantity of cells during delivery creates higher rates of competition between injected stem cells and the microenvironment depleting cell resourcefulness. Molecular approaches to enhance stem cell ability to thrive in the damaged myocardium should provide for enhanced proliferation and survival characteristics *ex vivo* and prior to delivery.

Exogenous expansion of adult stem cells is necessary to deliver adequate numbers of cells and support regeneration after damage especially in view of the inevitable losses of cells following adoptive transfer. Methodologies to invigorate stem cells by improving proliferation and survival capabilities for transplantation studies have employed genetic engineering with viral vectors (adeno-, retro- and lentiviruses). Boosting stem cell properties has been accomplished with genetic overexpression of serine threonine kinases Akt and a downstream activator Pim-1. Pim-1 is a constitutively active protein implicated in cardioprotection after

pathological stimulus and promotes CPC cycling and cardiomyogenic differentiation in mouse and human systems[48-51]. Bone marrow cells (BMCs) migrate to the heart after myocardial damage, yet do very little to maintain cardiac integrity with limited evidence of transdifferentiation[52]. In a study completed by our laboratory, delivery of Pim-1 over expressing BMCs enhanced structural integrity of the heart after damage compared to non-genetically modified stem cells possibly through increased persistence and secretion of paracrine factors from BMCs well into the third month after delivery[53]. Similarly, mouse and human CPCs support cardiac regeneration directly up to 8 months after delivery through means of increased engraftment and differentiation into mature cardiogenic cells[49, 53]. Pim-1 overexpression increases growth kinetics and provides for transient lengthening of telomeres in mouse CPCs[54]. Routine protocols in our laboratory allow for isolation of c-kit^{+} CPCs from patients exhibiting symptoms of severe heart failure before LVAD implantation[55]. Isolated human CPCs with slow proliferative indices correlate with shorter telomeres and increased susceptibility to oxidative stress[55, 56]. Genetic enhancement of human CPCs with Pim-1 increases telomerase activity, stabilizes telomere lengths and prevents premature cell cycle arrest in culture[55]. Senescent properties of CPCs can be reversed using Pim-1 and can further broaden the use of CPCs from patients regardless of suboptimal stem cell traits. Additionally, our group has identified nucleostemin (NS) as a downstream target of Pim-1[57]. NS is known to play a role in regulation of ribosomal biogenesis, proliferation and growth in proliferative stem cells making NS an ideal biomarker to identify youthful CPCs

derived from the heart[56, 58]. Stem cell therapy would benefit by isolation of proliferative and survival competent cells, but also cells that are receptive to molecular strategies to supplement inherent limitations in the reparative potential of the heart.

Stem Cell Fusion

Cell fusion for reprogramming of somatic cells has undergone a form of renaissance in the regenerative medicine era, sparking new interest in defining the optimal genetic factors to activate dormant cell types[59-61]. Fusion of slow growing MSCs with an immortal cell line produces hybrids that escape replicative senescence[60, 61]. Hematopoietic stem cells (HSCs)-hepatocyte hybrids observed *in vivo* results in silencing of transcription factors associated with HSC maintenance, increased acquisition of hepatocyte chromatin regulators and overexpression of growth factor genes in the bone marrow nuclei overall leading to liver specific commitment in combination with enhanced bone marrow derived features[62]. In the cardiac context, proliferative stem cells fused with cardiomyocytes results in hybrids with constitutive expression of DNA synthesis markers and maintenance of well-defined sarcomeres[59]. These studies validate that cell fusion conducted between a proliferative parent cell and a slow growing, committed or senescent cell population can facilitate in the creation of hybrids with more youthful phenotypes, pre-committed cells with an ability to proliferate and optimal properties to overcome an aging cardiac environment. Fortunately, cell fusion is being discussed at a critical time for improving cellular based

approaches, as stem cell transplantation to support cardiomyocyte replacement occurs through a process of uncontrolled fusion of stem cells with the myocardial milieu in order to salvage damaged tissue[41, 63, 64]. However, there has been a dearth of studies to delineate the most favorable stem cell types to be used in a cell fusion based protocol *ex vivo* and to support repair of the myocardium.

Defining the Optimal Stem Cell Properties

Efforts to publicize widespread application of cellular therapy are hindered by reports of little to no improvement in cardiac function after long-term follow up studies using a variety of stem cell strategies. This is further complicated by the fact that isolation of stem cells from aged organs display senescent phenotypes[65]. Improvement of stem cell engraftment and survival has been attempted with co-injection of stem cells with biomaterials[66, 67], cytokines and growth factors[68], or genetically engineering cells with pro-survival and anti-apoptotic genes[48, 69]. Despite recent advances in gene therapy, the discovery of the optimal protein(s) and/or activated signaling pathways, which tailor stem cells for paracrine secretion in combination with cardiomyogenic commitment is needed. Furthermore, it is imperative that genetic strategies promote enhancement of pro-survival pathways in stem cells without initiating extreme proliferative phenotypes. Collectively, the field continues to struggle with uncertainties regarding the potency of adult stem cells to mediate meaningful cardiac repair during development or after myocardial damage.

Despite established isolation techniques, there appears to be a lack of understanding of the native stem cell biology in culture. Optimal properties that encompass a composite stem cell would include enhanced survival and proliferation, commitment, and ability to communicate with the endogenous cardiac environment. Ultimately, a picture of the ideal stem cell population emerges from our assessment and overview, but predictably the collective characteristics needed indicate that such a population might not exist under natural conditions to mediate cardiac repair. Therefore, we posit that a combination of stem cells or a single stem population created by *ex vivo* engineering will be required to advance the next generation of cell-based therapy. Our goal is to point toward new avenues and novel transformative therapeutic angles that embrace the ideal properties of adult stem cells.

CHAPTER 1

Nuclear Calcium/Calmodulin-Dependent Protein Kinase II Signaling Enhances Cardiac Progenitor Cell Survival and Cardiac Lineage Commitment

INTRODUCTION

Cardiac regeneration, homeostatic or after acute myocardial damage, is in part supported by the migration of stem and progenitor cells from the bone marrow and endogenous cardiac niches[70, 71]. Stem cells with cardiomyogenic potential were identified based on expression of the receptor tyrosine kinase c-kit and termed as cardiac stem cells or CSCs present in early cardiac development and in the adult heart[40, 72]. Importantly, c-kit$^+$ cells are up regulated temporally after myocardial damage by undergoing proliferation and commitment towards the cardiomyogenic lineage confirmed by genetic lineage tracing[43, 73]. CSCs isolated and expanded *ex vivo* acquire cardiac specific transcription factors and are referred to as cardiac progenitor cells (CPCs) [74]. CPCs exhibit properties of self-renewal and multipotency and give rise to cardiomyocytes, endothelial and smooth muscle lineages *in vitro*[48]. The clinical relevance of CPCs has been further validated by isolation of stem cells from human cardiac tissue used in the **S**tem **C**ell **I**nfusion in **P**atients with **I**schemic Cardi**o**myopathy (SCIPIO) Phase I clinical trial[10]. However, the intrinsic mechanisms involved in the regulation of CPC survival, proliferation and direct cardiomyogenic commitment have not been elucidated.

Calcium (Ca^{2+}) is an integral second messenger, regulating cellular processes such as cellular survival, proliferation, growth and differentiation[75]. Increases in intracellular Ca^{2+} bind to calmodulin which then activates Ca^{2+}/calmodulin-dependent serine/threonine kinase, a class of enzymes known

as CaMKs[76]. CaMKII is the predominant enzyme expressed in cardiac tissue and can be activated with oxidative stress following cardiac injury[77]. Chronic up regulation of the kinase results in cardiomyocyte hypertrophy leading to cardiac failure in mouse models[78, 79]. CaMKIIδ, the main isoform expressed in the heart, is elevated in heart failure samples implicating CaMKII in the regulation of proper cardiomyocyte contractility[80, 81]. However, the distinct role of CaMKII and the main cardiac δ isoforms in resident CPCs has not been previously addressed.

CaMKIIδB and CaMKIIδC are the predominant splice variants described in the adult myocardium. CaMKIIδB localization remains differentiated from CaMKIIδC due to a nuclear localized sequence. Yet CaMKIIδB expression is not exclusive to the nucleus as the CaMKII holoenzyme is formed by a majority of δ subunits[82, 83]. Nuclear CaMKIIδ (B isoform) regulates cellular growth through indirect de-repression of myocyte enhancer factor 2 (MEF2) after phosphorylation and inactivation of the histone deacetylase 4 (HDAC4)[83-85]. Furthermore, CaMKIIδB has been shown to promote cellular protection by binding to the transcription factor GATA4 and indirectly inhibiting the expression of inflammatory genes[86-88].

CaMKIIδB regulates vascular smooth muscle cell migration, proliferation and growth suggesting kinase activity is not limited to cardiomyocytes[89, 90]. CaMKII is linked to the regulation of proliferation and differentiation of embryonic stem cells after inhibition of Class II HDACs[91]. CaMKIIδB phosphorylation of HDAC4 induces translocation to the cytosol, thereby relieving its inhibitory action and allowing transcription of genes involved in cell cycle arrest and lineage

specific differentiation in a variety of stem cells[83-85, 92-94]**.** Currently the use of HDAC inhibitors such as Trichostatin A and 5-aza cytidine are used to increase the efficiency of reprogramming and differentiation of stem cells, supporting the role of HDACs in maintaining pluripotency and proliferation[92]. Therefore, this study aims to characterize a CaMKIIδB-dependent mechanism of cardiac progenitor survival and cardiogenic commitment through class IIa HDAC inhibition.

METHODS

Cardiac progenitor cell isolation

Adult CPCs were isolated from 12 week-old FVB male mice. After anesthetizing mice with ketamine-xylazine solution, the chest was opened and the aortic arch was isolated and curved forceps were used to slip a 4-0 suture (Ethicon) underneath. A small incision was on the aortic arch to insert a 22-guage cannula (Radnoti LLC). Basic buffer, which consists of J-MEM (Sigma) supplemented with HEPES, Taurine, Insulin, Penicillin, Streptomycin, Glutamine, Amphotericin and Gentamycin and collagenase II (30Units/mL Worthington Biochemical) was slowly perfused through the heart after suspending from a Radnoti EZ Myocyte/Langendorff Isolated Heart System while being submerged in a 100mL reservoir for no more than 15 minutes. The heart was then removed from the cannula and placed in a sterile 15-mL conical tube in basic buffer supplemented with 0.5% bovine serum albumin. In a sterile hood, the heart was passed through a 100-μm filter followed by a 40-μm filter and collected in a 15 mL conical tube in basic buffer with BSA. Large cells and cardiomyocytes were separated by quick centrifugation (1 minute, 100g, at 4°C). The supernatant was then passed through a 30-μm filter (Miltenyi Biotec Inc.). Cells were counted and centrifuged (10 minutes, 600g, 4°C). The second supernatant was aspirated, and the pellet was resuspended in 80 μL per 10^7 cells in washing buffer (phosphate buffered saline supplemented with 0.5% BSA) and 20 μL of CD117-conjugated microbeads (Miltenyi Biotec Inc.). Cells were passed over Miltenyi Biotec

MiniMACS sorting columns to select for c-kit^{+} cells. Cells were resuspended in 10% embryonic stem cells fetal bovine serum supplemented cardiac stem cell medium (Dulbecco's modified Eagle's medium and Ham's F-12 medium (ratio, 1:1), insulin-transferrin-selenium (0.1%), leukemia inhibitory factor (10 ng/mL), basic fibroblast growth factor (10 ng/mL), epidermal growth factor (20 ng/mL), 10% embryonic stem cells grade FBS, and 1% penicillin-streptomycin-glutamine), plated on a 35-mm cell culture-grade dish, and placed in an incubator at 37°C. Media was changed 5–7 days later, and the resulting adherent cultures were passaged using Cell Stripper (Cellgro) combined with TryLE Express Enzyme (Life Technologies).

Differentiation media conditions

CPCs in growth media (GM) were cultured in full medium and used as a control. Differentiation was induced by culturing CPCs in α-minimal essential media alone or with the addition of 10nM dexamethasone for 6 days.

Lentiviral constructs and cell transduction

Bicistronic lentiviral constructs were created to over-express a HA tagged CAMKIIδ gene under control of a myeloproliferative sarcoma virus LTR-negative control region deleted promoter and enhanced green fluorescence protein (eGFP) driven off a vIRES. The control lentivirus drives expression of eGFP alone. Transduction of CPCs with bicistronic lentivirus expressing eGFP or HA-CaMKIIδB-eGFP was performed with a multiplicity of infection of 10. Cells were allowed 48 hours to express the eGFP (CPCe) and HA-CaMKIIδB-eGFP

(CPCeδB), then purified after fluorescence activated cell sorting (FACS) by placing one-cell per well of a 96-micro plate to allow for clonal expansion. Three CPCe clones were derived and five CPCeδB. Silencing lentiviral constructs utilized the U6 promoter to drive expression of small hairpin targeted RNA. Two shRNAs were created, a scrambled control and sh towards CaMKIIδB. Both constructs had an inserted cytomegalovirus (CMV) eGFP cassette to label transduced cells. Transduction with sh- scrambled control (sh-Ctrl) or sh to CaMKIIδB (sh-δB) was performed with a MOI of 10 and allowed 48 hours for knockdown before performing population sorts using FACS based on eGFP expression.

Evaluation of cell morphology

Images of cultured CPCs were obtained on a Leica DMIL microscope and outlines were traced using ImageJ software. Parameters such as area, “shape descriptors” and “Feret’s diameter” were measured, based on which the cross sectional area and roundness were determined. Feret/MinFeret was used to evaluate length to width ratio of each cell.

Proliferation assay and cell doubling time

Cell proliferation was determined using the CyQuant Direct Cell Proliferation Assay (Life Technologies) according the manufacturer’s instruction. CPCs were plated at a density of 500 cells in 100 µL of full growth media per well of a 96-well flat bottom microplate. Assay was started on day of plating, day 2 and day 4 and day 6 by adding of 100 µL of CyQuant direct green fluorescent

nucleic acid stain in each well and incubated for 60 minutes. Green fluorescence intensity was measured at 495 nm using a plate reader and represented as a fold change relative to fluorescence intensity measured on the day of plating (day 0). Population doubling times were calculated using the readings from CyQuant Direct Proliferation Assay and use of a population doubling time online calculator (http://www.doubling-time.com/compute.php).

Cell cycle analysis

Cells were fixed in 70% ethanol and stored overnight at -20°C. Cell cycle distribution was analyzed by staining with propidium iodide (PI) plus RNAse staining buffer (BD Biosciences) at 37°C for 15 minutes. Cell cycle was analyzed using a BD FACSCanto and FlowJo software to determine relative distributions of cells in G1 and G2/M phases of the cell cycle.

Metabolic activity assay (MTT-based assay)

CPCe and CPCeδB were subjected to a MTT colorimetric reducing assay which analyzes (3-(4,5-Dimethylthiazol-2-yl)-2,5-diphenyltetrazolium bromide), a yellow tetrazole being reduced to a purple formazan in living cells. This assay was used in order to determine relative rates of metabolic activity between cell lines. In this assay 500 cells were plated per well in a 96-well flat bottom plate incubated with 10μL of 5mg/mL MTT reagent for four hours. Reaction was stopped with 100μL of diluted HCL for lysis overnight. The MTT assay was performed on the day of plating, 3 or 7 days after plating and incubation with CPC growth media, Minimum essential media- α modification (α-MEM) with 10%

fetal bovine serum (FBS) or 10% FBS α-MEM supplemented with Dex. Absorbance was measured at 595nm in order to determine relative concentrations of cells at given days.

Cell death assay

CPCs were plated in a 6-well dish (80,000 cells per well) and incubated in starvation media (growth factor and FBS depleted media) with 1% PSG for 18 hours. Cells were treated with either 40 or 80 μM hydrogen peroxide for 4 hours. Analysis of cell death was initiated by collecting cells from suspension and adherent cells and pelleting at 1600rpm for 5 minutes. The pellet was resuspended in Annexin V binding buffer and incubated with Annexin V (1:40) from BD Biosciences combined with 7-amino-actinomycin D (7-AAD) staining to label apoptotic and necrotic cells collectively. Data was acquired using a FACS Canto from BD Biosciences and analyzed with FACS Diva software from BD Biosciences. Cell death was quantitated by co-labeling of Annexin V and 7-AAD and represented as a fold change or percentage of cell death relative to cells in starvation media alone.

Immunoblot

Protein lysates from whole hearts and cultured cells were prepared in sample buffer (containing 150mM Tris (pH 6.8), 150mg/ml sucrose, 2mM ethylene diamine tetraaceticacid (EDTA) (pH 7.5-8), 480mg/ml urea, 8mg/ml dithiothreitol, 0.2% sodium dodecyl sulfate, 0.2 mg/ml bromophenol blue at a final pH of 6.8, supplemented with protease and phosphatase inhibitor cocktails

(Sigma-Aldrich). Whole hearts from mice were prepared by homogenizing tissue in isolation buffer (containing 70 mM sucrose, 190 mM mannitol, 20mM HEPES solution, and 0.2 mM EDTA in de-ionized water) using a Next Advance bullet blender. Protein lysates from homogenized tissue were incubated 1:1 with sample buffer. CPCs were either lysed directly with sample buffer or were fractionated into nuclear and cytosolic compartments according to manufacturer's protocol prior to incubating in sample buffer (PARIS Kit, Life Technologies). All protein samples for western blot analysis were separated on a 4%–12% Bis-Tris mini-gel (Life Technologies) and transferred to a polyvinylidene difluoride membrane. Membranes were blocked for 1 hour with 10% milk in TBST (1%Tris-buffered saline/0.1% Tween) and then probed with primary antibody overnight in milk. Next day blots were washed with TBST buffer and incubated in secondary antibodies in milk for 1.5 hours. Primary antibodies for western blot are as follows: rabbit anti-CaMKIIδ (1:15000; UC Davis, Dr. Donald Bers), mouse anti-HDAC4 (1:1,000; Cell Signaling) rabbit anti-Phospho-HDAC4 (Ser632)/HDAC5 (Ser661)/HDAC7 (Ser486) (1:1000; Cell Signaling) goat anti-GFP (1:1000; Rockland), mouse anti-HA tag (1:200; Santa Cruz Biotechnology, Inc.), mouse anti-p16 (1:200, Santa Cruz Biotechnology), rabbit anti-p53 (1:500, Abcam), rabbit anti-α-sarcomeric actinin (1:500; Abcam), mouse anti-α-smooth muscle actin (1:1000; Sigma Aldrich), rabbit anti-Tie2 (1:100; Santa Cruz Biotechnology), mouse anti-mouse β-actin (1:500; Sigma Aldrich), mouse anti-GAPDH (1:3000; Chemicon), and rabbit anti-Lamin A (c-terminal) (1:1000; Sigma Aldrich).

Immunocytochemistry

CPCs were plated at a density of 15,000 per well of a two-chamber permanox slide. Cells were then fixed in 4% paraformaldehyde for 60 minutes then washed in phosphate buffered saline. Cells were permeabilized in 0.1% Triton X in PBS for two minutes and washed twice with PBS. Cells were then blocked in 10% horse serum in PBS for one hour and then incubated with primary antibody overnight. Next day, cells were washed in PBS and incubated with secondary antibody for 1.5 hours. Cells were imaged on a Leica TCS SP2. Primary antibodies are as follows: rabbit anti-CaMKIIδ (1:1500; UC Davis, Dr. Donald Bers) and rat-anti Tubulin (1:50, Harlan).

Immunohistochemistry

Heart sections were deparaffinized, and antigen was retrieved in 1 mmol/L citrate (pH 6.0), followed by a one-hour block in TNB. Primary antibodies were incubated overnight. Slides were washed in 1% Tris/NaC1 (TN buffer) followed by secondary antibody incubation for two hours. Cells were washed after secondary antibodies in TN followed by a final wash containing DAPI (1:10,000 in TN for 10 minutes to stain for nuclei). Primary antibodies are as follows: goat anti-CD117 (c-kit) (1:100, R&D Systems) and GFP anti-rabbit (Life Technologies 1:500), mouse anti-cardiac troponin T (1:100, Abcam). CD117 required tyramide amplification.

Quantitation of CaMKIIδ expression in CPCs in vivo

C-kit cells were identified in paraffin heart sections after

immunohistochemical staining and by using a Leica TCS SP8 confocal microscope. In the Leica software, a measuring tool was used to create a region of interest around the border of c-kit$^+$ cells and the nucleus separately. The mean fluorescence value was measured and used to represent the relative expression levels of CaMKIIδ in the whole cell and the nuclear compartment of c-kit$^+$ cells.

RNA extraction and quantitative real time PCR

Reverse transcriptase was performed using protocol described for iScript cDNA Synthesis Kit (BIORAD). cDNA was diluted 1:100 in nuclease free molecular grade water before performing qRT-PCR. cDNA was incubated with primers at 100nM concentration. Real time PCR was performed on all samples in triplicate using iQ SYBR Green (Bio-Rad) following the manufacturer's protocol. The fold change in gene expression was determined using the ddCt method. CaMKIIδB and CaMKIIδC forward and reverse primers were used as previously described[87]. Primer sequences are as follows: cardiac troponin t, forward 5'-ACCCTCAGGCTCAGGTTCA-3' and reverse 5'-GTGTGCAGTCCCTGTTCAGA-3'; α-smooth muscle actin mouse forward 5'-GTTCAGTGGTGCCTCTGTCA-3' and reverse 5'-ACTGGGACGACATGGAAAAG-3'; 18s forward CGAGCCGCCTGGATACC and reverse CATGGCCTCAGTTCCGAAAA.

Experimental animals

The review board of the Institutional Animal Care and Use Committee at San Diego State University approved all animal protocols and studies.

Statistical analysis

All data are expressed as mean $^{+}$/- SEM. Statistical analyses were done using paired or unpaired Student's t-test, one way-ANOVA with Tukey post-tests or using two way ANOVA with Bonferroni post-tests on Graph Pad Prism v5.0. A value of $p<0.05$ was considered statistically significant.

RESULTS

CaMKIIδ is expressed in CPCs during post-natal growth and is upregulated after pathological stress

In order to validate levels of CaMKIIδ isoforms during different post-natal stages, immunoblot and immunohistochemical analysis was performed using whole heart lysates and heart tissue sections from mouse origin. CaMKIIδB protein expression is elevated in hearts from post-natal day 2 through 30 and decreases with progression into adulthood (Figure 1.1A and 1.1B). CaMKIIδC protein levels steadily increase with hypertrophic growth maintaining protein expression in mouse adulthood (Figure 1.1A and 1.1C). Since both CaMKIIδB and CaMKIIδC are known to inhibit HDAC4 activity by phosphorylation on the serine 632, we assessed total and phosphorylated HDAC4 in the developing heart. HDAC4 and phosphorylated HDAC4 on the serine 632 (pHDAC4) decrease with aging consistent with the role of HDAC4 to suppress growth in cardiomyocytes (Figure 1.1D-1.1G). The increased presence of c-kit^{+} CPCs during development coincides with a burst in cardiomyocyte proliferation and hypertrophic growth[42]. In order to determine if endogenous c-kit^{+} CPCs express CaMKIIδ isoforms *in vivo*, CPCs were co-labeled with a pan CaMKIIδ antibody. CaMKIIδ protein is detected in cardiomyocytes during an early postnatal day heart (Figure 1.1H) and is down regulated in a 30-day-old heart based on immunohistochemical analysis (Figure 1.1I). At the same post-natal time points, CaMKIIδ protein was detected in c-kit labeled CPCs at low levels (Figure 1.1H

and 1.1I). CPCs up regulate both cytoplasmic and nuclear CaMKIIδB 7 days after myocardial infarction (MI) relative to c-kit cells discovered in 3-month-old sham surgery controls (Figure 1.1J-1.1L). Overall, differential expression of CaMKIIδ in CPCs *in vivo* suggests relevance of the kinase in stem cells after pathological stress and possibly differentiation

CaMKIIδB localizes to the nucleus and inhibits HDAC4 in CPCs undergoing cardiogenic commitment

In order to investigate CaMKIIδ expression and localization in CPCs during basal and differentiation conditions, CPCs were isolated from the adult myocardium based on established protocols[42]. CPC commitment is characterized by decreased proliferation and increased cellular size concomitant with increased expression of proteins of the cardiomyogenic lineage following dexamethasone (Dex) treatment[95]. Relative to basal levels, CaMKIIδB mRNA levels are up regulated in CPCs treated with Dex (Figure 1.2A), whereas CaMKIIδC mRNA levels remain unchanged when comparing cells treated without and with Dex (Figure 1.2B). Following Dex stimulation CPCs have increases in both CaMKIIδ isoforms in whole cell lysates visualized after immunoblotting (Figure 1.2C and 1.2D). CaMKIIδ is primarily localized in the cytosol of CPCs during regular growth media conditions (Figure 1.2E), and is upregulated after differentiation along with a marked presence of CaMKIIδB in the nucleus of CPCs (Figure 1.2F). Fractionated CPCs were analyzed for CaMKIIδ in the cytoplasmic and nuclear

compartments of the cells, confirming that CaMKIIδB localizes in the nucleus during commitment of CPCs (Figure 1.2G-1.2I).

CaMKIIδB dependent regulation of HDAC4 has been previously reported[84, 85], therefore we attempted to investigate if this also occurs in our isolated CPCs. Inactivated HDAC4 (pHDAC4) protein trended towards an increase in the cytoplasmic fraction of CPCs treated with differentiation media without and with Dex compared to growth media conditions (Figure 1.3C and 1.3D), indicating a correlative role during differentiation to increase CaMKIIδB in the nucleus and de-repress genes necessary for growth and differentiation. However, total HDAC levels were not significantly changed in CPCs without and with Dex treatment (Figure 1.3A and 1.3B). In order to validate that HDAC4 is a target of CaMKIIδ in CPCs, we used a lentivirus to overexpress CaMKIIδB (CPCeδB), as confirmed by immunoblot by the presence of an HA tag and green fluorescent protein (Figure 1.3E and 1.3F). Lentivirus expressing GFP alone was used as a control (CPCe) (Figure 1.3E and 1.3F). Although total HDAC4 levels were unchanged in CPCe relative to CPCeδB (Figure 1.3G and 1.3H), CPCeδB have increased cytosolic pHDAC4 relative to CPCe, correlating with a decreased level of pHDAC4 in the nuclear compartment (Figure 1.3I and 1.3J). These results suggest that CaMKIIδB overexpression facilitates the inactivation of HDAC4.

Nuclear CaMKIIδ overexpression in CPCs increases cellular size and decreases cell proliferation

Overexpression of CaMKIIδB in CPCs presented phenotypic characteristics that are relevant to increased cardiomyogenic differentiation[55]. In support of this, CPCeδB show decreased proliferative potential (Figure 1.4A) and increased doubling time (Figure 1.4B) compared to CPCe. CPCeδB are less present in the G2/M phase of the cell cycle compared to CPCe (Figure 1.4C). Interestingly, CPCeδB exhibits increases in cellular size based on measurement of cell surface area (Figure 1.4F) and cell length to width ratio (Figure 1.4G) during basal growth conditions relative to CPCe (Figure 1.4D-1.4G). Cellular senescence was not evident in CPCeδB based on p53 or p16 protein levels relative to CPCe (Figure 1.4H-1.4J). Therefore, the decreased proliferative rate and larger cell morphology exhibited by CPCeδB is not due to increased senescence or irreversible cell cycle arrest.

CaMKIIδB overexpression in CPCs increases cell commitment towards the cardiomyogenic lineage

CPCeδB treated with Dex for six days shows a strong up regulation of cardiac and smooth muscle markers such as *cardiac troponin T* (*tnnt3, cTNT*) and *α-smooth muscle actin* (*α-SMA*) based on mRNA levels relative to CPCe (Figure 1.5A and 1.5B). Consistent with increased differentiation phenotype, CPCeδB have increased metabolic activity during growth conditions and during differentiation, where CPCe has increased metabolic activity only with the

addition of Dex (Figure 1.5C). Cardiac marker α-sarcomeric actinin was upregulated in Dex treated CPCeδB based on protein expression (Figure 1.5D and 1.5E). CPCeδB commitment to the vascular endothelial and smooth muscle differentiation is increased relative to CPCe based on immunoblot analysis of endothelial marker Tie2 (Figure 1.5F and 1.5G) and smooth muscle marker α-SMA (Figure 1.5F and 1.5H). This data indicates that CaMKIIδB can drive the differentiation of CPCs and enhance the transition to mature cells of the cardiac, endothelial and smooth muscle lineages.

CaMKIIδB expression in CPCs antagonizes apoptotic cell death after oxidative stress stimuli

Expression of CaMKIIδB prevents apoptosis in cardiomyocytes following doxorubicin or hydrogen peroxide (H_2O_2) stimulation[86, 87]. Overexpression of CaMKIIδB in CPCs similarly improves survival after 40μM and 80μM H_2O_2 induced death compared to CPCe (Figure 1.6A and 1.6B). In order to establish a pro-survival role of CaMKIIδB in CPCs, a small hairpin RNA to CaMKIIδB (sh-δB) was used to decrease the expression of the kinase before stimulation with oxidative stress (Figure 1.6C and 1.6D). CPCs with reduced levels of CaMKIIδB had increased susceptibility to cell death at increasing concentrations of H_2O_2 (Fig. 1.6E and 1.6F). Collectively, CaMKIIδB plays an integral role in early commitment of CPCs while enhancing cell survival during oxidative stress.

DISCUSSION

There is debate as to the stem cell type that is needed to treat myocardial damage. CPCs, although limited, have been validated as a cell type to treat heart disease due to their cardiomyogenic potential[10, 73]. In this study, we present a canonical calcium-signaling cascade implicated in growth and survival of CPCs by CaMKII. CaMKIIδ isoforms are studied in the context of maladaptive hypertrophy in transgenic mice[78]. However, recent studies have implicated CaMKIIδB to reduce expression of inflammatory factors in a global CaMKIIδ knockout model, indicating a protective role of the δB kinase in the cardiac context after pathological damage[88]. Until now, it remained unknown whether CaMKIIδ isoforms are present in resident CPCs although expression is reported in smooth muscle cells in the heart[89, 90]. Our study is the first to identify nuclear translocation of the CaMKIIδB isoform during lineage commitment of CPCs (Figure 1.1 and Figure 1.2). Furthermore, overexpression of CaMKIIδ supports distinct morphological changes and increases differentiation accompanied by decreased cell cycle progression (Figure 1.3 and Figure 1.4). Consistent with cardiomyocyte data, CaMKIIδB confers survival in CPCs, which is abrogated when δB expression is reduced and subjected to oxidative stress stimuli (Figure 1.6). Collectively, this data supports the ability of CPCs to acquire growth and differentiation phenotypes regulated by CaMKIIδ signaling to the nucleus.

Currently, there is interest in identifying proteins and signaling cascades in CPCs related to mature cardiomyocytes. During basal conditions, CPCs express the B2-adrenergic receptor (B2-AR) regulating stem cell proliferation but acquire

the mature B1-AR after co-culture with cardiomyocytes[96]. Ca^{2+} in fetal CSCs supports cellular growth, proliferation and commitment[97]. Inositol-1,4,5-triphosphate (IP3) receptors on the sarcoplasmic reticulum induce spontaneous Ca^{2+} oscillations in mouse and human CPCs [97, 98]. CPCs are validated to not only express IP3 receptors, but also purinergic G protein-coupled receptors (P2Y) and SERCA2, which are functionally stimulated and activated after introduction of Ca^{2+} and/or ATP [98, 99]. Furthermore, IP3 receptors promote an influx of Ca^{2+} in the nucleus activating CaMKII/MEF2 and cellular growth [100]. In Figure 1.1, expression levels of CaMKIIδ are increased and localized to the nucleus during acute stress, indicating that a short-term stimulus is sufficient to prime cardiac commitment of stem cells. This was further validated in isolated CPCs, as our differentiation protocol induced nuclear accumulation of CaMKIIδB (Figure 1.2), correlating with inactivated p-HDAC4 in the cytosolic fraction (Figure 1.3). These studies suggest that the transitory fate of CPCs during cell division and differentiation can be defined by a complex interplay of calcium-regulated molecules prior to acquiring cardiomyogenic fate.

CPCs under genetic modification with mature cardiomyocyte genes increase our knowledge as to the potential of stem cells to promote cardiac repair after adoptive transfer in the heart. CPCs express Ca^{2+} receptors and pumps, however, expression of the Ryanodine receptors and B1-AR are not present in CPCs indicating that these cells hold a primitive molecular cardiac signature[99]. Related to our study, CPCs transfected with a siRNA targeting HDAC4, and therefore inhibiting the repression of growth genes, increased differentiation of

CPCs *in vivo* supporting myocardial regeneration[94]. In cardiomyocytes, HDAC4 and HDAC5 form a complex to inhibit MEF2 and serum response factor elements[83, 84]. Inactivation of Class IIa HDACs by CaMKII and protein kinase D promotes shuttling of HDAC4 from the nuclear compartment by the chaperone 14-3-3 [101, 102]. Our data shows a decrease of nuclear p-HDAC4 in our non-modified CPCs (Figure 1.3). Conversely, p-HDAC was increased in the cytosol of Dex treated CPCs or CPCeδB (Figure 1.3). However, the results were modest indicating that additional factors affect the kinase activity of CaMKII and/or inhibition of Class IIa HDACs. In contrast, HDAC inhibition, including inhibition of Class I HDACs, has been shown to decrease the proliferative and differentiation potential of mesenchymal stem cells indicating that HDACs are essential for maintenance of proper stem cell function [103].

We evaluated if overexpression of CaMKIIδB can enhance the differentiation patterns of CPCs. Here a lentiviral protocol was employed and characteristics such as increased cellular size and decreased proliferation were immediately apparent after overexpression of CaMKIIδB (Figure 1.4). In order to delineate a CaMKIIδB dependent role to enhance stem cell survival relative to the CaMKIIδC isoform, we subjected CPCs to oxidative stress and observed a decrease in late apoptotic cells (6-fold reduction) relative to control CPCs (Figure 1.6). In contrast, knockdown of CaMKIIδB increases cell susceptibility to apoptosis (Figure 1.6). This data confirms that CaMKIIδB is essential in CPC survival consistent with other reported cell types. Interestingly, we observed an increase in mRNA expression of CaMKIIδC following the knockdown of

CaMKIIδB. Models of CaMKIIδC overexpression exaggerates maladaptive cardiac remodeling during development and after trans aortic constriction surgery relative to overexpression of CaMKIIδB[78]. At the cellular level, cardiomyocyte apoptosis and sensitivity to stress stimuli are increased by overexpression of CaMKIIδC[104]. Furthermore, proliferation and differentiation was not significantly altered relative to control cells after transfection of CPCs with shRNA to CaMKIIδB. This data may indicate that CaMKIIδB is not required for growth and commitment of CPCs and there are alternative compensatory mechanisms that sustain CPC self-renewal capabilities. This brings into question the diverse forms of CaMKII, the differential isoforms and interplay in the entire cell. Currently, identification of calcium-associated proteins brings validation to CPC origin and potency status and supports the potential of CPCs as a cardiac regenerative population.

SUMMARY POINTS

- CaMKIIδ isoforms are expressed in endogenous CPCs during post-natal growth and is induced after injury.
- Isolated CPCs upregulate CaMKIIδ in the cytosol concurrent with CaMKIIδB localization in the nuclear compartment during commitment.
- CaMKIIδB overexpression in CPCs inactivates HDAC4.
- CaMKIIδB overexpression in CPCs reduces proliferation, improves survival and increases cardiomyogenic commitment.
- Knockdown of CaMKIIδB in CPCs increases susceptibility to death stimuli but does not impair differentiation capacity.
- CaMKIIδ expression in CPCs may serve as a regulatory kinase to enhance therapeutic properties.

FIGURES

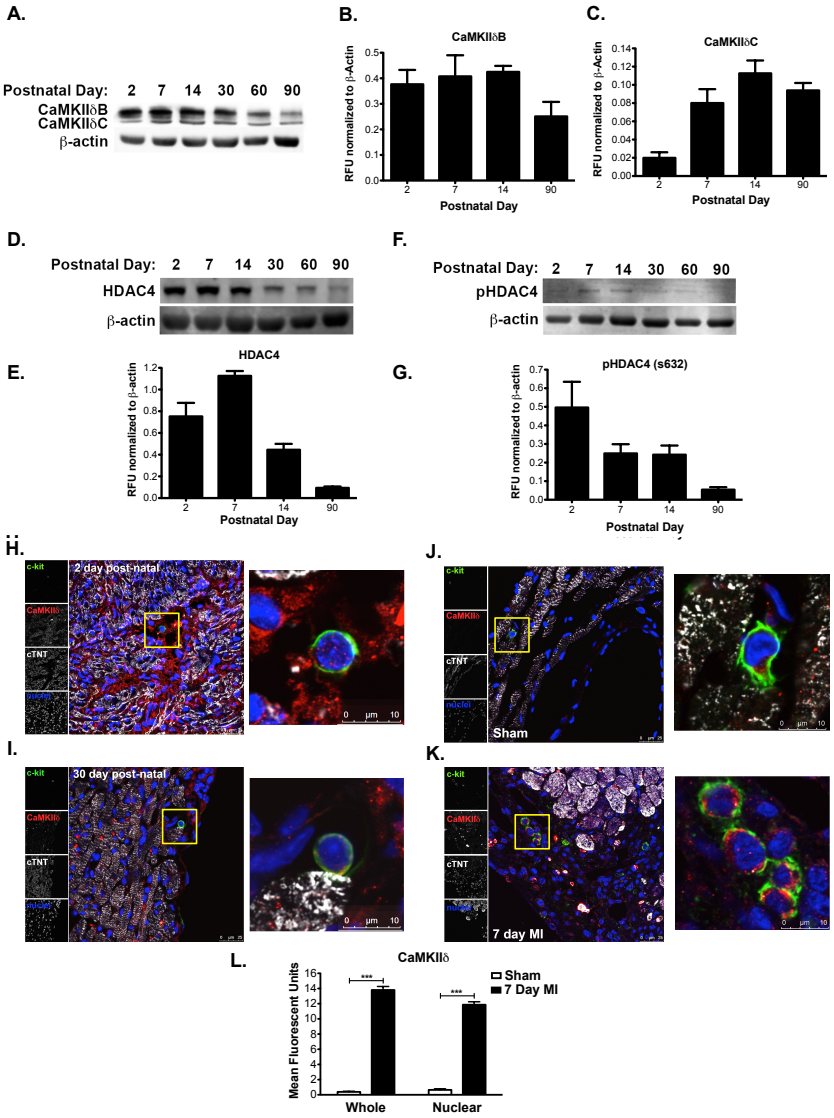

Figure 1.1: CaMKIIδ is expressed in CPCs during post-natal growth and is upregulated after pathological stress.

(A) CaMKIIδB (top band) and CaMKIIδC (bottom band) protein expression in whole heart lysates at increasing postnatal days. (B) Quantitation of CaMKIIδB and (C) CaMKIIδC expression levels represented as relative fluorescent units (RFU) normalized to β-actin. (D) Total HDAC4 levels at different postnatal days in the mouse heart. (E) Quantitation of HDAC4 expression normalized to β-actin represented as RFU. (F) Phosphorylated HDAC4 on the serine 632 in the developing mouse heart. (G) Quantitation of pHDAC4 expression normalized to β-actin represented as RFU. (H) 2 day and (I) 30-day-old hearts visualized for expression and localization of CaMKIIδ in myocytes and c-kit^{+} CPCs. (J) CaMKIIδ labeling in CPCs after sham or (K) Following MI surgery for 7 days. (L) Quantitation of CaMKIIδ expression and localization (whole or nuclear) in endogenous CPCs in sham and 7 day MI treated mice. Mice are 3 months of age prior to MI surgery. Cardiac troponin T (cTNT) and TO-PRO-3 iodide were used to label myocardium and nuclei respectively. *** $p<0.0001$ Sham vs. 7 Day MI.

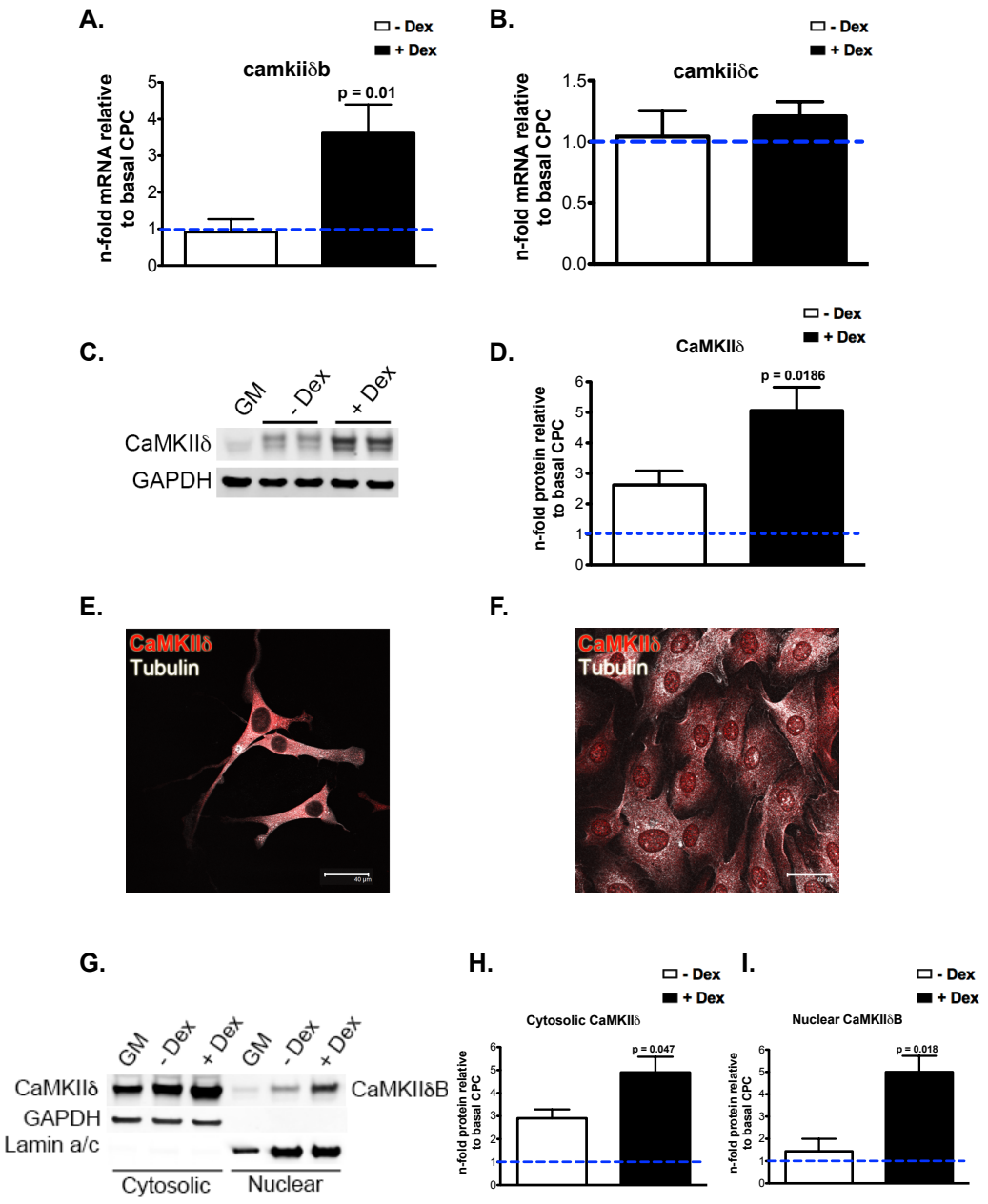

Figure 1.2: CaMKIIδB localization to the nucleus is increased in CPCs during commitment.
(A) CaMKIIδB and (B) CaMKIIδC mRNA in CPCs with and without Dexamethasone (Dex) stimulation for seven days represented as a fold change relative to CPCs maintained in growth media (GM). (C) CaMKIIδ protein levels in whole cell lysates with and without Dex stimulation. (D) Quantitation of total CaMKIIδ levels relative to GM treated CPCs. (E) CaMKIIδ protein is primarily cytosolic in CPCs without differentiation stimulus. (F) CaMKIIδ increases in expression and localizes to the nuclear compartment of CPCs after six days of Dex treatment. (G) CaMKIIδ expression in the cytosolic and nuclear fractions of CPCs after induction with differentiation media. (H) Quantitation of cytosolic CaMKIIδ and (I) nuclear CaMKIIδB. Graphs are represented as a fold change relative to basal CPCs in cytosolic and nuclear fractions. GAPDH is probed as a loading control for immunoblots. P values compare CPCs in 10% FBS α-MEM without Dex to CPCs treated with Dex.

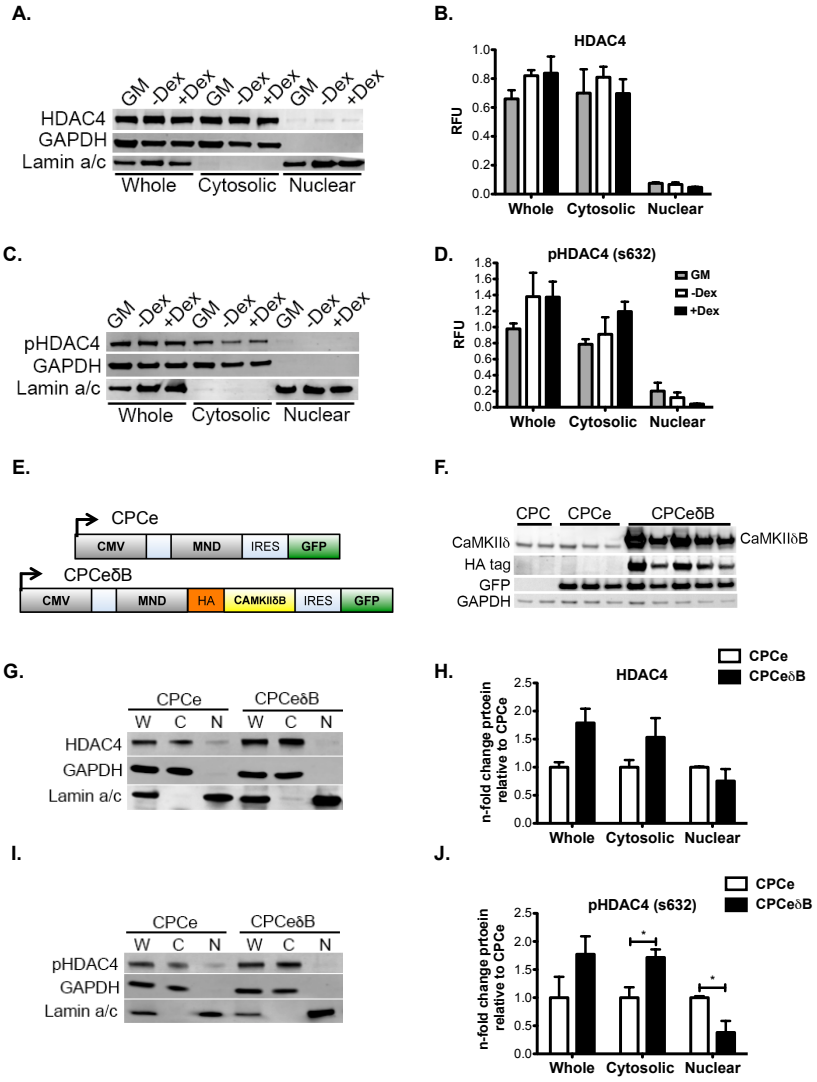

Figure 1.3: CaMKIIδB localizes to the nucleus and inhibits HDAC4 in CPCs undergoing cardiogenic commitment.
(A) Immunoblot of total HDAC4 protein levels in whole, cytosolic and nuclear fractions of CPCs treated with GM, -Dex or $^{+}$ Dex supplemented media. (B) Quantitation of total HDAC4. (C) Immunoblot pHDAC4 (s632) protein levels in whole, cytosolic and nuclear fractions of CPCs treated with GM, -Dex or $^{+}$ Dex supplemented media. (D) Quantitation of pHDAC4 (s632) Immunoblots are presented as a fold change relative to CPCs in GM and normalized to GAPDH or Lamin A (C-terminus) ** $p<0.01$ –Dex vs. $^{+}$Dex. (E) Lentiviral constructs to establish CPCe and CPCedδB lines. (F) CPCeδB lines overexpress CaMKIIδB as well as the HA tag. CPCe overexpress eGFP. GAPDH was probed as a loading control. (G) CPCe and CPCeδB lines probed for total HDAC4 levels by immunoblot and (H) Quantitation in whole cell lysates, cytosolic and nuclear fractions. (I) Phosphorylated HDAC4 on the serine 632 protein levels in CPCe or CPCeδB by immunoblot and (J) Quantitated from whole cell lysates, cytosolic and nuclear fractions. Immunoblots are probed with GAPDH to normalize for protein loading of the whole and cytosolic lysates. Lamin A (C-terminus) antibody was utilized to normalize for loading of the nuclear fraction. Total and phosphorylated HDAC4 are represented as a fold change relative to CPCe. * $p<0.05$ CPCe vs. CPCeδB. W=Whole cell, C=cytosolic fraction and N=nuclear fraction

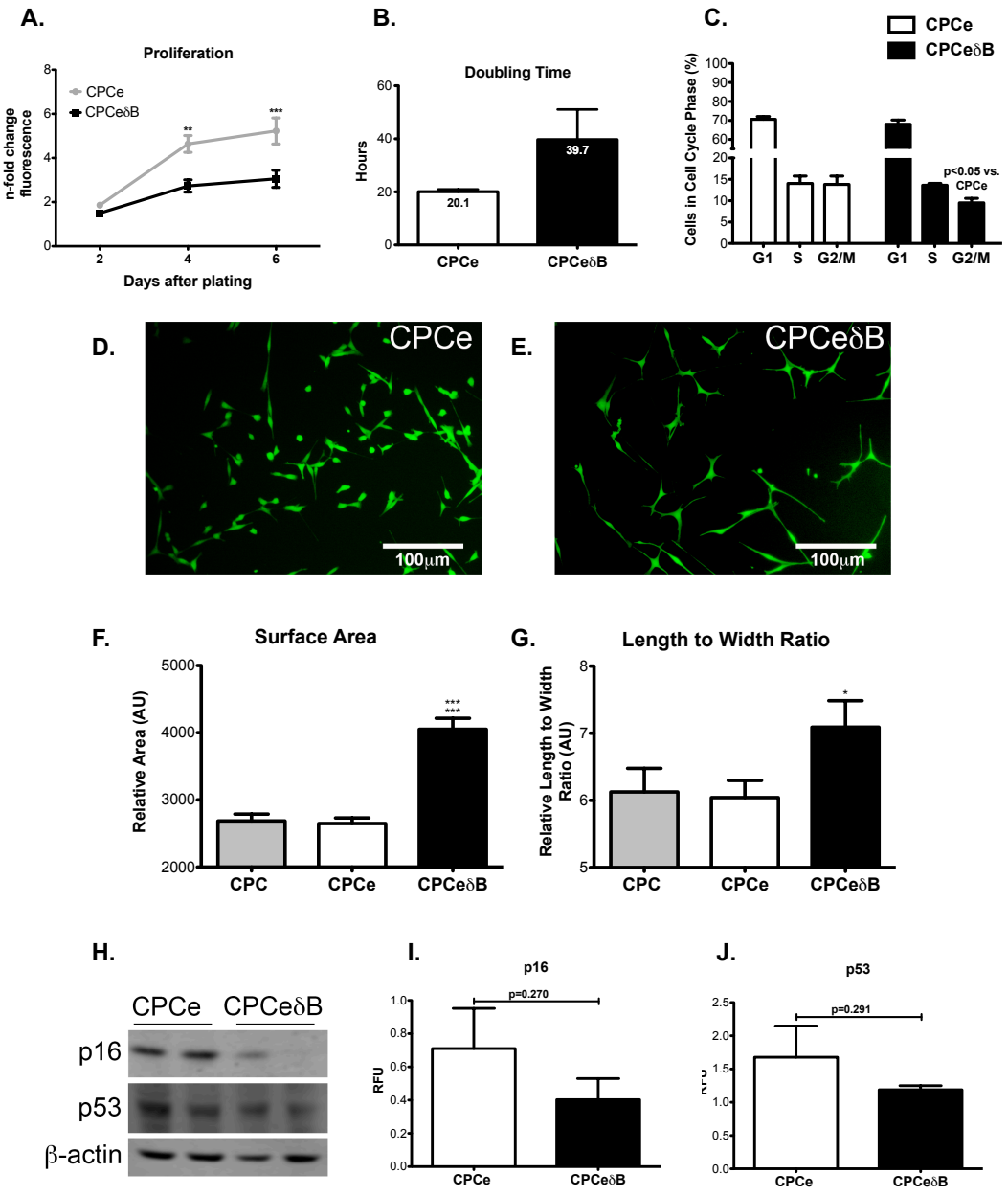

Figure 1.4: Nuclear CaMKIIδ overexpression in CPCs increases cellular size and decreases cell proliferation.
(A) CPCeδB has decreased proliferative capacity relative to CPCe based on a fluorescent nucleic acid stain measured at 2, 4 and 6 days after seeding equal cell numbers. ** and *** p<0.01 and p<0.0001 CPCeδB relative to CPCe. (B) CPCeδB populations shows an increased doubling time relative to CPCe. (C) Cell cycle analysis using flow cytometry in CPCe and CPCeδB. (D) Fluorescent images of CPCe and (E) CPCeδB populations in growth media. (F) CPCeδB shows an increase in relative cell surface area. *** p<0.0001 CPCeδB relative to CPC and CPCe. (G) CPCeδB shows an increase in length to width ratio relative to non-modified CPCs and CPCe. * p<0.01 CPCeδB relative to CPCe. (H) Expression of senescence markers p16 and p53 by immunoblot. β-actin was probed as a loading control. (I) Quantitation of p16 and (J) p53 in CPCe and CPCeδB populations.

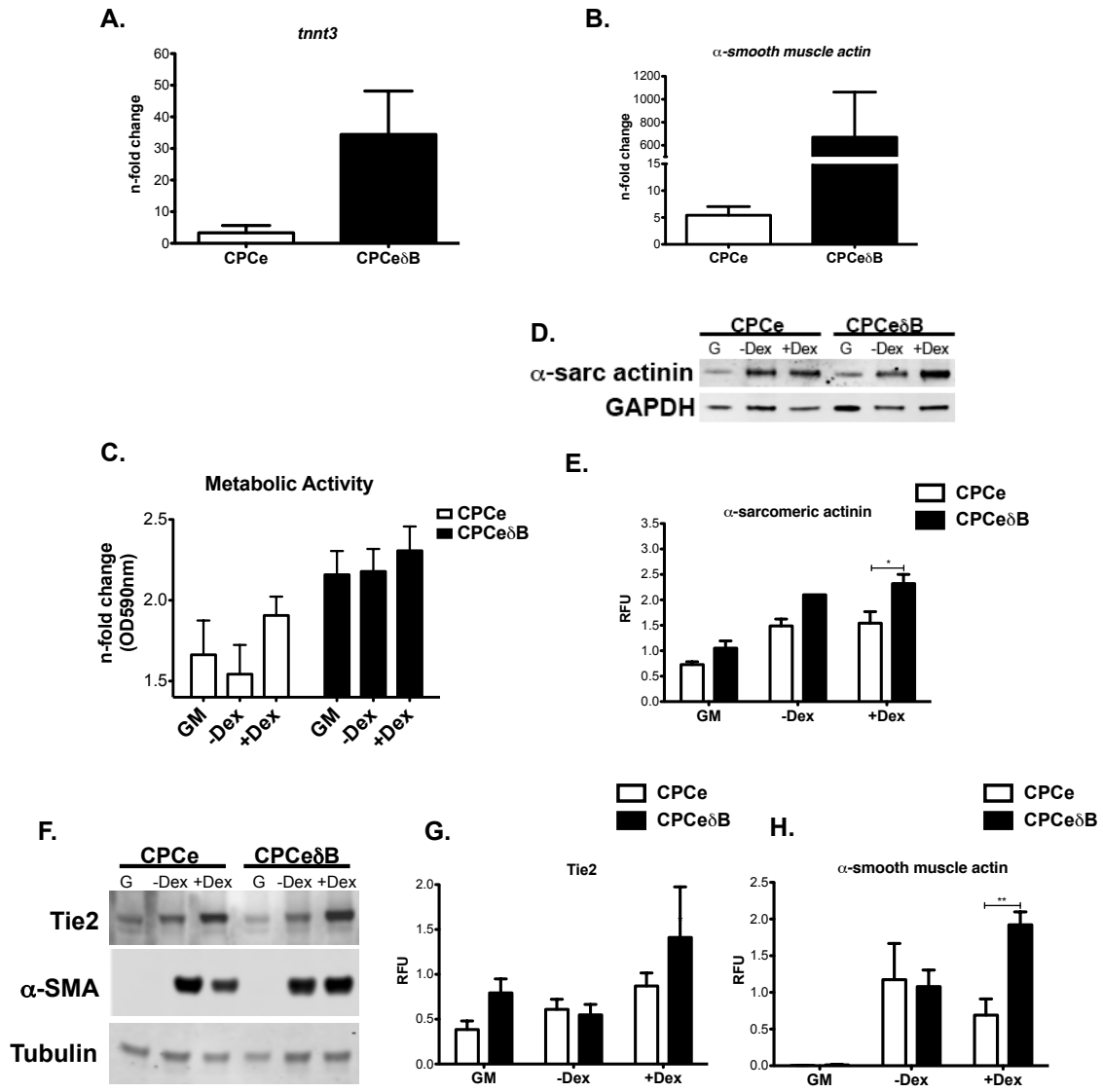

Figure 1.5: CaMKIIδB overexpression in CPCs increases cell commitment towards the cardiomyogenic lineage.
(A) CPCeδB stimulated with Dex for six days show increased expression of cardiogenic marker cardiac troponin T (tnnt3) and (B) α-smooth muscle actin based on mRNA expression. (C) Cardiac marker α-sarcomeric expression and (D) Quantitation in CPCe and CPCeδB in normal growth conditions, -Dex and $^{+}$ Dex. (E) Metabolic activity under GM, -Dex or $^{+}$ Dex growth conditions. (F) Endothelial (Tie2) and smooth muscle (α-SMA) were probed in CPCe and CPCeδB grown in normal growth conditions, -Dex or $^{+}$ Dex. (G) Quantitation of Tie2 and (H) α-SMA, which is upregulated in Dex treated CPCeδB. Values are represented as relative fluorescent units (RFU) normalized to GAPDH or tubulin. * $p<0.05$ and ** $p<0.01$ CPCe vs. CPCeδB.

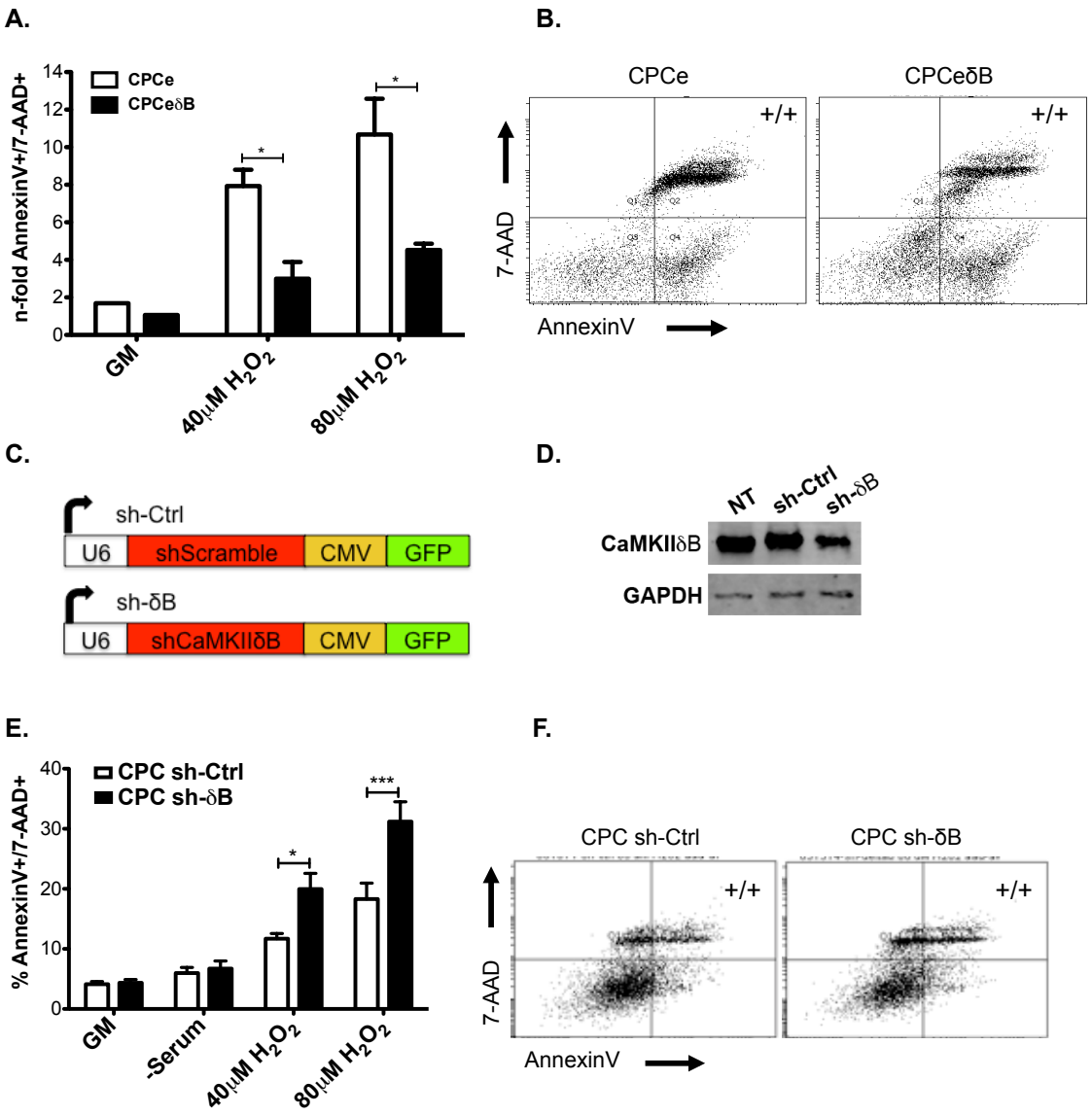

Figure 1.6: CaMKIIδB expression in CPCs antagonizes apoptotic cell death after oxidative stress stimuli.
(A) Quantitation of Annexin V and 7-AAD double positive cells (to label for cells in late apoptosis) in (B) CPCe and CPCeδB after incubation in growth media GM, 40 or 80 μM H_2O_2. Values are represented as a fold change relative to GM treated cells. (C) Schematic of constructs (top) and (D) confirmation of knockdown of CaMKIIδB in CPCs relative to controls (NT: non-treated and sh-Ctrl). (E) Quantitation of late apoptosis in CPCs transfected with (F) small hairpin (sh) control or Sh to knockdown CaMKIIδB and subjected to growth media, serum starvation, 40 or 80 μM H_2O_2. Values are represented as a percentage based on flow cytometric analysis.

Chapter 1, in full, is prepared for submission. Nuclear Calcium/Calmodulin-Dependent Protein Kinase II Signaling Enhances Cardiac Progenitor Cell Survival and Cardiac Lineage Commitment. Pearl Quijada, Nirmala Hariharan, Jonathan Cubillo, Kristin M. Bala, Lucia Ormachea, Donald M. Bers, Mark Sussman and Coralie Poizat. The dissertation author was the primary author and investigator on this publication.

CHAPTER 2

Cardiac Stem Cell Hybrids Enhance Myocardial Repair

INTRODUCTION

Cell therapy for regeneration of the myocardium after myocardial infarction (MI) involves two concurrent processes: 1) stimulation of endogenous repair, and 2) exogenous cellular commitment. Regenerative medicine would benefit tremendously from identification of optimal stem cell population(s) that exert both direct and indirect mechanisms to mediate survival of existing cardiomyocytes, support proliferation and differentiation of endogenous stem cells, reduce inflammation and prevent scar formation. Coupling intrinsic mechanisms of myocardial repair with the propensity of stem cells to undergo cardiomyogenesis should be carefully balanced and integrated with the existing heart scaffold. Delivery of single stem cell types promote relatively modest functional and structural recovery of the heart owing to limited reparative capacity of donated cell populations derived from cardiac and bone marrow origin. Increasing cell numbers can enhance beneficial cellular properties, but excess reactive oxidative species and inflammation after acute damage contribute to elimination of more than 90% of delivered cells after one-week[46, 47]. While the genetic engineering of stem cells prior to delivery remains a promising alternative to enhance persistence and regeneration[48, 49], potential additional benefits of combinatorial cell therapy remain largely unexplored.

Resident c-kit$^+$ cardiac progenitor cells (CPCs) are a desirable cell choice due to enhanced proliferative capacity and ability to form cardiomyocytes, vascular smooth muscle and endothelial cells *ex vivo*[105]. Endogenous c-kit$^+$ cells

have limited capacity towards cardiomyogenic commitment during development and after myocardial injury[73]. Despite limited regenerative capability, clinical application of CPCs confers improvements in myocardial structure and function as highlighted in the Cardiac **S**tem **C**ell **I**nfusion in **P**atients With **I**schemic Cardi**O**myopathy (SCIPIO) patient trial[10]. Bone marrow is the most popular source of adult-derived stem cells because of proven safety and efficacy after transplantation[14]. In particular, mesenchymal stem cells (MSCs) are commonly used for autologous and allogeneic clinical therapies[32]. MSCs are valued for paracrine-mediated effects such as reducing inflammation and promoting pro-survival and growth cascades to surrounding cells[106]. MSC injection after infarction promotes robust recruitment of c-kit$^+$ CPCs, induces cardiomyocyte cycling and facilitates the outgrowth of stem cells from myocardial biopsies *ex vivo*[107]. Recently, combining these two distinct stem cells types, CPCs and MSCs, was investigated in a porcine model of myocardial damage[108]. Functional recovery and detection of human derived cells in the myocardium was improved over injection of single cells alone, indicating synergism of combining two cell types[108]. However, cellular mechanisms of myocardial recovery were not addressed and cell numbers were skewed towards increased MSCs in order to confer protective effects *in vivo*[108].

Cell fusion to create syncytia is an endogenous and homeostatic process coupled with differentiation and organ development[63]. Although low at basal levels, fusion increases in acute and chronic settings of inflammation, DNA damage and apoptotic events after bone marrow cell (BMC) transplantation[109,

[110]. Artificial cell fusion between the same or different cell types to produce heterokaryons can be accomplished with addition of polyethylene glycol, electric pulses or viral fusogens[111]. In rare events, mononucleated hybrids (synkaryons) from bi-nucleated cell states occur, which is largely dependent on the ability of one cell type to undergo DNA synthesis after fusion[112]. BMCs and MSCs have been observed to readily fuse to more mature cells, allowing successful transfer of mitochondria and phenotypic traits such as increased survival and proliferation[59, 64, 113]. Spontaneous *in vivo* cell fusion as a mechanism to support regenerative therapy have been underwhelming leading to the conclusion that cell fusion alone is not a major contributor to heart regeneration.

In this manuscript, we present the creation and characterization of CPC and MSC hybrids, referred to as CardioChimeras (CCs), generated by *ex vivo* viral cell fusion. CCs exhibit enhanced molecular and phenotypic traits relative to individual stem cells and these distinct hybrids were evaluated for *in vivo* therapeutic effects after myocardial damage in a mouse model. Recovery of anterior wall thickness (AWT) and ejection fraction (EF) were markedly improved, concomitant with increased engraftment and expression of early cardiomyogenic lineage markers in CC treated hearts. CardioChimeras represent a novel therapy that complements the paracrine effects of MSCs to orchestrate endogenous repair with direct cell contributions from CPCs in promotion of *de novo* cellular regeneration.

METHODS

Study design

These studies were designed to test the reparative capacity of CPCs, MSCs, CPC + MSC and CCs in a mouse model of MI. Initially, we expanded 18 CCs and chose two phenotypically distinct hybrids, CC1 and CC2. Inclusion of CCs was contingent on pro-proliferative and pro-survival capabilities. Furthermore, co-culturing CCs with NRCMs mediated the identification of CCs that facilitate survival and growth of cardiomyocytes as compared to parent MSCs. Overall, all 18 CCs were analyzed for optimal profiles in proliferation, survival and stem cell properties and/or differentiation before an *in vivo* mouse trial. We required approximately 16 animals per cell group to allow for analysis of at 3-5 mice per time point (4, 12 and 18 WPI) without impacting statistical significance obtained during longitudinal assessment by echocardiography. This number was chosen based on an average of 65-75% survival rate immediately after injury. Mice with a measured EF between 35-50% one-week post infarction were included in the experiment. EF >50% or <35% were excluded from the experiment. Throughout the time course, mice were not subjected to echocardiography if mice were perceived to be in distress. The study was concluded after determining statistical significance in wall thickness recovery and EF at 18 WPI. The study was not randomized, but was blinded to the operator during echocardiographic acquisition and analysis.

CPC and MSC isolation

CPCs were isolated and maintained as previously described[114]. CPCs were used during passages 10-20. Mesenchymal stem cells were isolated from 12 week old female FVB mice by flushing the femur and tibiae with 5% Fetal Bovine Serum in PBS through a 40-μm filter and centrifuged (10 minutes, 600g, 4°C). Cells were resuspended in media consisting of α modified minimum essential media and 15% FBS. Cells were plated in 150mm dish and media was changed every two days to remove non-adherent cells. Adherent cells created colonies in approximately two weeks. MSCs were passaged using 0.25% Trypsin and used during passages 2-4 for experiments.

Lentiviral constructs

A third generation enhanced green fluorescent protein (eGFP) lentivirus with a phosphoglycerate kinase (PGK) and puromycin (puro) selection marker was purchased from Addgene (pLenti PGK GFP Puro (w509-5) was a gift from Eric Campeau, plasmid # 19070). pLenti PGK GFP Puro was used as a backbone to sub clone mcherry in the place of eGFP and bleomycin (bleo) to replace the puro gene in order to create pLenti PGK mcherry Bleo.

Stem cell transduction with lentivirus

MSCs at passage 1 were lentivirally transduced with pLenti PGK GFP Puro at a multiplicity of infection (MOI) of 50 and maintained in puromycin supplemented MSC media for one week starting at 48 hours post-infection. CPCs at passage 10 were lentivirally transduced with pLenti PGK mcherry Bleo

at a MOI of 10 and subjected to fluorescent activated cell sorting (FACS) to purify mcherry positive CPCs. Fluorescent protein expression in MSCs (MSC-GFP) and CPCs (CPC-mcherry) was confirmed by fluorescent light microscopy and flow cytometric analysis.

Cell fusion and creation of CardioChimeras

Cell fusion was conducted using the GenomONE™ - CF EX Sendai virus (Hemagglutinating Virus of Japan or HVJ) Envelope Cell Fusion Kit (Cosmo Bio. USA). According to the manufacturer's protocol, we subjected MSCs and CPCs to the plating method for cell fusion. Here, 100,000 MSC-GFP in a 100mm dish were incubated in CPC media for 24 hours. Next day, 100,000 CPC-mcherry cells were suspended in 20μL of cell fusion buffer and 10μL of Sendai virus and placed on ice for 5 minutes for absorption of the virus on the cell membrane. Media from MSC-GFP plate was removed and washed once with cell fusion buffer, and CPC-mcherry $^{+}$ Sendai virus was added. The plate was then centrifuged (10 minutes, 1200rpm at 4°C) to force cell-to-cell contact. To induce cell fusion, cells were placed at 37°C for a total of 15 minutes. Non-fused CPC-mcherry cells were removed by aspiration and CPC media was added back to the plate. The next day, media was changed, and within 48 hours cells were trypsinized and subjected to FACS to place one-cell per well of a 96-micro plate and allow for clonal expansion of double positive cell populations expressing GFP and mcherry. 18 double positive clones expanded from single cell sorted

were confirmed by secondary flow cytometric analysis. Two representative clones were chosen for experiments outlined in this paper.

Light microscopy and measurement of cell morphology

Images of stem cells were obtained on a Leica DMIL microscope and cell outlines were traced using ImageJ software. Relative surface area was determined as previously described[115].

Neonatal rat cardiomyocyte (NRCM) co-culture with stem cells

NRCMs were isolated and plated as previously described[116]. After enzymatic digestion, cells were plated in M199 media (Life Technologies) with 15% FBS (Omega Scientific Inc.) at a density of 260,000 cells per well of a 6-well culture dish pretreated with 1% gelatin (Sigma-Aldrich). Within 18 hours, myocyte cultures were washed with PBS and incubated with M199 with 10% fetal bovine serum for 24 hours. The next morning, the cells were subjected to serum starvation (0.5% FBS in M199) for 24 hours. After low serum conditions, stem cells were added to the plate at a ratio of 1:10 (CPCs, MSCs, CPC $^{+}$ MSC combined, CC1 and CC2) and allowed to incubate with NRCMs for an additional 24 hours in low serum conditions. Controls for NRCMs included leaving cells in 0.5% alone, adding back 10% M199 or maintaining NRCMS in 10% M199 for the duration of the experiment. NRCM size was measured after staining cardiomyocytes with sarcomeric actinin (1:100, Sigma-Aldrich) and nuclei with TO-PRO-3 iodide and as previously described[117]. Separation of NRCM and stem cells was accomplished with fluorescent activated cell sorting (FACS) of

negative cells (NRCMs) versus GFP^+, $mcherry^+$ or GFP^+/ $mcherry^+$ stem cells. After sorting, cells were centrifuged and suspended in RNAse buffer for isolation and quantitation of mRNA from NRCMs or stem cells.

Immunocytochemistry

Stem cells were placed at a density of 15,000 per well of a two-chamber permanox slide and stained according to previous studies[53]. Before scanning, cells were washed in PBS containing TO-PRO-3 iodide (1:10,000, Life Technologies) to stain for nuclei. Slides were visualized using a Leica TCS SP2 confocal microscope. Primary antibodies are as follows: rat anti-mcherry (1:100, Life Technologies); rabbit anti-GFP (1:100, Life Technologies).

Flow cytometric analysis

Cells in suspension were counted (2.0 X 10^5 per sample) and stained with primary and secondary antibodies according to previous studies[53]. Samples were analyzed using a FACS Canto (BD Biosciences). Primary antibodies are as follows: goat anti-CD117 (1:40, R&D Systems); or goat anti IgG as a control (1:40, Santa Cruz Biotechnology, Inc.). Secondary antibody: donkey anti-goat 647 (1:400, Jackson Immunoresearch).

Centromere labeling

Cells were fixed on glass two chamber slides in 3:1 ethanol: acetic acid for 30 minutes and then passed through graded alcohol series 70, 90, 100% (2 minutes each step). Slides were baked at 65°C for 15 minutes and then transferred to acetone for 10 minutes. Slides were then incubated for 1h at 37°C

in 2X SSC (NACl/NA Citrate) plus RNAse (100µg/ml). Cell were treated with pepsin, 10mM HCl mixed with 0.5µl of stock pepsin solution (1mg/ml) at room temperature for 2-3 minutes and then dehydrated through ethanol series. Denaturing cellular DNA was done by immersing slides in 70% formamide in 2X SSC at 70°C for 2 minutes and then placed in ice cold 70% ethanol for 2 minutes followed by passing through an ethanol series. Prior to hybridization the centromere probe, CENPB-Cy3 (PNA Bio; ATTCGTTGGAAACGGGA), was warmed to 37°C for 5 minutes. The probe was denatured for 10 minutes at 85°C then immediately chilled on ice before applying probe to the slides. The hybridization protocol required 16 hours at 37°C. Post hybridization washes for 5 minutes at 37°C in 2X SSC were followed by two washes in 50% formamide/2X SSC 37°C, for 5 min each time and final wash in 2X SSC, twice for 5 min each time. DAPI (Sigma-Aldrich) was added to the final wash. Cell nuclei were visualized using a Leica TCS SP8 confocal microscope and the Z-stacking feature. Measurements of nuclear size and centromere intensity were determined after outlining the nucleus and getting the area (μm^2) and mean gray values (fluorescent intensity/μm^2) after creating a projection of Z-Stack scans.

Proliferation assay and cell doubling time

Cell proliferation was determined using the CyQuant Direct Cell Proliferation Assay (Life Technologies) according the manufacturer's instruction and as previously described[115]. Population doubling times were calculated using

the readings from CyQuant Direct Proliferation Assay and use of a population doubling time online calculator (http://www.doubling-time.com/compute.php).

Cell death assay

Stem cells were plated in a 6-well dish (80,000 cells per well) and incubated in starvation media (growth factor and FBS depleted media) with 1% PSG for 18 hours. The cells were then treated with either 40μM or 80μM hydrogen peroxide for 4 hours. Cells were resuspended with Sytox Blue (1:2,000, Life Technologies) to label necrotic cells. Data was acquired on a FACS Aria (BD Biosciences) and analyzed with FACS Diva software (BD Biosciences). Cell death was quantitated by measurement of Sytox Blue positive cells and represented as a fold change relative to cells in starvation media alone.

In co-culture conditions of stem cells with NRCMs, whole populations were analyzed and stained with Annexin V (1:40, BD Biosciences) and Sytox Blue and only the negative (non-fluorescent NRCM) population was analyzed for cell death. Cell death of NRCMs was represented as a fold change relative to cells in growth media (10% M199). NRCMs in 0.5% M199 and 0.5% plus add back of 10% M199 at the time of stem cell addition were maintained as positive and negative controls for cell death.

mRNA isolation, cDNA synthesis and quantitative RT-PCR

RNA was enriched using the Quick RNA Mini Prep kit from ZymoResearch according to the manufacturers instructions. Reverse transcriptase was performed using protocol for the iScript cDNA Synthesis Kit (BIORAD). qRT-PCR

was read after incubation of cDNA, primers (100nM) and IQ SYBR Green Supermix (BIORAD) as previously described[115]. Data was analyzed using the ΔΔC(t). Primers are as follows: cardiac troponin t, forward 5'-ACCCTCAGGCTCAGGTTCA-3' and reverse 5'-GTGTGCAGTCCCTGTTCAGA-3'; connexin 43 forward 5'-GGACCTTGTCCAGCAGCTT-3' and reverse 5'-TCCAAGGAGTTCCACCACTT-3'; smooth muscle 22 forward 5'-GACTGCACTT CTCGGCTCAT-3' and reverse 5'-CCGAAGCTACTCTCCTTCCA-3'; platelet endothelial cell adhesion molecule forward 5'-TGCTCTCGAAGCCCAGTATT-3' and reverse 5'-TGTGAATGTTGCTGGGTCAT-3'; p53 forward 5'-GCAGGGCTCA CTCCAGCTACCT-3' and reverse 5'-GTCAGTCTGA GTCAGGCCCCACT-3'; p16 forward 5'-CGTACCCCGATTCAGGTGATG-3' and reverse 5'-CGGGCGGG AGAAGGTAGT-3'; interleukin-6 forward 5'-ATCCAGTTGC CTTCTTGGGACTGA-3' and reverse 5'-TAAGCCTCCGA CTTGTGAAGTGGT-3'; 18s forward CGAGCCGCCTGGATACC and reverse CATGGCCTCAGTTCCGAAAA.

Enzyme-Linked Immuno Assay (ELISA)

The ELISA assay was performed in NRCMs alone (0.5%, 0.5% $^{+}$ 10% rescue, and 10% M199 treated cells), NRCMs incubated with stem cell groups and stem cells alone in normal growth media. Briefly, after 24 hour incubation with serum or stem cells, the 96-well microplate was centrifuged for 5 minutes at 1200rpm and 100μL of media supernatant was removed and used for IL-6 Mouse ELISA Kit (Life Technologies) performed according the company's instructions.

Myocardial infarction and intramyocardial injection

Myocardial infarctions were carried out in eleven-week old female FVB mice under 2-3% isoflurane anesthesia and by tying off the left anterior descending artery (LAD) using a modified protocol[118]. After ligation, injections with either PBS (5μL per injection, 5 injections total per mouse), parents (CPCs or MSCs), parents combined (CPC $^{+}$ MSC) CC1 or CC2 (20,000 cells per 5μL injection, 5 injections making a total of 100,000 cells injected per mouse) were introduced to the pre-ischemic border along the infarcted region. Placing the heart out of the chest and placing it back in the chest without ligation of the LAD was considered a sham surgery.

Echocardiography and hemodynamics

Echocardiography was used to evaluate cardiac function after MI and injections using the Vevo 2100 (Visual Sonics) and as previously described[53]. Closed-chest hemodynamic assessment was performed after insertion of a microtip pressure transducer (FT111B, Scisense) and as previously described[53]. Cardiac function assessed by echocardiography 2 days post-infarction was not statistically different between infarcted/injected groups. The review board of the Institutional Animal Care and Use Committee at San Diego State University approved all animal protocols and studies.

Retroperfusion

Mice were sacrificed under chloral hydrate sedation before removing hearts from mice and as previously described[53]. After retroperfusion, hearts were processed for paraffin embedding.

Immunohistochemistry

Heart sections were deparaffinized, and incubated with primary and secondary antibodies as previously described[53]. Subsequent tyramide amplification was performed as necessary. Slides were incubated in DAPI (Sigma-Aldrich) for 10 minutes to stain for nuclei. Primary antibodies are as follows: goat anti-CD117 (c-kit) (1:100, R&D Systems); rabbit anti-GFP (1:500, Life Technologies); rat anti-mcherry (1:200, Life Technologies); mouse anti-cardiac troponin T (1:100, Abcam); CD117, GFP and mcherry required subsequent tyramide amplification.

Quantitation of c-kit cells, infarct size and cellular engraftment

Paraffin sections were probed with primary antibodies for proteins cardiac troponin T (cTNT), c-kit, GFP and mcherry and visualized on a Leica TCS SP8 Confocal Microscope. Nuclei were visualized after DAPI staining. For infarct size, cTNT was probed to visualize live myocardium and DAPI to determine nuclei distribution and area of infarction. Area of live versus dead myocardium was measured using the drawing tool in the Leica Software and normalized to the total area of the left ventricular free wall and converted to percentage. In this area, c-kit$^+$ cells were counted. For engraftment, area of mcherry$^+$ (CPCs, CPCs

in CPC $^{+}$ MSC group, CC1 and CC2) or GFP^{+} (MSCs alone and MSCs in CPC $^{+}$ MSC group) was measured and normalized to total area. 4 and 12 week sections had an n=3-4 per group.

Masson's Trichrome

Trichrome (Masson) kit was used to stain for collagen deposition in infarcted hearts according to manufacturer's protocol and based on previous reports[114]. Staining was visualized using a Leica DMIL microscope.

Statistical analysis

All data are expressed as mean $^{+}$/- SEM. Statistical analyses was done using paired or unpaired Student's t-test, one-way ANOVA with a Tukey post-test or using two-way ANOVA with Bonferroni post-tests on Graph Pad Prism v5.0. A value of $p<0.05$ was considered statistically significant.

RESULTS

Phenotypic characterization of CardioChimeras

CardioChimeras (CCs) were created after fusion of fluorescently labeled CPCs (mcherry) and MSCs (eGFP) with an inactivated RNA Sendai virus (Figure 2.1A). After fusion, dual fluorescent hybrids were purified by fluorescent activated cell sorting and allowed to undergo clonal expansion (Figure 2.2A). 18 mono-nucleated hybrids were successfully expanded one-month after initial sorting, and two unique CCs (CC1 and CC2) were maintained for this study based upon comparable proliferative and survival properties to the parental cells. CC2 exhibits a proliferative rate similar to CPC parent while CC1 shows modest proliferation, and all cells had increased proliferation over the MSC parent based on a fluorescent dependent cell proliferation assay and cell doubling time (Figure 2.1B and 2.1C). CCs are not increasingly susceptible to cell death compared to parent cells (Figure 2.1D) and did not exhibit elevated expression of cell cycle arrest or senescence markers based on mRNA for p16 or p53 (Figure 2.1E and 2.1F). CC1 has increased cell size and is morphologically similar to MSCs (Figure 2.1G, 2.1I and 2.1J). CC2 displays a slight increase in cell size but is not significantly different from CPCs (Figure 2.1G, 2.1H, and 2.1K). Mononucleated CC1 and CC2 exhibit increased nuclear size and centromere intensity relative to parent cells after nuclear hybridization (Figure 2.2B-2.2F). Collectively, CCs represent a novel stem cell population where increased DNA content does not negatively impact on survival or proliferation after induced cell fusion.

CardioChimeras exhibit increased basal expression of cardiomyogenic commitment markers

MSCs and CC1 populations have little to undetectable c-kit^{+} cells, while CC1 and CPCs maintain 20% and 50% c-kit positivity (Figure 2.3A). Gap junction marker *connexin43* and *platelet endothelial cell adhesion molecule* (*pecam or cd31*) mRNA are modestly upregulated in CC2 at basal levels (Figure 2.3B and 2.3C). MSCs express high levels of endothelial and smooth muscle markers as indicated by *cd31* and *smooth muscle 22* (s*m22*) gene expression (Figure 2.3C and 2.3D)[119]. Although *sm22* was not upregulated in CCs, co-incubation of CPCs with MSCs at a 1:1 ratio increased mRNA expression of s*m22* (Figure 2.3D). Interestingly, CC1 has increased mRNA for *cardiac troponin T* (*cTNT or tnnt3*) (Figure 2.3E). This data supports CCs potential for increased cardiomyogenic activity making them an attractive cellular source for cardiac therapy.

CardioChimeras promote cardiomyocyte growth after co-culture

In order to test the beneficial effects mediated by CCs and parental cells before *in vivo* cell transfer, neonatal rat cardiomyocytes (NRCMs) were co-incubated with stem cell groups (CPC, MSCs, CPC + MSC, CC1 and CC2) at a ratio of 1:10 in serum depleted conditions. NRCMs maintained in low serum conditions (0.5%) resulted in smaller cardiomyocytes relative to NRCMs maintained in high serum conditions (10%) (Figure 2.4A, 2.4B and 2.4G). Addition of MSCs, CPC + MSC, CC1 or CC2 to low serum treated NRCMs significantly increased cardiomyocyte size within 24 hours (Figure 2.4C-E and

2.4G), but CPCs could not induce significant growth of NRCMs (Figure 2.4F and 2.4G). Slow twitch *β-myosin heavy chain* (*mhy7*) over fast twitch *α-myosin heavy chain* (*mhy6*) gene expression was not significantly elevated in cardiomyocytes after 24 hours co-incubation with stem cell groups but is highly expressed in low serum conditions indicating the stem cells do not induce a maladaptive hypertrophic responses in cardiomyocytes (Figure 2.4H). Regardless of the stem cell population added to cardiomyocytes, NRCMs were protected from cell death based on flow cytometric analysis of apoptotic and necrotic markers (Figure 2.4I). With the addition of CC1 and CC2, NRCMs had increased mRNA for *stromal derived factor-1* (*sdf-1*) (Figure 2.4J) a cardioprotective cytokine and homing ligand for C-X-C chemokine receptor type 4 (CXCR-4) positive stem cells[120].

CardioChimeras have increased gene expression of commitment and paracrine markers after co-culture with cardiomyocytes

After co-culture with cardiomyocytes, *sm22* was not significantly upregulated in CC groups (Figure 2.5A). However, CPC + MSC and CC2 displayed the largest induction of endothelial marker expression of *pecam*, whereas CC2 induced *cTNT* gene expression after 7 days of co-culture with NRCMs (Figure 2.5B and 2.5C). Paracrine factors are routinely touted as a mechanism for cardioprotection[121], therefore we analyzed stem cells for expression of growth and immunomodulatory factors. Gene expression for *interleukin-6* (*Il-6*) and protein expression is upregulated in CC2 after 24-hour incubation with serum starved NRCMs (Figure 2.5D and 2.5E). Early release of

immunomodulatory factors such as IL-6 after acute cardiac damage is anti-apoptotic[122].

CardioChimeras improve left ventricular structure and cardiac function after myocardial injury

To establish therapeutic efficacy of CCs relative to parent cells or parent cells combined, we injected a total of 100,000 cells within the border zone region of an acutely damaged mouse heart (left anterior descending artery ligation). At 1-week post injury (WPI), all groups had similar reductions in AWT and EF (Figure 2.6A and 2.6D and Table 2.1). CC1 and CC2 exhibited increased AWT at 4 WPI, but only CC1 treated hearts preserved AWT up to 18 WPI (Figure 2.6A). Heart weight to body weight ratios (HW/BW) at 12 and 18 weeks did not increase in CC treated hearts indicating that hypertrophy was not a contributing phenotype to increases in AWT (Figure 2.6B and 2.6C). Rather, CC1 hearts had significantly reduced HW/BW relative to vehicle control (PBS) (Figure 2.6C). EF was increased in CC1 and CPC + MSC hearts starting at 3 WPI, and CC1 and CC2 had increased EF over PBS at 6 WPI (Figure 2.6D). CC and CPC + MSC-treated groups exhibited improved EF starting at 12 WPI, whereas the CPC-treated group was beneficial for cardiac function only at 18 WPI (Figure 2.6D). Heart rates and structural/functional data are detailed in Table 2.1. Correlating with improved EF, CC1 treatment significantly improved positive developed pressure over time (dP/dT) (Figure 2.6E) and negative dP/dT (Figure 2.6F). CC1, CC2, CPC + MSC and CPC had smaller infarct sizes relative to PBS (Figure 2.6G).

MSC groups exhibited increased infarct size when measuring scar between 4 and 12 WPI, CPC and CPC + MSC hearts remain unchanged, and CC1 and CC2 treatment reduced infarct size as represented by Masson's Trichrome staining (Figure 2.6G-2.6N).

Cellular engraftment of CardioChimeras 4 weeks after damage

Scar size measured at 4 WPI was not significantly different among infarcted heart groups (Figure 2.7A and 2.7B-2.7E). Next, we were interested in determining cell persistence at this time point and were able to detect CPCs labeled with mcherry in CPC alone and CPC + MSC treated hearts (Figure 2.7F and 2.7G). Interestingly, mcherry$^+$ CPCs were detected near small c-kit$^+$/cTNT$^+$ cardiomyocytes in the infarct area (Figure 2.7H). CC1 was detected by both GFP and mcherry expression, but did not display evidence of commitment at this early time point (Figure 2.7I-2.7K).

CardioChimeras have increased engraftment, expression of cardiomyogenic markers and support the increased presence of c-kit$^+$ cells in the myocardium 12 weeks after damage

C-kit$^+$ cell recruitment in damaged regions supports endogenous differentiation and myocardial repair[121]. Although infarction sizes were similar at the 4-week time point, induction of endogenous c-kit cells in the infarcted area was increased in MSC, CPC + MSC, and CC1 treated hearts (Figure 2.8A-2.8C). At 12 WPI, a high number of c-kit$^+$ cells were observed in PBS and MSC treated hearts, yet c-kit$^+$ cells remained visually present in CPC + MSC, CC1 and CC2

treated hearts surrounding mcherry^{+} cells in the border zone regions (Figure 2.8D-2.8G). The percentage of cell engraftment was increased in CC1 and CC2 hearts at 1.9% and 1.1% respectively relative to 0.21% and 0.29% in CPC and CPC + MSC hearts (Figure 2.8H and 2.8K-2.8O). MSCs were detected at a much lower level or 0.04% of the total left ventricular free wall (Figure 2.8H, 2.8I, and 2.8J). CPCs discovered in the border zone areas co-expressed c-kit and mcherry in CPC hearts and expressed mcherry alone in CPC + MSC hearts (Figure 2.8K and 2.8L). However, both CC1 and CC2 showed increased levels of engraftment and co-localized with cTNT, surrounded by endogenous c-kit^{+} cells (Figure 2.8M-2.8O).

CardioChimeras increase capillary density in the infarct area

Capillary density was measured in the border zone and infarcted areas at 12 WPI. Shams, non-injured controls, are included as a standard for capillary density compared to injured hearts (Figure 2.9A, 2.9B, and 2.9C). Parent cells, individual or combined, or CC treatment did not significantly increase capillary density in the border zone regions relative to PBS (Figure 2.9A and 2.9C-2.9I). MSC, CPC or CPC + MSC treated hearts similarly did not affect the number of capillaries discovered in the infarct zone (Figure 2.9B and 2.9J-2.9M). Notably, CC1 and CC2 treated hearts had significant increases in isolectin^{+} structures in the infarct regions at 12 WPI (Figure 2.9B and 2.9N-2.9O).

CPC, MSC and CardioChimera treatment normalizes cardiomyocyte size in the remote and infarcted regions

Cellular treatment and long term engraftment of cells is reported to induce compensatory hypertrophy in areas of damage preventing progression of heart failure after MI[123]. MSC and vehicle controls had increased cardiomyocyte size in the remote area relative to sham, displayed no significant changes in the border zone cardiomyocytes and revealed decreased average cardiomyocyte size in the infarct regions (Figure 2.10A-2.10F). CPC + MSC, CC1 and CC2 treated hearts maintained cardiomyocyte size in the remote region similar to non-injured controls (Figure 2.10A, 2.10D and 2.10H-2.10J). Although stem cell treatments did not modify border zone cardiomyocyte size (Figure 2.10B and 2.10K-2.10P), injection of CPC, CPC + MSC, and both CCs increased cardiomyocyte size in the infarcted regions relative to PBS and MSC treated hearts up to 12 WPI (Figure 2.10C and 2.10Q-2.10V). This data indicates that improved engraftment of stem cells correlates with the presence of microvascular structures and preservation of cardiomyocyte size in the remote and infarct regions relative to failing and severely damaged hearts.

DISCUSSION

The restorative impact of cell therapy to advance regenerative medicine remains to be fully realized and continues to be the focus of intense investigation. Increased knowledge of stem cell biology emerges from the use and application of a variety of adult stem cells. Unfortunately, ideal cellular properties are compromised by massive cellular death upon introduction into damaged myocardium[47]. In this report, we demonstrate a novel approach by using cell fusion to enhance delivery of novel and unique stem cell properties created within a single cell. Cardiac-derived CPCs and bone marrow derived MSCs were chosen for this study as both of these cell types have established roles in the heart: CPCs contribute to direct cardiomyogenic differentiation whereas MSCs provide for protective immunomodulatory and growth factor paracrine secretion[105, 106]. CCs were not significantly impaired in proliferation and did not exhibit signs of genomic instability due to increased DNA content (Figure 2.1 and 2.2). Furthermore, CCs had decreased expression c-kit^{+} and increased expression of cardiac specific factors at basal levels and after co-culture with cardiomyocytes, which is concurrent with the ability of stem cells to provide for increases in cardiomyocyte growth, survival and *sdf-1* mRNA in stressed cultured conditions (Figure 2.3, 2.4, and 2.5). CCs injected into the acutely damaged heart improved structural integrity and reduced infarct size (Figure 2.6). Furthermore, functional improvements were observed in CC treated hearts, and increased engraftment was apparent in the border zones after 12 WPI (Figure 2.8). In conclusion, CardioChimeras are a superior cellular therapy to single cell

injections of either CPCs or MSCs alone, comparable to CPC + MSC treatment but with the advantage of increased survival and persistence relative to either parental cell line.

BMCs, the most common stem cell for cardiac therapy, apparently undergo engraftment through a combination of cell fusion and to a lesser degree by direct transdifferentiation events[124]. Membrane fusion is dependent upon signaling mechanisms involving paxillin induced focal adhesions and recycling of integrins as demonstrated between macrophages and myoblasts[125]. In the heart, cell fusion is increased between exogenous stem cells and apoptotic cardiomyocytes similar to enhanced myoblast fusion in the presence of phosphatidylserine presenting cells[110, 126]. Altered DNA content has been raised as an issue following fusion events as genomic instability leads to cellular aging[127]. However, CCs display normal stem cell function and continue to expand without undergoing replicative senescence after long-term culture (Figure 2.1). Somatic cells exhibiting chromosomal mosaicism such as through the loss or deletions of chromosomes do not significantly affect stem cell properties or cell fate[128]. As a result, CCs do not appear transformed but rather retain properties of CPCs and MSCs to support enhanced myocardial repair.

Increased basal expression of cardiomyogenic factors was observed in CCs (Figure 2.3). Pre-committed cells, but not fully mature stem cell derived cardiomyocytes improve exogenous cell coupling and formation of gap junction proteins[129]. CCs display coordinated phenotypic properties of commitment and increased paracrine abilities to promote cardiomyocyte health much like the MSC

parent and CPC + MSC parents combined (Figure 2.4). Furthermore, CC2 in particular had enhanced IL-6 production (Figure 2.5) indicating potential to mediate anti-inflammatory functions after acute MI compared to MSC alone[122]. Factor(s) that promote growth of cardiomyocytes and stabilization or the creation of microvasculature (Figure 2.9 and 2.10) remain to be established in our model of mouse CCs, but is certainly a subject of future investigations. Gene dosage effects as well as modifying the ratio of cell numbers before cell fusion leads to unique phenotypic properties such as proliferation and inhibition of senescence[60, 61, 130]. Embryonic stem cell (ESC) fusion with somatic cells facilitates reprogramming using equal cellular ratios indicating that ESCs are the more dominant cell type[131]. In this report, the CPC parent phenotype dominates in the fused progeny and most likely mediates early cardiomyogenic factors in CCs, whereas paracrine mediated effects from the MSC parent is secondary. For future studies, selecting the optimal cells and gene dosage for fusion will allow us to more effectively design hybrids for stronger traits towards commitment or paracrine effects.

Therapeutic delivery of MSCs improves cardiac function and structure mainly through paracrine mediated effects. Secretion of factors such as SDF-1 and IGF-1 support endogenous recruitment of c-kit$^+$ progenitor cells and further facilitates cardiomyocyte cell cycle entry and survival[132-134]. Immunomodulatory functions of MSCs to inhibit excess scar formation is an attractive therapy for several disease states[135]. In this study, we did not see any significant improvements in AWT or EF over vehicle treated controls using the MSC

parental cells alone (Figure 2.6). The MSC treatment was unable to prevent increases in scar size or decreases in cardiac function up to 18 weeks similar to the deteriorating PBS treated hearts. Although, MSC addition did maintain size and survival of the responding cardiomyocytes, these beneficial effects were not recapitulated *in vivo* after MSC transfer (Figure 2.4 and 2.6). Apoptosis and slow proliferation rate are likely contributing factors to the disappearance of MSCs at later time points (Figure 2.1 and 2.6). Instead, MSC and PBS treated hearts sustained increases in c-kit^{+} cells, which are most likely increased through chronic inflammation and recruitment of hematopoietic derived c-kit^{+} mast cells (Figure 2.8).

The optimal cell number chosen for therapy is a critical aspect to promote structural and functional recovery after MI. Delivery of human CPC + MSC in a pig model of ischemia resulted in positive remodeling and engraftment using 200-fold more MSCs relative to CPCs[108]. For our study, we placed CPCs to MSCs at a one-to-one ratio as the appropriate control compared to our CCs. The engraftment efficiency of MSCs could have been greatly limited from the beginning of the experiment due to reduced MSC cell numbers (Figure 2.8). Benefits of co-culture of CPCs with MSCs are consistent with previous findings as MSC co-incubation with CPCs at equal ratios increased basal differentiation markers such as *sm22*, which was not observed in CCs (Figure 2.3). Furthermore, during co-culture with NRCMs, CPC + MSC groups exhibited increased cardiomyogenic markers *sm22*, *pecam* and *cTNT* (Figure 2.5). It remains unclear if differentiation resulted from CPCs alone in culture with MSCs,

although significant cell death of MSCs alone was observed when co-cultured with NRCMs for seven days. The comparatively modest therapeutic benefit of unmodified CPCs has been previously shown from our laboratory[48, 49]. Clearly, pinpointing the mechanistic contribution of MSCs to support CPCs in our CPC + MSC treated hearts is an important unanswered question to be resolved in future investigations. Although engraftment efficiency of CPCs co-injected with MSCs was not significantly improved relative to CPC hearts alone, function was improved in CPC + MSC hearts at a much earlier time point. We can hypothesize that MSCs in the acute stages of damage (<4weeks) facilitated protective endogenous cell reprogramming without long-term persistence, which was not sufficient to impact on exogenous CPC proliferation and/or engraftment, consistent with reports from other groups[107, 136].

From the numerous cell types touted to be efficacious for cardiac clinical therapy, CPCs and MSCs are particularly promising because of established protocols for cell isolation and expansion in clinical settings[10, 32]. Although MSCs show much lower rates of persistence in the damaged heart than CPCs, cell therapeutic practices could benefit from investigation of how to enhance immunomodulatory effects of MSCs[106]. Currently, “Off-the-shelf” allogeneic cellular options include cardiosphere derived cells and MSCs that may exert beneficial effects after MI but suffer from poor persistence following delivery[32, 137]. In comparison, ESCs and induced pluripotent stem cells exhibit extended proliferation and are less prone to immuno rejection and/or cell senescence after transplantation[138]. However, ESCs have reduced capacity for integrative

cardiomyogenesis as demonstrated by arrhythmogenic events in large animal models[139]. Our cell fusion approach aims to capitalize on adult stem cells that have validated cardiac therapeutic effects in order to create a superior composite hybrid with anti-inflammatory functions. Additionally, fusion of aged stem cells with more youthful cells could confer cell rejuvenation and reverse signs of cellular aging[60, 140]. In the era of human cord blood banking, the isolation of immunoprivileged stromal cells from the same patient can be easily fused with stem cells harboring tissue specific regenerative capacity, resulting in a novel cell type that is resistant to rejection in addition to having desired cellular effects such as proliferation and direct tissue commitment[141]. From a translational perspective, cell fusion is an adaptable genetic engineering strategy that qualitatively enhances adult stem cell properties such as persistence, anti-inflammatory and growth factor secretion and direct cardiomyogenesis to sustain long-term cardiac repair.

SUMMARY POINTS

- Cell fusion of CPCs with MSCs creates unique hybrids that have similar proliferative rates and survival capabilities compared to the parental cell lines.
- Hybrids or CardioChimeras have increased DNA content after fusion but do not exhibit signs of genetic instability and/or senescence.
- CardioChimeras have increased expression of cardiomyogenic markers during normal growth conditions.
- CardioChimeras co-cultured with cardiomyocytes improve myocyte growth, survival and expression of SDF-1 a beneficial paracrine factor.
- Intramyocardial transplantation of CardioChimeras improves myocardial structure and reduces infarct size at 12 weeks.
- CardioChimeras and dual transplantation of CPCs and MSCs increase cardiac function as measured by ejection fraction.
- CPC injection improves ejection fraction 18 weeks after MI.
- CardioChimeras promoted an increase in capillary density and normalized cardiomyocyte size in the infarct area 12 weeks after damage.
- CardioChimeras have increased engraftment in the left ventricle relative to groups treated with parental cells individually or combined.
- CardioChimeras combine the beneficial and cardioprotective properties of distinct stem cells into a single cell type for effective cardiac repair.

FIGURES

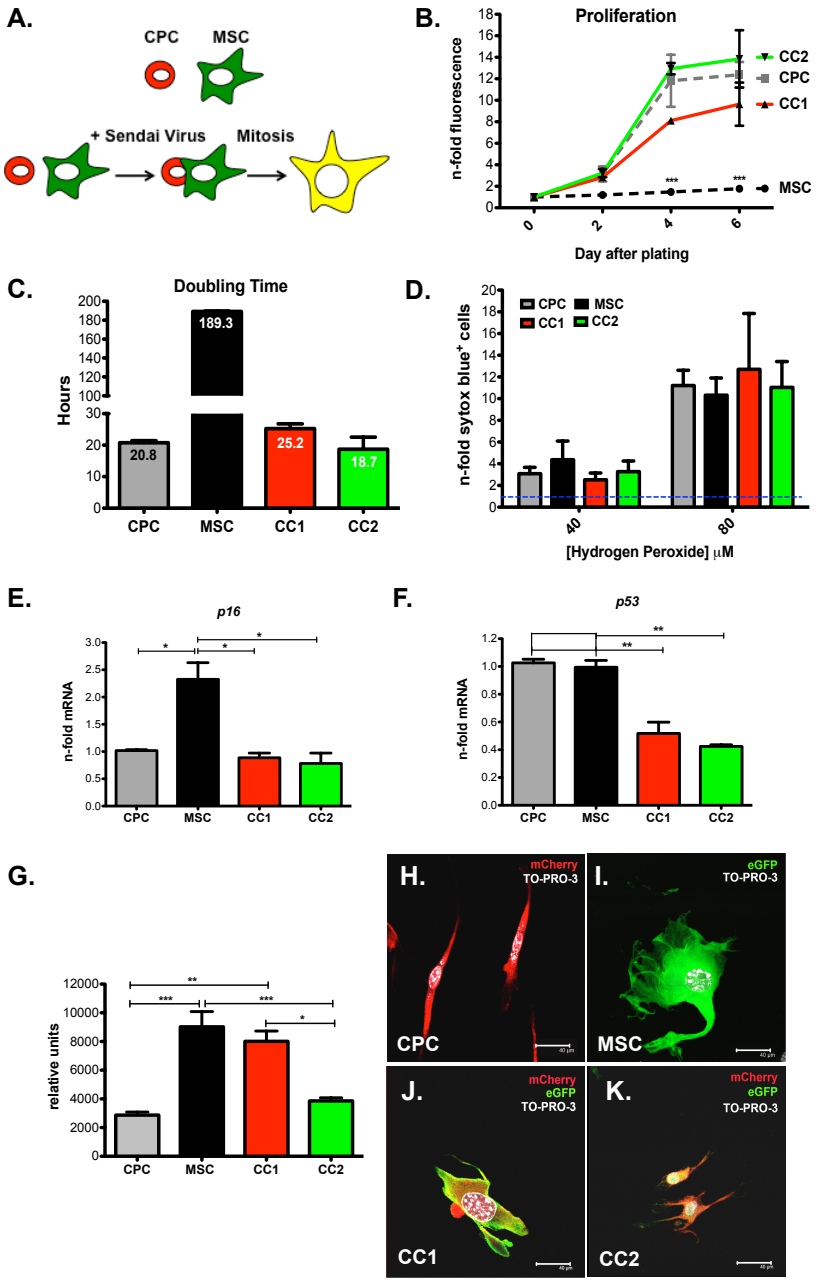

Figure 2.1: Phenotypic characterization of CardioChimeras.
(A) Schematic representation of the creation of CardioChimeras. (B) Proliferation of CCs, CPCs and MSCs represented as a fold change relative to day of plating. (C) Cell doubling time in hours. (D) Cell death assay of CCs and parents cells after treatment with 40µM or 80µM hydrogen peroxide represented, as a fold change relative to cells not treated with hydrogen peroxide. (E) p16 and (F) p53 gene expression normalized to ribosomal 18s and represented as a fold change relative to CPCs. (G) Surface area of (H) CPC, (I) MSC, (J) CC1 or (K) CC2. * $p<0.05$, ** $p<0.01$, *** $p<0.001$. Scale bar is 40µm.

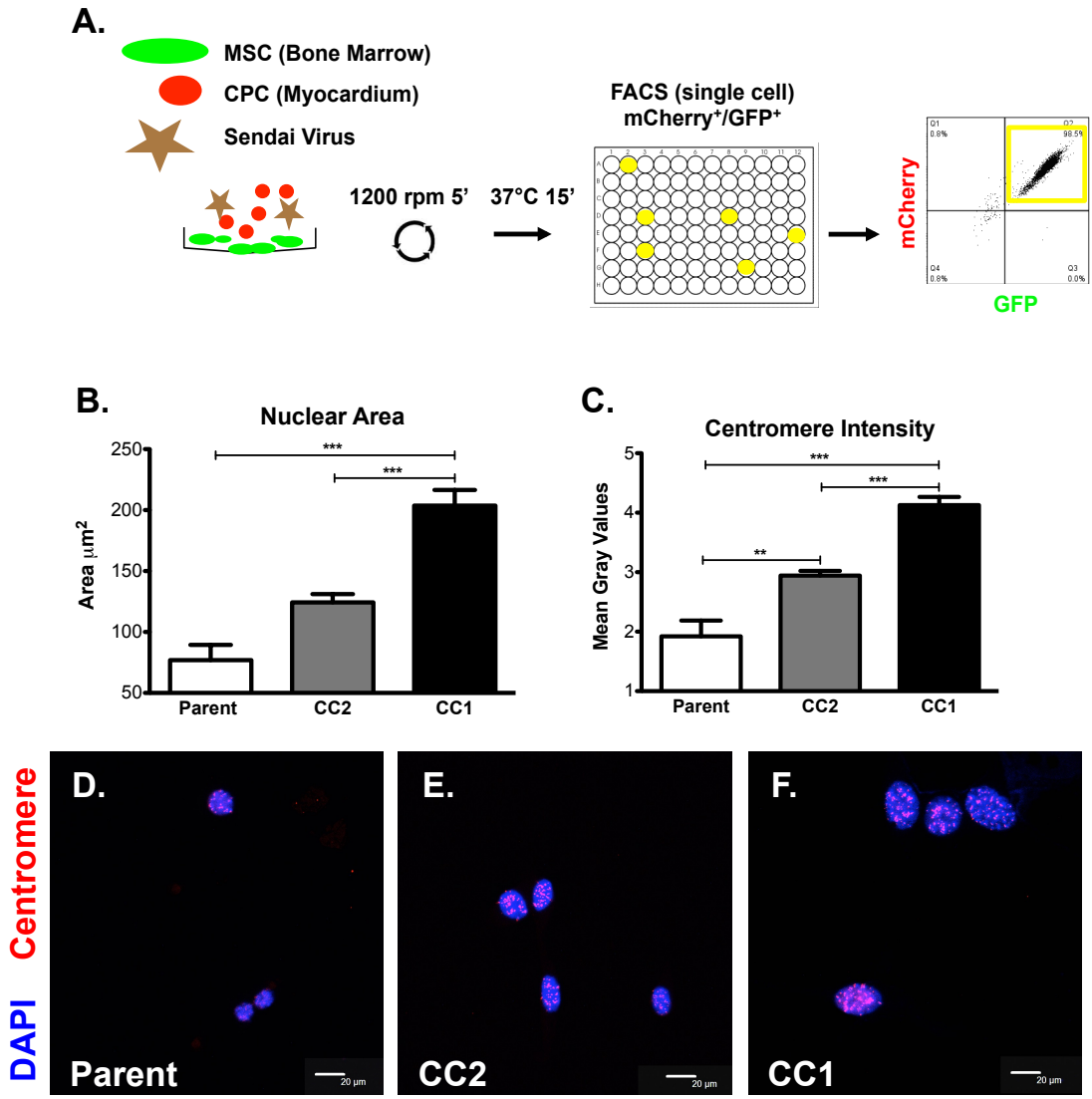

Figure 2.2: CardioChimeras have increased nuclear size and DNA content.
(A) Detailed protocol for the fusion and clonal expansion of CardioChimeras. Briefly, mouse CPCs were co-incubated with mouse MSCs at a 1:1 ratio with addition of Sendai virus. Cells were centrifuged to force cell contact and single cell sorted based on fluorescent expression of mcherry and GFP. Clones were confirmed by flow cytometric analysis. (B) Measurement of nuclear size and (C) Centromere intensity in parent MSCs, CC2 and CC1. (D) Representative images of nuclei in parent (E) CC2 and (F) CC1. Blue represents DAPI staining of DNA content and red represents centromere probe binding. Scale bar is 20µm. * $p<0.05$, ** $p<0.01$, *** $p<0.001$.

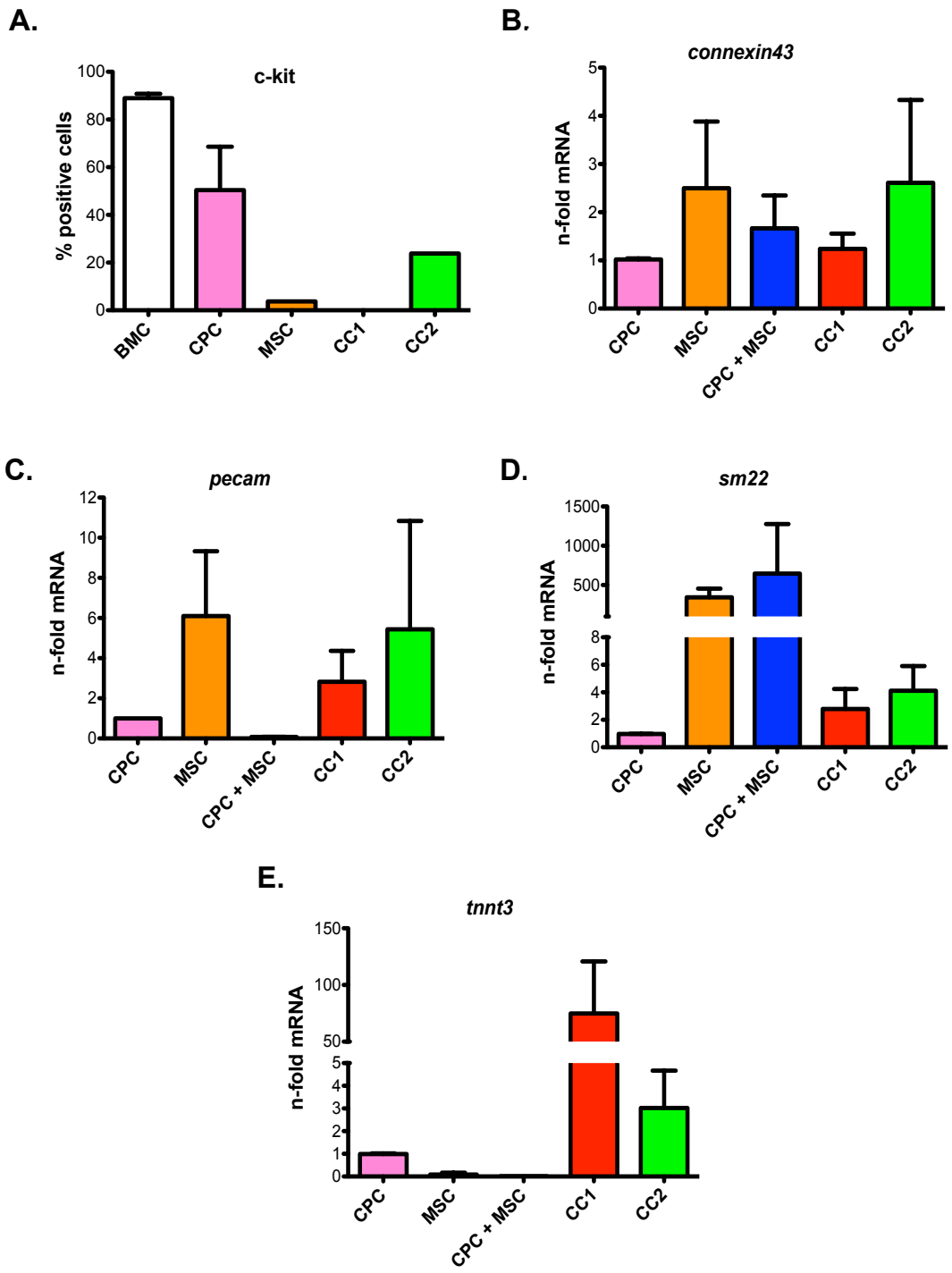

Figure 2.3: CardioChimeras have increased expression of cardiomyogenic commitment markers at basal levels.
(A) C-kit protein expression as analyzed by flow cytometry. C-kit purified bone marrow cells were utilized as a positive control. (B) *connexin 43*, (C) *pecam* (*cd31*), (D) *sm22* and (E) *cTNT* (*tnnt3*) gene expression was analyzed by qRT-PCR in CPC, MSC, CPC + MSC, CC1 and CC2 after normalization to ribosomal 18s. Values are represented as a fold change relative to CPCs.

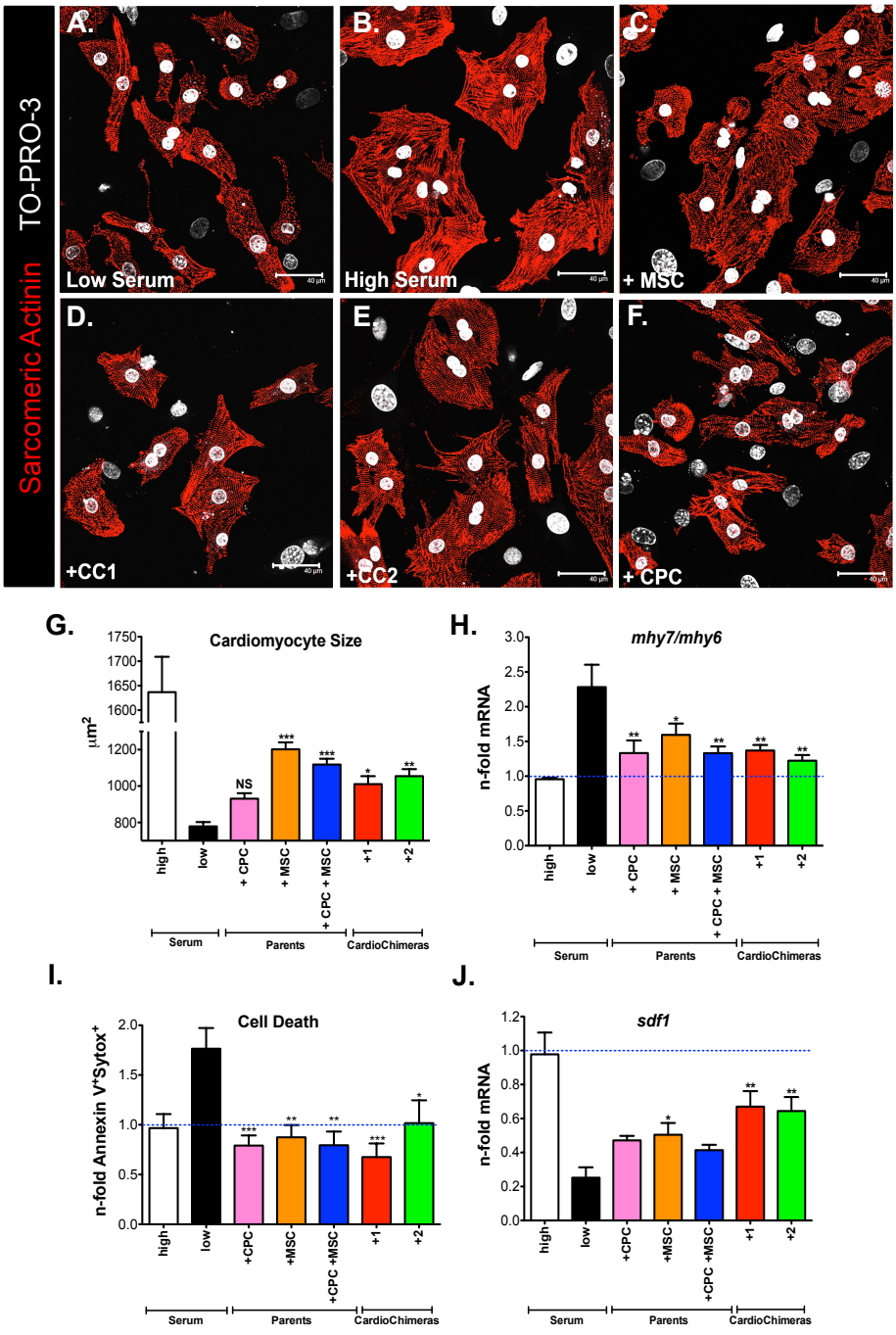

Figure 2.4: CardioChimeras promote cell growth after co-culture with cardiomyocytes.
(A) NRCMs in low serum. (B) NRCMS in high serum. (C) NRCMs in low serum and the addition of MSCs, (D) CC1, (E) CC2 or (F) CPC for 24 hours. Cardiomyocytes were visualized by staining with sarcomeric actinin. TO-PRO-3 iodide was used to visualize nuclei. (G) Quantitation of cardiomyocyte size. (H) Gene expression of *mhy7* over *mhy6* represented as fold change relative to high serum. (I) Cardiomyocyte cell death. Values are represented as fold change of Annexin V^+ and Sytox $Blue^+$ cells relative to high serum. (J) *sdf-1* gene expression in cardiomyocytes alone after the addition of stem cells. * $p<0.05$, ** $p<0.01$, *** $p<0.001$. Scale bar is 40µm.

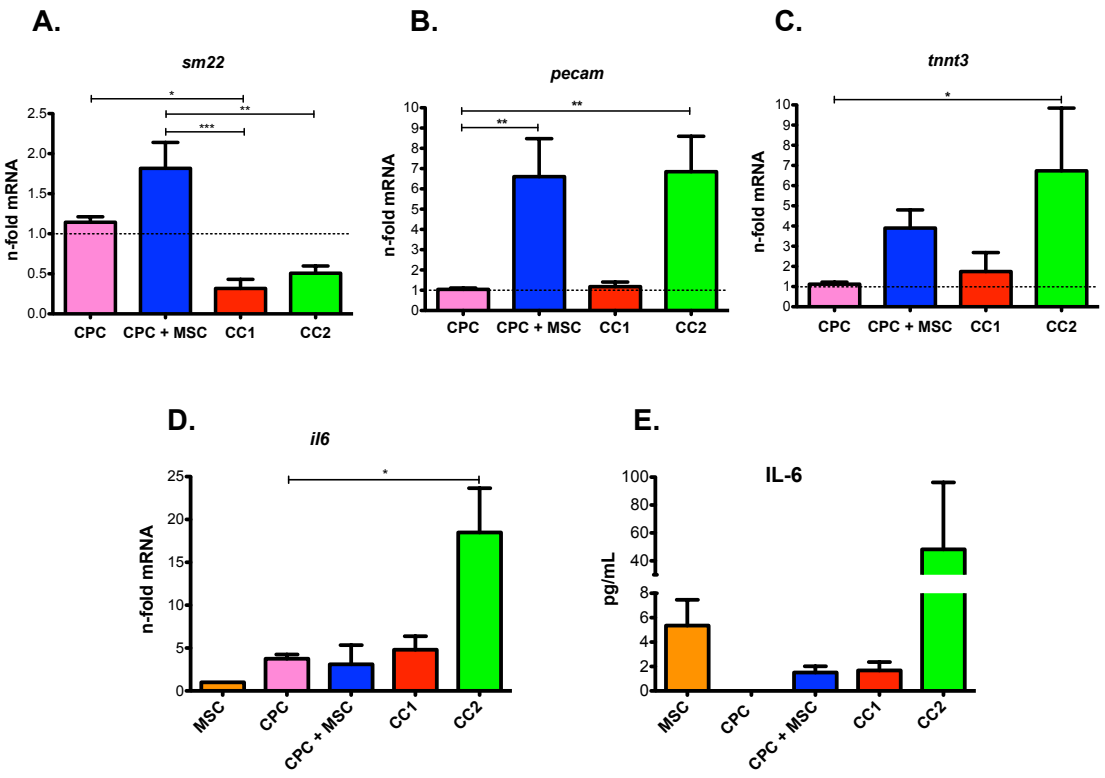

Figure 2.5: CardioChimeras have increased commitment and paracrine gene expression after co-culture with cardiomyocytes.
(A-C) Gene expression in stem cells after 7-day co-culture with NRCMs. (A) sm22 (B) pecam and (C) cTNT. (D) il6 gene expression was analyzed in stem cells after 24-hour co-culture with NRCMs. (E) IL-6 protein expression was confirmed by ELISA.(G-J) Statistical values were determined by one-way ANOVA compared to low serum controls. * $p<0.05$, ** $p<0.01$, *** $p<0.001$.

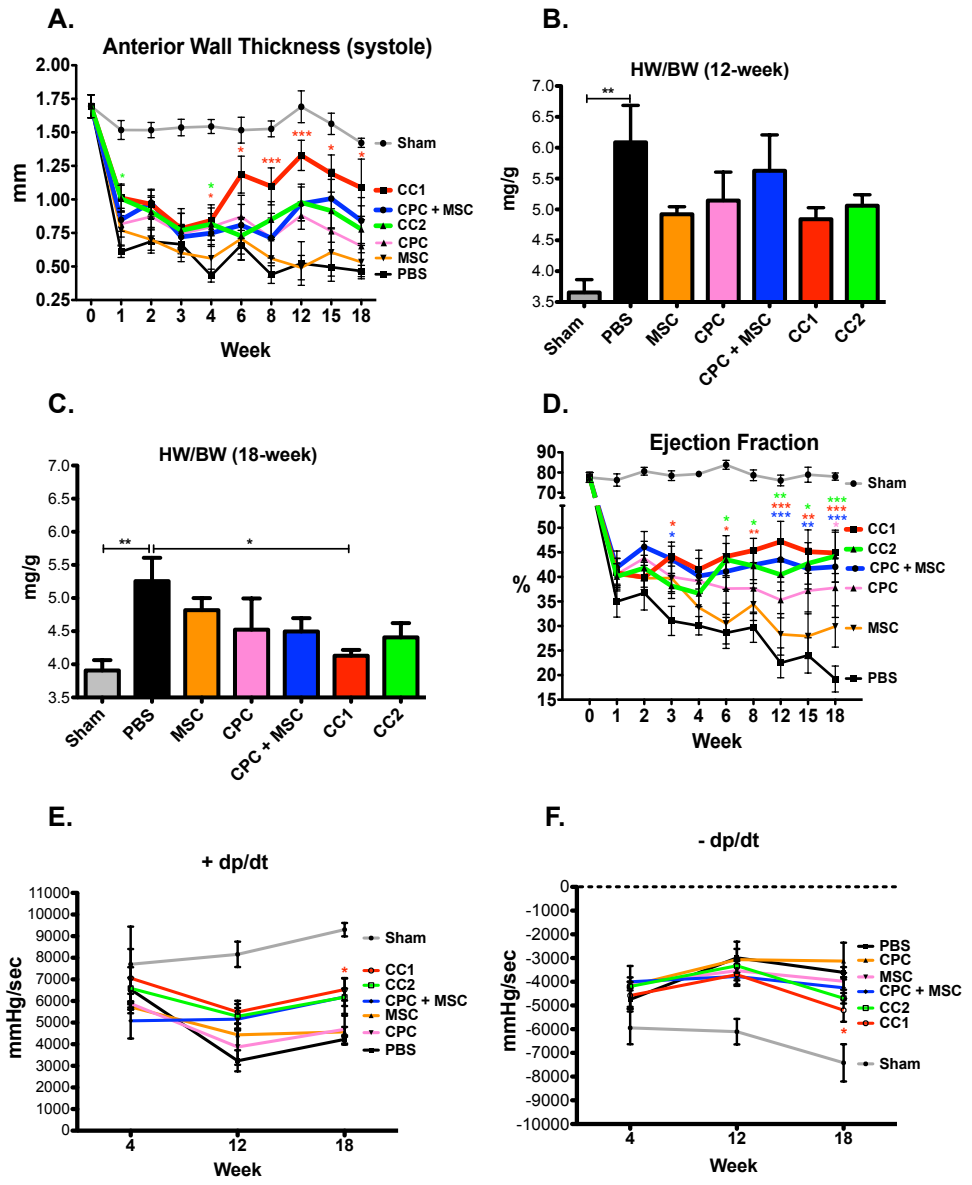

Figure 2.6: CardioChimeras improve left ventricular wall structure and cardiac function after myocardial injury.
(A) Longitudinal assessment of anterior wall thickness during systole (mm) over 18 weeks. (B) Heart weight to body weight ratio (mg/g) at 12 weeks and (C) 18 weeks post treatment and infarction. Sample sizes of at 3-5 mice per group. (D) Longitudinal assessment of ejection fraction (%). (E) Positive and (F) Negative developed pressure over time represented as mmHg/sec at 4, 12 and 18 weeks. (G) Change in infarct size between 4 and 12 weeks time points. P values were determined by one-way ANOVA compared to PBS treated controls. (H-N) Masson's Trichrome staining and representative images of infarct size and fibrosis in (H) Sham, (I) PBS, (J) MSC, (K) CPC, (L) CPC + MSC, (M) CC1 and (N) CC2. Sample sizes are specified in Table S1. All statistical values were determined by two-way ANOVA compared to PBS treated hearts. * $p<0.05$, ** $p<0.01$, *** $p<0.001$. Colors of asterisk(s) correspond to heart group. Scale bar is 250μm.

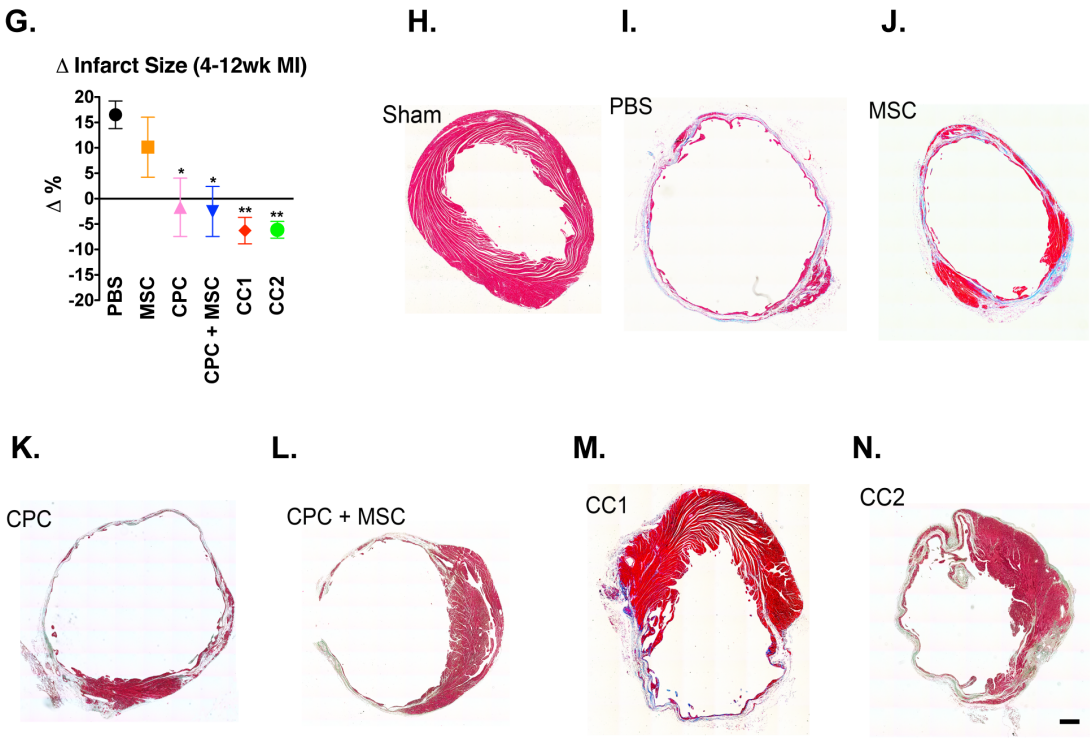

Figure 2.6: CardioChimeras improve left ventricular wall structure and cardiac function after myocardial injury, Continued.
(G) Change in infarct size between 4 and 12 weeks time points. P values were determined by one-way ANOVA compared to PBS treated controls. (H-N) Masson's Trichrome staining and representative images of infarct size and fibrosis in (H) Sham, (I) PBS, (J) MSC, (K) CPC, (L) CPC + MSC, (M) CC1 and (N) CC2. Sample sizes are specified in Table S1. All statistical values were determined by two-way ANOVA compared to PBS treated hearts. * $p<0.05$, ** $p<0.01$, *** $p<0.001$. Colors of asterisk(s) correspond to heart group. Scale bar is 250μm.

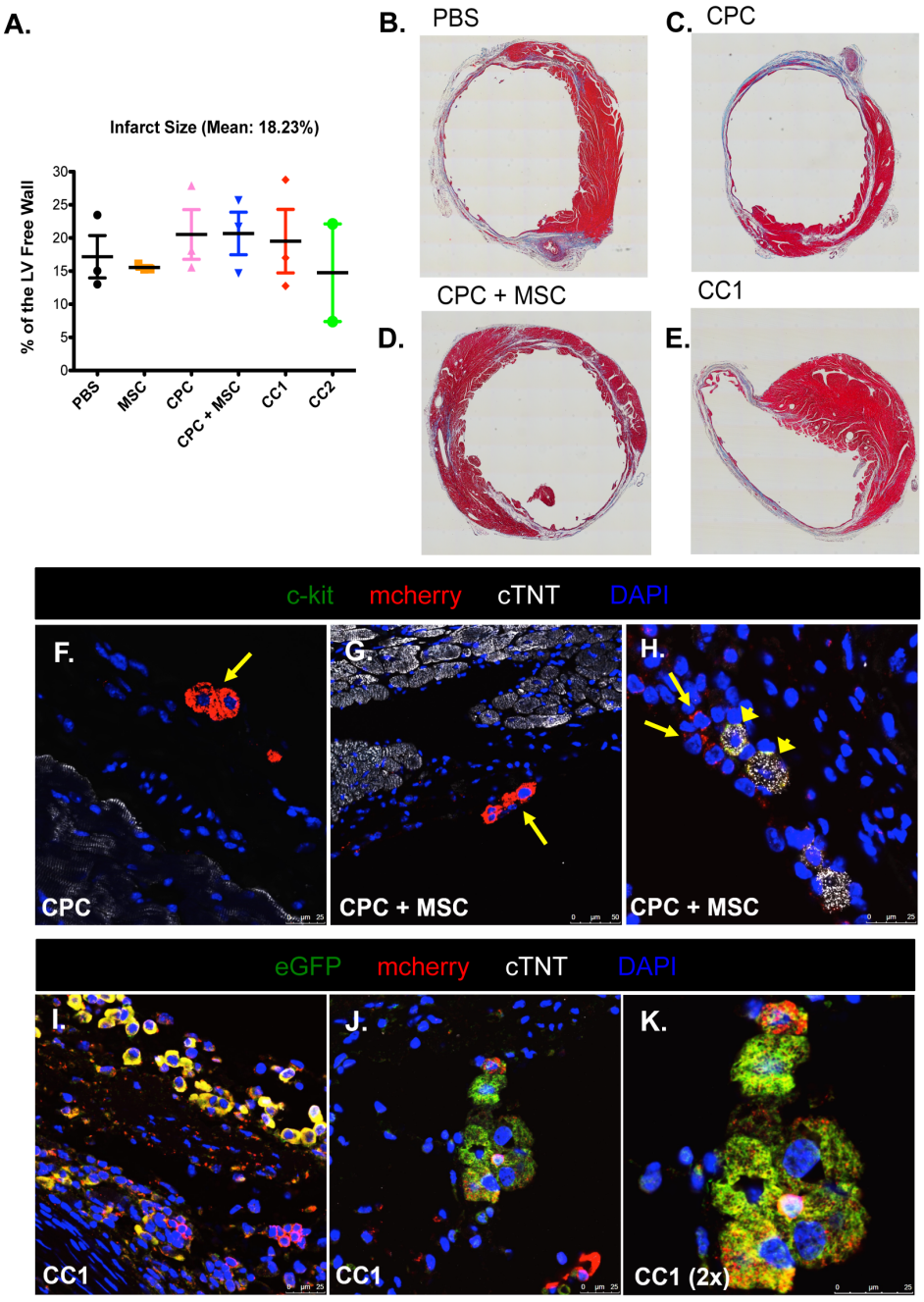

Figure 2.7: Cellular engraftment of CardioChimeras 4 weeks after damage.
(A) Infarct size was not significantly different between infarcted groups (mean=18.23%). N=2-4 per group. (B-E) Masson's Trichrome staining and representative images of (B) PBS, (C) CPC, (D) CPC + MSC and (E) CC1 hearts to visualize scar size and fibrosis. Scale bar is 250μm.(F) Mcherry^{+} CPCs detected in the infarct area in CPC treated hearts. (G) Mcherry^{+} CPCs detected in the infarct area in CPC + MSC treated hearts. (H) Mcherry^{+} CPCs adjacent to c-kit^{+} /cTNT^{+} cardiomyocytes in CPC + MSC treated hearts. (I) and (J) CC1 expressing eGFP and mcherry in the infarcted area. (K) 2x zoom of CC1. Scale bar is 25μm for confocal images. Scale bar is 50μm in (G).

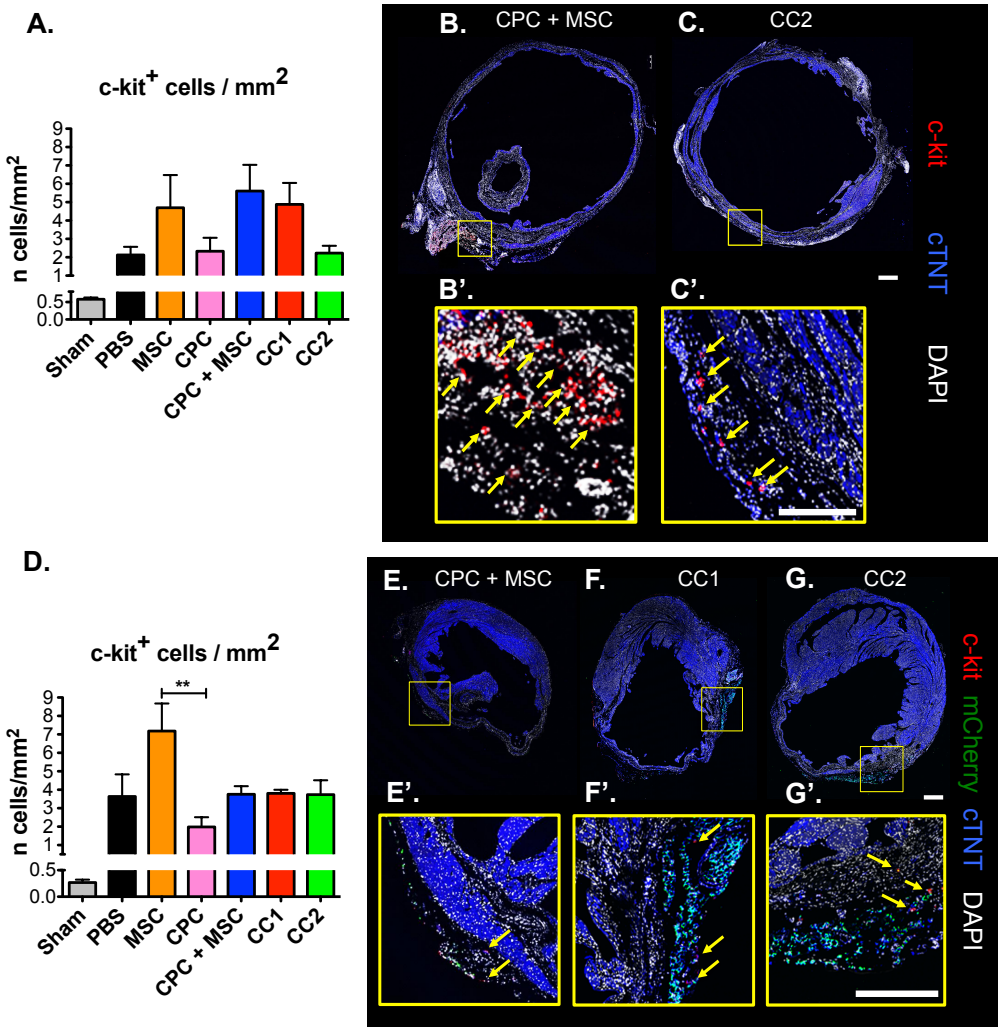

Figure 2.8: CardioChimeras have increased engraftment, expression of cardiomyogenic markers and support the increased presence of c-kit positive cells in the myocardium 12 weeks after damage.

(A) Number of c-kit$^+$ cells represented as number of cells over the area of left ventricular free wall (mm^2) in 4-week damaged hearts. Sample size of 3 mice per group. Representative whole heart scans of (B) CPC + MSC and (C) CC2 treated hearts to visualize c-kit$^+$ cells (red). Scale bar is 100μm. (B') and (C') C-kit$^+$ cells are identified by yellow arrows. Scale bar is 50μm. (D) Number of c-kit$^+$ cells in 12-week damaged hearts. Sample size of 3 mice per group. Representative whole heart scans of (E) CPC + MSC, (F) CC1 and (G) CC2 treated hearts to visualize exogenous mcherry$^+$ cells (green) and c-kit$^+$ cells (red). Scale bar is 100μm. (E'), (F') and (G') C-kit$^+$ cells are identified by yellow arrows. Scale bar is 100μm.

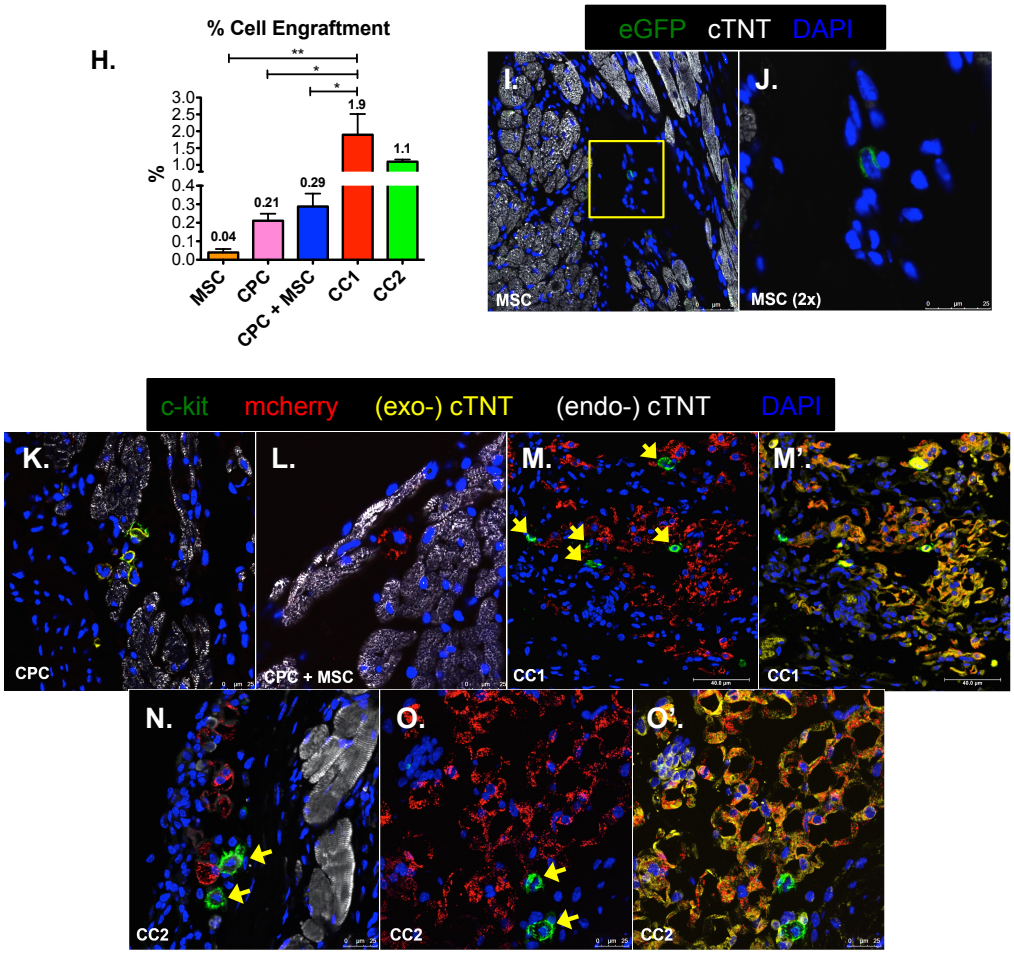

Figure 2.8: CardioChimeras have increased engraftment, expression of cardiomyogenic markers and support the increased presence of c-kit positive cells in the myocardium 12 weeks after damage, Continued.

(H) Cell engraftment efficiency (%). Sample size of 3 mice per group. (I) MSC detected by GFP protein staining at 12 weeks. (J) 2x zoom of MSC in the border zone area. (K) C-kit^{+} /mcherry^{+} CPCs in the border zone area. (L) Mcherry^{+} CPC in CPC + MSC treated heart. (M) Mcherry^{+} CC1 visualized in the infarcted area surrounded by c-kit^{+} cells (green). (M') Overlay of cTNT (exogenous-cTNT, yellow) in CC1 mcherry labeled cells. (N) Mcherry^{+} CC2 visualized in the infarcted area surrounded by c-kit^{+} cells (green). (O) Mcherry^{+} CC2 (red) visualized in the infarcted area surrounded by c-kit^{+} cells (green). (O) Overlay of cTNT (exogenous-cTNT, yellow) in CC2 mcherry labeled cells. Endogenous-cTNT (white) labels existing cardiomyocytes. * $p<0.05$, ** $p<0.01$, *** $p<0.001$.

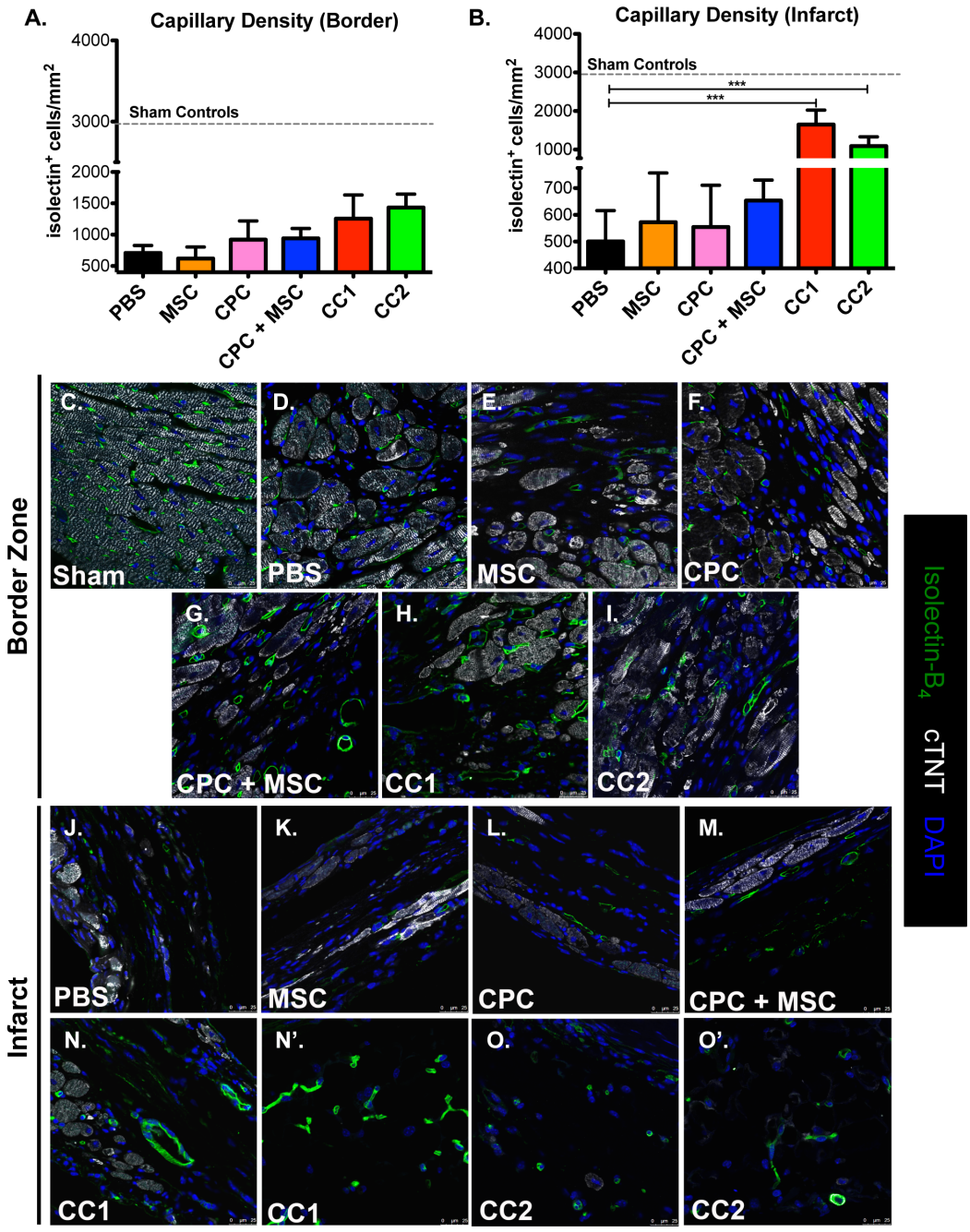

Figure 2.9: CardioChimeras increase capillary density in the infarct area.
(A) Capillary density in the border zone and (B) Infarcted heart regions. Sample sizes are 3-4 mice per group. Sham controls (dashed line) are represented as control for baseline density of isolectin$^+$ structures per mm^2. (C-I) Representative border zone images to visualize isolectin$^+$ structures. (J-O) Representative infarct zone images to visualize and quantitate isolectin$^+$ structures. Green= Isolectin B_4, White=cardiac troponin T and Blue= DAPI to stain for nuclei. Scale bar is 25μm. * $p<0.05$, ** $p<0.01$, *** $p<0.001$.

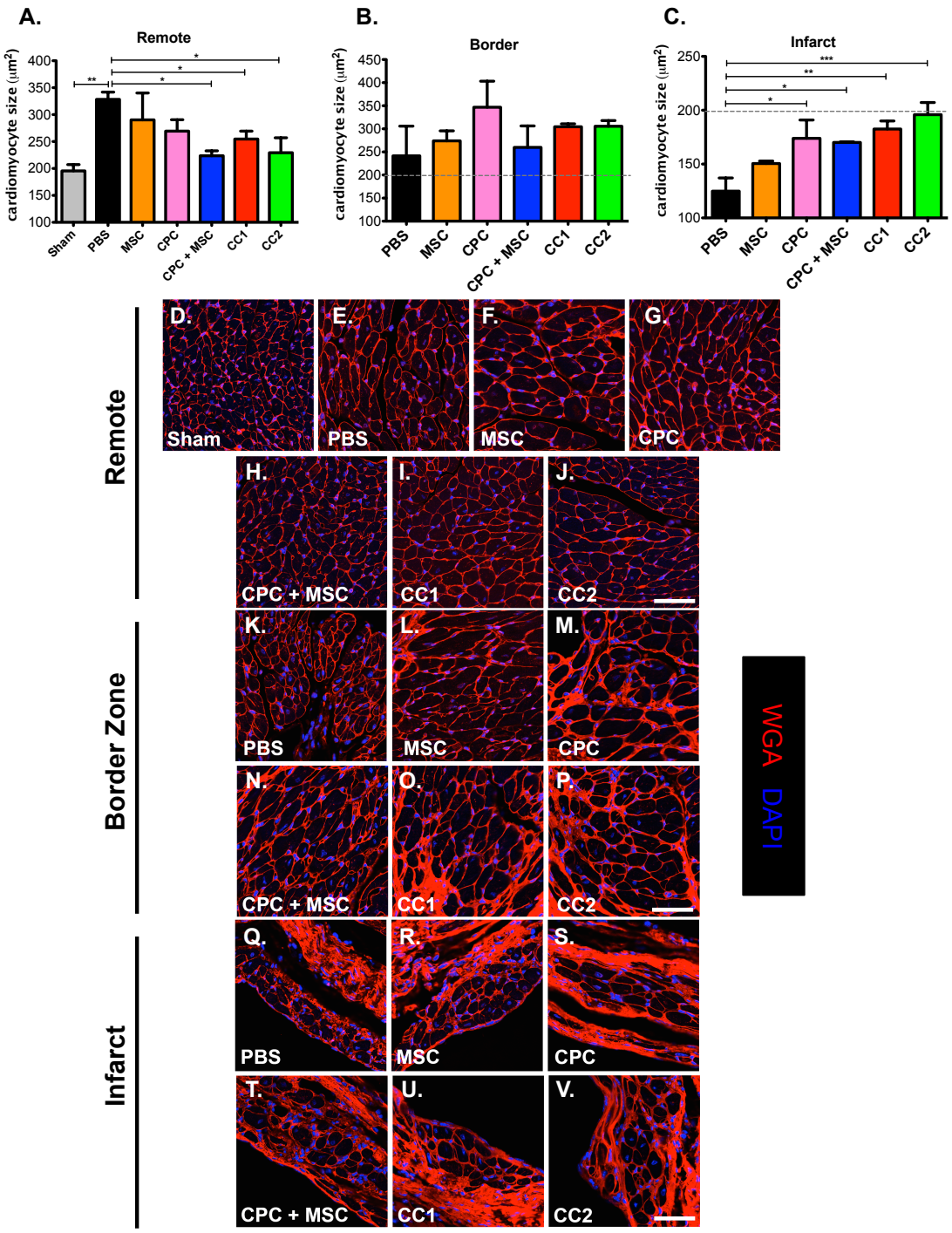

Figure 2.10: CPC, MSC and CardioChimera treatment normalizes cardiomyocyte size in the remote and infarcted regions.
(A) Mean cardiomyocyte size in the remote, (B) Border zone and (C) Infarct regions. Sample size is 3-4 mice per group. (D-J) Representative images of remote area cardiomyocyte size. (K-P) Representative images of border zone area cardiomyocytes. (Q-V) Representative images of infarct area cardiomyocytes. Red=Wheat germ agglutinin, White=cardiac troponin T and Blue=DAPI to stain for nuclei. Scale bar is 25μm. * $p<0.05$, ** $p<0.01$, *** $p<0.001$.

Table 2.1: Heart rate and echocardiographic data.

Echocardiographic data represented as mean ± SEM. Heart rate, anterior wall thickness, posterior wall thickness, left ventricular volume, ejection fraction and fractional shortening were measured at specified times after MI. (N) indicates the number of mice used in each group at the given time point.

HEART RATE (bpm)

	SHAM			PBS			CPC			MSC			CPC + MSC			CC1			CC2		
WEEK	MEAN	SEM	N	MEAN	SEM	N	MEAN	SEM	N	MEAN	SEM	N	MEAN	SEM	N	MEAN	SEM	N	MEAN	SEM	N
1	442.01	9.59	14.00	437.76	31.15	16.00	470.12	14.68	10.00	430.31	22.14	9.00	482.20	17.02	13.00	447.60	14.93	12.00	471.75	13.97	16.00
2	481.89	21.14	15.00	388.82	35.11	15.00	432.29	21.09	10.00	456.65	16.74	13.00	451.13	13.77	16.00	435.68	12.17	12.00	455.07	12.08	15.00
3	463.60	20.09	15.00	418.29	30.32	15.00	458.29	13.70	10.00	481.08	8.04	13.00	474.35	17.10	15.00	428.87	18.10	11.00	437.59	10.37	14.00
4	410.89	15.05	15.00	415.45	31.30	15.00	468.65	14.55	12.00	448.78	11.57	13.00	448.64	10.43	16.00	454.86	10.32	12.00	453.41	14.50	16.00
6	450.04	14.43	13.00	408.62	37.45	12.00	452.84	30.45	9.00	460.82	21.66	10.00	432.77	16.38	11.00	456.33	12.18	10.00	442.09	8.87	12.00
8	462.46	16.23	13.00	418.66	33.42	13.00	448.29	10.66	8.00	437.37	16.02	10.00	431.76	15.49	11.00	443.27	16.91	9.00	446.78	12.22	13.00
12	447.88	10.27	10.00	402.83	62.11	7.00	418.22	18.53	9.00	398.17	18.97	8.00	399.69	21.15	9.00	450.84	13.17	10.00	444.61	16.72	13.00
15	415.57	6.42	7.00	390.88	65.85	6.00	431.98	40.89	6.00	412.93	33.16	6.00	451.78	25.30	6.00	465.01	14.56	6.00	448.01	14.28	8.00
18	459.99	20.90	6.00	375.44	75.95	5.00	411.75	23.07	6.00	427.62	23.90	6.00	492.13	9.90	7.00	436.17	18.29	6.00	454.12	21.22	8.00

ANTERIOR WALL THICKNESS; SYSTOLE (mm)

	SHAM		PBS		CPC		MSC		CPC + MSC		CC1		CC2	
WEEK	MEAN	SEM	MEAN	SEM	MEAN	SEM	MEAN	SEM	MEAN	SEM	MEAN	SEM	MEAN	SEM
1	1.52	0.07	0.61	0.04	0.82	0.10	0.77	0.11	0.85	0.09	1.01	0.10	1.01	0.10
2	1.52	0.06	0.69	0.09	0.87	0.14	0.70	0.08	0.98	0.10	0.96	0.10	0.91	0.12
3	1.54	0.06	0.67	0.10	0.75	0.15	0.60	0.06	0.72	0.09	0.78	0.15	0.77	0.13
4	1.54	0.05	0.43	0.05	0.80	0.10	0.56	0.10	0.75	0.10	0.84	0.12	0.82	0.12
6	1.52	0.10	0.60	0.10	0.87	0.16	0.71	0.16	0.81	0.15	1.19	0.14	0.73	0.14
8	1.53	0.06	0.44	0.06	0.71	0.18	0.56	0.14	0.71	0.15	1.10	0.14	0.85	0.13
12	1.69	0.12	0.52	0.16	1.04	0.18	0.49	0.09	0.97	0.13	1.33	0.11	0.98	0.14
15	1.56	0.08	0.57	0.11	0.98	0.21	0.88	0.21	1.23	0.21	1.07	0.17	0.86	0.21
18	1.42	0.03	0.47	0.04	0.65	0.20	0.57	0.17	0.84	0.17	1.09	0.21	0.78	0.18

ANTERIOR WALL THICKNESS; DIASTOLE (mm)

	SHAM		PBS		CPC		MSC		CPC + MSC		CC1		CC2	
WEEK	MEAN	SEM	MEAN	SEM	MEAN	SEM	MEAN	SEM	MEAN	SEM	MEAN	SEM	MEAN	SEM
1	0.99	0.05	0.46	0.03	0.60	0.07	0.58	0.07	0.65	0.07	0.73	0.08	0.72	0.08
2	1.02	0.05	0.54	0.06	0.62	0.10	0.54	0.07	0.67	0.06	0.74	0.10	0.72	0.10
3	0.97	0.05	0.55	0.08	0.49	0.09	0.45	0.04	0.54	0.07	0.63	0.10	0.59	0.09
4	0.96	0.05	0.30	0.04	0.54	0.08	0.41	0.07	0.56	0.09	0.61	0.08	0.56	0.08
6	0.98	0.05	0.45	0.09	0.61	0.13	0.54	0.13	0.58	0.11	0.83	0.11	0.56	0.10
8	1.01	0.05	0.33	0.04	0.55	0.14	0.40	0.12	0.58	0.11	0.82	0.12	0.66	0.09
12	1.06	0.05	0.40	0.14	0.73	0.11	0.38	0.09	0.70	0.10	1.02	0.11	0.84	0.11
15	1.02	0.08	0.46	0.10	0.66	0.15	0.57	0.14	0.92	0.15	0.79	0.13	0.65	0.16
18	0.99	0.03	0.31	0.05	0.42	0.13	0.46	0.13	0.57	0.11	0.78	0.17	0.60	0.10

POSTERIOR WALL THICKNESS; SYSTOLE (uL)

	SHAM		PBS		CPC		MSC		CPC + MSC		CC1		CC2	
WEEK	MEAN	SEM	MEAN	SEM	MEAN	SEM	MEAN	SEM	MEAN	SEM	MEAN	SEM	MEAN	SEM
1	1.40	0.08	0.70	0.08	0.64	0.07	0.73	0.07	0.71	0.07	0.65	0.04	0.75	0.07
2	1.44	0.06	0.62	0.06	0.79	0.13	0.71	0.07	0.72	0.05	0.58	0.08	0.79	0.10
3	1.55	0.07	0.63	0.06	0.64	0.10	0.61	0.05	0.72	0.06	0.57	0.07	0.62	0.09
4	1.34	0.05	0.61	0.09	0.52	0.08	0.72	0.10	0.53	0.08	0.64	0.06	0.74	0.10
6	1.59	0.09	0.49	0.06	0.66	0.11	0.50	0.07	0.54	0.09	0.56	0.07	0.68	0.11
8	1.43	0.05	0.50	0.06	0.61	0.07	0.62	0.07	0.65	0.12	0.58	0.09	0.70	0.11
12	1.52	0.07	0.49	0.06	0.45	0.06	0.40	0.04	0.54	0.08	0.61	0.08	0.75	0.11
15	1.45	0.08	0.45	0.08	0.46	0.05	0.68	0.14	0.56	0.08	0.66	0.14	0.79	0.19
18	1.38	0.12	0.50	0.09	0.51	0.07	0.50	0.13	0.62	0.08	0.59	0.10	0.87	0.13

POSTERIOR WALL THICKNESS; DIASTOLE (mm)

	SHAM		PBS		CPC		MSC		CPC + MSC		CC1		CC2	
WEEK	MEAN	SEM	MEAN	SEM	MEAN	SEM	MEAN	SEM	MEAN	SEM	MEAN	SEM	MEAN	SEM
1	0.99	0.05	0.68	0.06	0.57	0.06	0.65	0.08	0.67	0.05	0.62	0.05	0.70	0.06
2	1.00	0.04	0.56	0.06	0.67	0.10	0.69	0.05	0.70	0.04	0.58	0.06	0.66	0.08
3	1.09	0.06	0.56	0.05	0.62	0.08	0.61	0.06	0.68	0.05	0.53	0.07	0.56	0.07
4	0.93	0.06	0.53	0.07	0.48	0.05	0.70	0.08	0.54	0.06	0.59	0.05	0.64	0.08
6	1.23	0.08	0.41	0.05	0.58	0.08	0.46	0.07	0.51	0.08	0.48	0.06	0.57	0.10
8	1.08	0.07	0.46	0.04	0.57	0.07	0.66	0.06	0.59	0.09	0.56	0.06	0.69	0.10
12	1.16	0.05	0.35	0.04	0.46	0.06	0.37	0.03	0.52	0.07	0.56	0.07	0.65	0.10
15	1.18	0.08	0.43	0.03	0.44	0.04	0.59	0.13	0.54	0.10	0.50	0.06	0.74	0.14
18	1.06	0.07	0.55	0.07	0.52	0.11	0.50	0.12	0.57	0.07	0.57	0.06	0.83	0.11

LEFT VENTRICULAR VOLUME; SYSTOLE (uL)

	SHAM		PBS		CPC		MSC		CPC + MSC		CC1		CC2	
WEEK	MEAN	SEM	MEAN	SEM	MEAN	SEM	MEAN	SEM	MEAN	SEM	MEAN	SEM	MEAN	SEM
1	8.23	1.31	32.47	2.71	21.03	1.80	24.51	2.00	25.37	2.80	30.37	3.60	26.51	1.92
2	5.71	0.74	42.31	4.03	27.89	3.09	31.23	3.13	27.85	4.27	36.91	3.65	31.34	2.55
3	6.53	0.74	45.85	4.12	35.43	4.58	38.66	4.70	37.90	4.67	33.21	3.28	37.42	2.90
4	6.65	0.64	49.14	6.23	34.82	4.42	37.97	4.64	30.97	3.27	34.27	3.91	38.98	3.51
6	4.34	0.74	54.55	7.42	32.75	6.76	37.03	4.55	33.67	4.71	33.84	5.29	35.89	4.63
8	6.90	1.08	59.25	6.65	33.71	6.31	39.67	4.93	31.64	4.58	35.42	4.08	38.15	4.12
12	6.23	0.63	72.93	6.54	37.02	7.69	45.63	6.28	33.84	4.06	35.66	6.08	43.39	5.92
15	7.06	1.30	77.61	8.10	38.78	9.59	53.58	9.01	33.34	8.37	34.60	7.44	38.17	7.43
18	6.41	0.65	85.10	6.17	42.06	8.13	61.12	13.11	38.13	9.37	36.42	6.82	34.07	5.75

LEFT VENRICULAR VOLUME; DIASTOLE (uL)

	SHAM		PBS		CPC		MSC		CPC + MSC		CC1		CC2	
WEEK	MEAN	SEM	MEAN	SEM	MEAN	SEM	MEAN	SEM	MEAN	SEM	MEAN	SEM	MEAN	SEM
1	31.91	2.09	49.27	2.55	34.91	1.94	40.96	2.62	42.59	2.54	50.25	3.95	43.68	1.83
2	28.32	1.96	65.28	3.08	49.28	4.10	51.34	4.23	49.19	4.97	60.17	3.95	52.86	2.77
3	30.11	1.13	65.36	4.57	57.79	5.91	62.22	5.49	64.60	4.82	58.81	4.31	60.18	3.55
4	31.41	1.75	70.07	6.64	55.35	5.91	55.36	4.85	50.18	3.14	57.21	4.38	60.50	3.57
6	25.73	1.62	76.12	7.76	51.35	6.48	54.04	4.28	54.65	4.94	56.34	5.98	61.18	5.75
8	26.87	2.04	80.00	6.85	55.63	6.67	60.41	5.19	53.88	5.76	63.32	5.31	64.31	4.37
12	26.59	1.40	93.79	7.14	57.87	8.50	63.91	5.37	58.94	4.86	64.08	7.96	68.67	6.68
15	33.36	2.32	101.45	7.32	58.48	10.74	72.01	8.69	55.19	11.01	61.14	9.31	60.26	8.81
18	29.43	2.67	105.34	6.58	67.10	8.31	83.06	14.89	61.47	11.20	63.69	8.03	59.45	5.41

EJECTION FRACTION (%)

	SHAM		PBS		CPC		MSC		CPC + MSC		CC1		CC2	
WEEK	MEAN	SEM	MEAN	SEM	MEAN	SEM	MEAN	SEM	MEAN	SEM	MEAN	SEM	MEAN	SEM
1	76.28	3.05	35.00	3.18	40.56	2.31	40.45	3.29	41.91	3.37	40.84	2.98	40.10	2.59
2	80.65	1.92	36.74	3.47	43.81	3.45	39.75	1.84	46.12	3.14	39.90	2.46	41.80	2.61
3	78.46	2.40	31.04	2.97	40.02	3.02	39.77	3.12	43.66	3.43	44.24	2.03	38.18	2.57
4	79.27	1.39	32.57	2.39	39.12	2.46	33.76	3.12	40.19	3.57	41.50	3.95	36.64	2.71
6	83.83	2.20	30.89	3.27	40.23	5.32	32.86	4.39	41.10	3.62	42.82	4.03	43.54	3.28
8	75.09	3.33	27.78	3.36	41.97	4.85	35.76	3.24	42.44	2.98	45.39	2.47	42.24	3.58
12	76.06	2.66	22.51	3.04	39.22	5.06	31.09	4.69	43.53	3.57	47.20	4.13	39.45	3.16
15	78.93	3.73	24.03	3.60	37.19	4.32	27.93	4.55	41.69	4.12	45.15	4.43	40.31	4.39
18	77.99	1.77	19.22	2.64	37.79	6.04	29.91	4.21	40.33	3.46	44.89	4.21	44.23	5.29

Fractional Shortening (%)

	SHAM		PBS		CPC		MSC		CPC + MSC		CC1		CC2	
WEEK	MEAN	SEM	MEAN	SEM	MEAN	SEM	MEAN	SEM	MEAN	SEM	MEAN	SEM	MEAN	SEM
1	28.15	2.75	13.18	1.37	17.96	2.01	17.04	0.87	18.02	2.12	14.90	1.51	15.80	1.70
2	28.66	2.58	13.58	1.51	16.88	1.97	18.18	2.03	19.14	1.93	14.74	1.38	11.91	1.43
3	25.71	1.95	11.61	0.94	14.82	1.45	14.58	1.31	15.15	1.71	11.68	1.06	15.75	1.45
4	28.48	1.47	11.88	1.51	15.38	1.10	13.77	1.24	16.33	1.47	14.02	1.63	12.70	1.55
6	31.55	2.61	11.48	1.37	13.96	1.31	11.65	1.23	10.30	1.85	13.20	2.15	18.01	1.02
8	23.11	2.11	9.26	0.64	16.07	3.45	15.21	1.70	16.48	1.71	19.97	2.55	15.12	1.18
12	26.82	3.39	9.60	1.75	10.78	1.91	10.05	1.74	11.34	1.10	13.31	1.50	16.01	1.25
15	27.00	2.24	8.27	0.95	11.74	2.36	9.54	0.85	11.81	2.27	14.82	1.86	14.05	2.07
18	25.99	2.03	8.75	1.87	17.02	1.32	10.66	2.13	12.96	2.38	14.66	2.64	12.84	2.35

Chapter 2, in full, is prepared for submission. Cardiac Stem Cell Hybrids Enhance Myocardial Repair. Pearl Quijada, Hazel T. Salunga, Nirmala Hariharan, Jonathan Cubillo, Farid El-Sayed, Maryam Moshref, Kristin M. Bala, Jaqueline M. Emathinger, Andrea De La Torre, Lucia Ormachea, Roberto Alvarez Jr., Natalie A. Gude, and Mark A. Sussman. The dissertation author was the primary author and investigator on this manuscript.

CHAPTER 3

Characterization of Adult Stem cells with Altered DNA Content

INTRODUCTION

Physiological deterioration due to aging is coupled with the progression of cardiovascular disease. Myocardial aging is associated with reduced cardiac contractile and relaxation hemodynamics, metabolic dysfunction and cellular senescence[142]. Of the hallmarks of aging, stem cell exhaustion or a decline in stem cell regenerative capacity is particularly detrimental as resident c-kit$^+$ cardiac progenitor cells (CPCs) give rise to cardiomyogenic structures during development and after damage[73, 142]. In the era of cardiac cellular therapy, the ability to streamline the derivation of the most regenerative human adult stem is crucial. Isolation of youthful stem cells characterized by long telomeres and high telomerase activity is important for long-term maintenance of stem cell clonogenicity, self-renewal and differentiation[143-146].

Growth properties of adult stem cells *ex vivo* are an important metric to predict endogenous cardiac repair. Patient recovery after infarction has been positively correlated with robust CPC proliferation[144]. In addition, the cell surface receptor tyrosine kinase c-kit influences downstream signaling related to survival and proliferation in stem cells[55, 115, 147, 148]. The heart contains a heterogeneous population of adult stem cells including resident mesenchymal stem cells (MSCs). MSCs from the heart are of pro-epicardial origin, express platelet derived growth factor-α (PDGF-α) and exhibit multipotency towards smooth muscle and endothelial lineages[149, 150]. Although basic characteristics of

myocardial MSCs have been reported, the application of MSCs for cardiac therapy has not been investigated.

Diploid adult stem cells acquire tetraploidy after extended *in vitro* passaging leading to signs of cellular senescence and cell death[151]. Adipose derived MSCs frequently exhibit polyploidy in culture concurrent with increased p53 expression[152]. Chromosomal mosaicism or aneuploidy is reported in stem cells *in vivo*, yet chromosomal deletions or losses do not negatively effect stem cell properties such as self-renewal and/or differentiation[153]. Aneuploidy is associated with extreme proliferative properties and decreased sensitivity to growth inhibitors[154]. Recently, the stem cell field has highlighted the potential use of hybrids created through cell fusion as a potential therapeutic strategy to oppose cellular senescence and aging despite increased DNA content.

Cell fusion based nuclear reprogramming of somatic cells is a validated approach for production of pluripotent stem cells[155]. Cross-species hybrids are utilized for ease in the identification of species-specific factors that aid in reprogramming[148]. Identification of reprogramming factors after fusion between somatic fibroblasts and embryonic stem cells (ESCs) is accomplished with RNA sequencing (RNA-seq) of heterokaryons. Nuclear hybridization after fusion between human fibroblasts and immortalized mouse ESCs results in viable hybrids with enhanced survival and proliferation conferred by the ESC partner[61]. Related to our transplantation studies, electrofusion of MSCs with pancreatic islet cells improve βeta-cell insulin release and cell survival compared to the co-injection non-fused βeta-cells with MSCs in a diabetes mellitus mouse model[156].

Therefore, cell fusion may serve a novel therapeutic strategy to support the rejuvenation of somatic cells.

In this study we created a protocol to derive cross-species hybrids between mouse CPCs and human myocardial MSCs. CPCs were chosen due to enhanced proliferative properties and overall youthful cellular phenotype. Myocardial MSCs were utilized to further investigate paracrine-mediated secretion of stromal cells from the heart. Overall, we have identified an *ex vivo* strategy that allows for the successful propagation of mouse-human CardioChimeras. Furthermore, we have gained further understanding of the role ploidy plays in the regulation of stem cell characteristics and senescence.

METHODS

Stem cell isolation (mouse and human)

C-kit$^+$ CPCs isolated from 3 month old male FVB mice hearts and CD90$^+$/CD150$^+$ MSCs were isolated from spontaneously aborted human fetuses and were cultured as previously described[48, 54, 55]. Briefly, MSCs were isolated from whole fetal myocardial tissue, which was minced in small pieces and digested in collagenase (Worthington Bio Corporation) for 2 hours at 37°C. The cells were then passed through 100μm and 50μm filters (BD Biosciences), centrifuged at 1200rpm for 5 min and the pellet is incubated with c-kit labeled beads (Miltenyi Biotec,). The c-kit negative population was collected, washed once by centrifugation and cells were labeled with magnetic beads against CD90$^+$/CD150$^+$ (Miltenyi Biotec) and sorted according to manufacturer's protocol. MSCs were cultured in α-minimum essential media supplemented with 15% fetal bovine serum. Experiments with mCPCs and hMSCs were conducted between passages 10-20 and 4-10 respectively.

Lentivirus production

A third generation enhanced green fluorescent protein (eGFP) lentivirus with a phosphoglycerate kinase (PGK) and puromycin (puro) selection marker was purchased from Addgene (pLenti PGK GFP Puro (w509-5) was a gift from Eric Campeau, plasmid # 19070). pLenti PGK GFP Puro was used as a backbone to sub clone mcherry in the place of eGFP and bleomycin (bleo) to replace the puro gene in order to create pLenti PGK mcherry Bleo.

Stem cell transduction with lentivirus

Human MSCs at passage 6 were lentivirally transduced with pLenti PGK GFP Puro at a multiplicity of infection (MOI) of 10 and maintained in puromycin supplemented MSC media for one week starting at 48 hours post-infection. CPCs at passage 10 were lentivirally transduced with pLenti PGK mcherry Bleo at a MOI of 10 and subjected to fluorescent activated cell sorting (FACS) to purify mcherry positive CPCs. Fluorescent protein expression in MSCs and CPCs (CPC-mcherry) was confirmed by fluorescent microscopy and flow cytometric analysis.

Cell fusion and creation of cross-species CardioChimeras

Cell fusion was conducted using the GenomONE™ CF EX Sendai virus (Hemagglutinating Virus of Japan or HVJ) Envelope Cell Fusion Kit (Cosmo Bio. USA). According to the manufacturer's protocol, we subjected MSCs and CPCs to the suspension method. Here, human MSC labeled with GFP were mixed with mouse CPC labeled with mcherry at ratio of 3:1 and suspended in 20μL of cell fusion buffer and 10μL of Sendai virus and placed on ice for 5 minutes for absorption of the virus on the cell membrane. To induce cell fusion, cells were placed at 37°C for a total of 15 minutes. Cells were suspended in cell fusion media consisting of Hams F12 (Fisher Scientific), 15% FBS, 1% PSG, 5mU/mL human erythropoietin (Sigma Aldrich), 10ng/mL basic fibroblast growth factor (Peprotech) 0.2mM L-Glutathione (Sigma Aldrich), 10ng/mL leukocytye inhibitory factor (LIF) and 10ng/mL interleukin-6 (IL-6). The next day, media was changed,

and within 48 hours cells were trypsinized and subjected to fluorescence activated cell sorting (FACS) to purify GFP and mcherry double positive cells as a population. Once the population expanded, the cells were subjected to puromycin and bleocin selection for one week to remove single positive stem cells. The population was then subjected to a second round of FACS to purify GFP and mcherry double positive cells and placed as a single cell per well of a 96 well microplate and allowed to undergo clonal expansion. 12 double positive clones expanded from single cell sorted were confirmed by secondary flow cytometric analysis.

Cell proliferation assay

Cell proliferation was determined using the CyQuant Direct Cell Proliferation Assay (Life Technologies) according the manufacturer's instruction and as previously described[115].

Cell death assay

Stem cells were plated in a 6-well dish (80,000 cells per well) and incubated in starvation media (growth factor and FBS depleted media) with 1% PSG for 18 hours. The cells were then treated with either 40μM or 80μM hydrogen peroxide for 4 hours. Cells were resuspended with TO-PRO-3 iodide to label for dead cells. Data was acquired on a FACS Canto (BD Biosciences) and analyzed with FACS Diva software (BD Biosciences). Cell death was quantitated by measurement of TO-PRO-3 positive cells and represented as a percentage of the entire population.

G-band karyotype analysis

Karyotype analysis was carried in cultured cells during the growth phase of cells. G-banding reports were performed by Cell Line Genetics, Inc. Chromosome analysis was measured in at least 20 cells per cell line.

Immunoblotting

Protein lysates from cultured cells were prepared as previously described[115]. All protein samples for western blot analysis were separated on a 4%–12% Bis-Tris mini-gel (Life Technologies) and transferred to a polyvinylidene difluoride membrane. Membranes were blocked for 1 hour with 10% milk in TBST (1%Tris-buffered saline/0.1% Tween) and then probed with primary antibody overnight in milk. Next day blots were washed with TBST buffer and incubated in secondary antibodies in milk for 1.5 hours. Primary antibodies for western blot are as follows: mouse anti GAPDH (1:1000, Millipore); goat anti HP1γ (1:200, Santa Cruz Bio.).

Immunocytochemistry

Stem cells were placed at a density of 7,000 cells per well of a two-chamber permanox slide and stained according to previous studies[53]. Before scanning, cells were washed in PBS containing DAPI (Sigma Aldrich) to stain for nuclei. Slides were visualized using a Leica TCS SP8 confocal microscope. Primary antibodies are as follows: rat anti-mcherry (1:100, Life Technologies); rabbit anti-GFP (1:100, Life Technologies); goat anti-GFP (1:100, Rockland); rabbit anti-tubulin (1:40, Sigma Aldrich); goat-anti-c-kit (1:40, mouse specific,

R&D Systems); goat anti-c-kit (1:40, human specific, R&D); mouse anti-cardiac troponin T (1:40, Abcam); mouse anti-smooth muscle actin (1:40, Sigma Aldrich); mouse anti p16 (clone F9) (1:10, Santa Cruz Bio.); rabbit anti p53 (1:40, Abcam).

RESULTS

Analysis of ploidy in adult stem cells from mouse and human origin

Mouse c-kit$^+$ CPCs are abnormal tetraploid (4N), whereas myocardial human stem cells are diploid (2N) as confirmed by G-band karyotyping (Figure 3.1A and 3.1B). Bone marrow derived c-kit$^+$ cells (BMCs) are euploid based on karyotype reports (Figure 3.1C). Non-transformed tetraploid cells which fail to undergo cell division exhibit signs of phenotypic and molecular senescence[157]. Therefore, we were interested in evaluating the proliferation and expression of senescent makers in 2N and 4N cells. C-kit$^+$ BMCs have slower proliferative capabilities relative to mono-nucleated 4N CPCs (Figure 3.1D). Low passage BMCs are p16 and p53 negative (Figure 3.1E), proteins that are involved in cell cycle inhibition and senescence associated cell death[115]. Mouse CPCs express p16 during normal growth conditions (Figure 3.1F). Additionally, 4N and 6N cells express high levels of p53 based on immunoblot analysis, while 2N BMCs express low levels of p53 (Figure 3.1G). Heterochromatin protein 1 (HP1γ) is involved in chromatin regulation and transcriptional silencing by association with heterochromatin complexes[158]. HP1γ is highly expressed in 4N and 6N cell lines indicating that increased ploidy is correlated with suppression of transcription (Figure 3.1G).

Phenotypic properties of cross-species CardioChimeras

Mouse CPCs labeled with mcherry fluorescence and human MSCs labeled with GFP fluorescence were incubated at a ratio of 1:3 before fusion with

an inactivated RNA sendai virus. Cross-species hybrids were purified by these successive steps: 1) population sort by FACS 2) puromycin (puro) and bleocin (bleo) antibiotic treatments in culture and 3) clonal expansion after FACS single cell sorting (Figure 3.2A). 12 clones were confirmed to co-express mcherry and GFP based on flow cytometric analysis (Figure 3.2A). Of the 12 clones, two mouse and human CardioChimeras (MH-CCs) were characterized for properties of proliferation, cell survival and expression of stem and differentiation markers relative to the parental cell lines. MH-CCs were confirmed to express mcherry and GFP from mouse CPC and human CPC parents (Figure 3.2B and 3.2C). Clones are mono-nucleated indicating that cells underwent nuclear hybridization after fusion (Figure 3.2C). MH CCs exhibit a modest increase in proliferation relative to human MSCs (Figure 3.2D). Furthermore, cell survival between MH-CCs was comparable (blue) or slightly elevated (purple) relative to the parent cells during serum free and hydrogen peroxide conditions (Figure 3.2E).

Mouse/Human CardioChimeras have increased expression of mature cardiomyogenic markers and reduced c-kit expression

CPCs express c-kit *in vitro* and *in vivo*[74] and do not express mature markers such as cardiac troponin T (cTNT) during basal growth conditions (Figure 3.3A and 3.2B). Human derived MSCs are c-kit and cTNT negative (Figure 3.3D). However, both mouse CPCs and human MSCs express high levels of α-smooth muscle actin (α-SMA) (Figure 3.3C and 3.3D). MH-CC expresses low levels of c-kit using a mouse specific c-kit antibody (Figure 3.2E)

and express cTNT (Figure 3.2F). MH-CCs are uniformly α-SMA positive similar to parental cell lines (Figure 3.3G).

DISCUSSION

Myocardial CPCs and MSCs contribute to the heart during development and human cardiac disease[73, 150]. In order to make advanced use of the distinct mechanistic properties of CPCs to directly contribute to regeneration and MSCs to provide for paracrine secretion we turned to the technique of cell fusion to create stem cells hybrids or CardioChimeras. We utilized two distinct stem cell types derived from different species allowing for use of species-specific reagents to better understand the basic phenotypic and molecular characterization of resulting CardioChimeras. Mouse CPCs in combination with human myocardial MSCs were used to create cross-species CCs, which undergo nuclear hybridization and exhibit distinct proliferative and survival properties (Figure 3.2 and 3.3).

Initial analysis of chromosome number in our stem cells revealed c-kit$^+$ BMCs are 2N and c-kit$^+$ CPCs are 4N confirmed by karyotyping although cells were derived from the same mouse strain (FVB/NJ) (Figure 3.1A and 3.1C). Long-term passaging of HSCs show decreased telomerase activity leading to genomic instability and cellular senescence[159]. Furthermore, up regulation of p53 and p16 in polyploid cells is a reported mechanism to induce cell cycle arrest[115, 152]. Tetraploid complementation, or the combination of a tetraploid embryo with a diploid embryo, results in a fetus that comes to term as tetraploid cells are confined to the extraembryonic tissue and removed by p53-mediated apoptosis[160]. It is possible that the clearance of tetraploid cells from the embryo is incomplete leaving behind aneuploid cells with tissue specific residency in the

adult mouse. Currently, the source of 4N c-kit$^+$ CPCs is not known and/or if this is an artifact of extended culture, but future investigations are currently underway to determine if 4N cells exist in the intact heart.

Mono-nucleated tetraploidy is a hallmark of cancer stem cells, which bypass G1 and G2/M cell cycle check points leading to a transformed cellular phenotype[154]. Adult human CPCs from the myocardium have been shown to undergo replicative senescence as early as passage 15 out of the heart[55]. In contrast, mouse CPCs display an indefinite replicative potential while expressing high levels of p53 (Figure 3.D, 3.F, 3.G), yet CPCs still possess the ability to undergo cardiomyogenic commitment[48]. In our laboratory, mouse CPC senescence is induced after down regulation of stem cell maintenance protein nucleostemin as evidenced by senescence associated β-galactosidase staining and bi-nucleated cell cycle arrest[115]. Recent reports suggest that replicative and oxidative stresses are strong agents for increasing genomic instability and aneuploidy in proliferative cell types[161, 162]. Future studies will investigate the relation of ploidy and senescence in c-kit$^+$ CPCs, which may facilitate our understanding of stem cell exhaustion associated with cardiac aging.

Fusion between two human derived stem cells has been attempted, but nuclear hybridization was not observed. We posit that creation of heterokaryons between two human cells may up regulate p53 and inhibit nuclear fusion. Although observed at a low frequency, fusion of mouse CPCs to human MSCs yielded hybrids with optimal proliferative properties (Figure 3.2D). Interestingly, MH CCs express c-kit and retain expression of smooth muscle markers while up

regulating cTNT (Figure 3.3E and 3.3G). Aneuploidy is observed in MSCs undergoing osteogenic differentiation[163]. Furthermore, aneuploidy is observed in induced pluripotent stem cells, which retain properties of ESCs such as alkaline phosphatase expression and pluripotency[164].

Our initial cell fusion approach focused on the functions of mouse derived stem cell hybrids in Chapter 2, yet this technology can be applied for the creation of cross-species and human-to-human hybrids. Fusions between two different species facilitates our understanding of novel expression patterns, enabling production of critical factors that define stem cells for commitment, paracrine secretion or both. The inability of human adult stem cells to accomplish high impact restoration of myocardial structure and function continues to frustrate and impede progress in the regenerative medicine field because of limited inherent properties of the stem cell types employed. Hybrids are an attractive and provocative novel method for developing innovative paracrine-based and genetically linked cellular properties that will enhance efficacious actions of a single cell population preceding adoptive transfer to the injured myocardium. The ultimate goal of cardiac stem cell hybrids therapy is to empower the adult stem cell with multiple properties in order to blunt myocardial scar formation, stimulate endogenous regeneration and survival and repopulate the damaged myocardium with new cardiomyogenic cells and structures. Genetic modification of stem cells through cell fusion creates hybrids that have never existed in nature but can be formulated as a superior regenerative tool.

SUMMARY POINTS

- Stem cells for cardiac therapy display differences in DNA content, which may affect cellular properties such as cell division and cellular senescence.
- Cell fusion followed by nuclear hybridization is feasible between stem cells derived from different species.
- Mouse and human CardioChimeras exhibit proliferative capabilities comparable to human MSCs.
- Mouse and human CardioChimera clones exhibit variability in survival, which may be dependent on genomic stability after nuclear hybridization.
- Mouse and human CardioChimeras down regulate expression of c-kit and up regulate expression of cardiomyogenic markers.

FIGURES

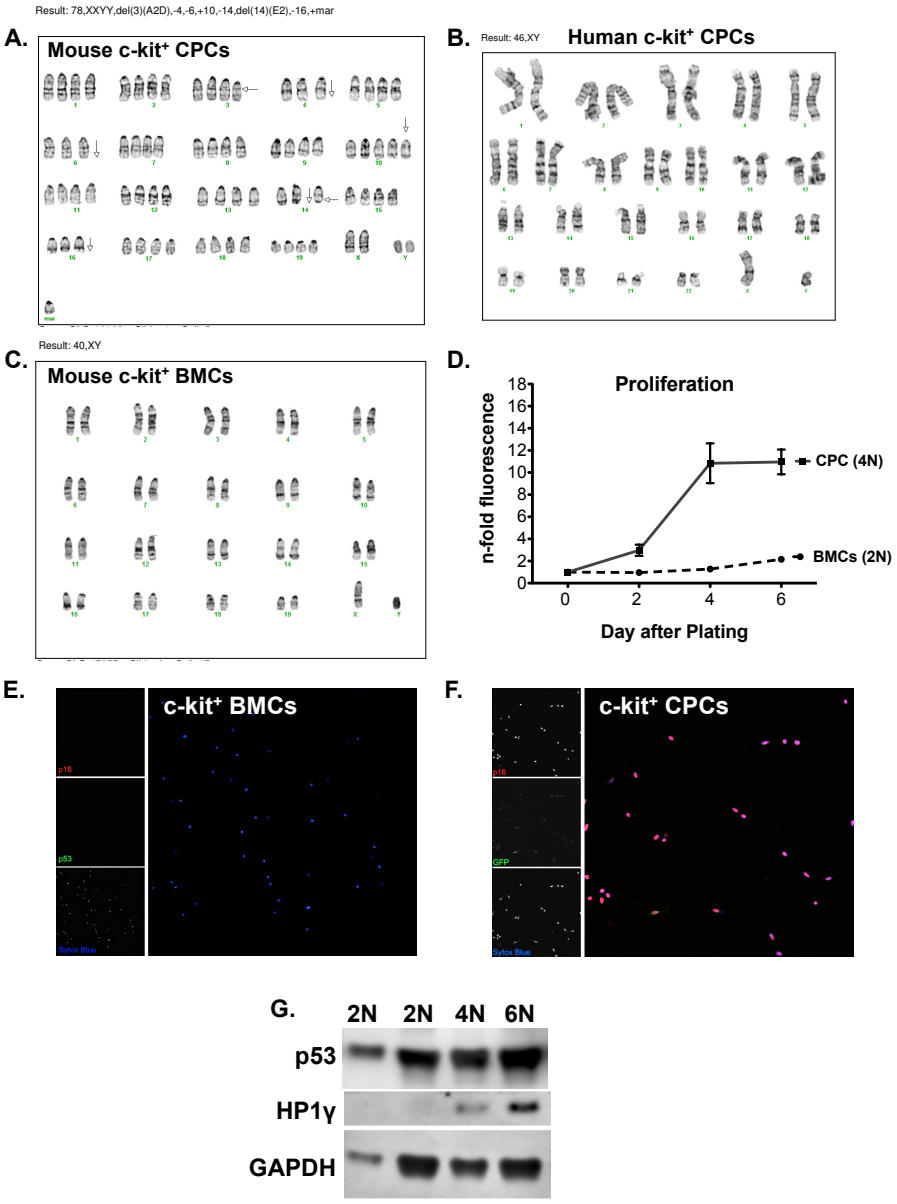

Figure 3.1: Analysis of ploidy in stem cells from mouse and human origin.
(A) Karyotype report of c-kit$^+$ CPCs from mouse cardiac origin. Cells were characterized as abnormal tetraploidy with loss and deletion of chromosomes across all chromosomes. Cell line is derived from male FVB/NJ. (B) Karyotype report of human c-kit$^+$ CPCs derived from a male fetal heart. (C) Karyotype report of c-kit$^+$ bone marrow cells derived from mouse bone marrow. Cell line is derived from male FVB/NJ. (D) Proliferation of mouse diploid (2N) BMCs and tetraploid (4N) CPCs based on fluorescent based assay to stain for nucleic acid. (E) Expression of p16 and p53 in mouse BMCs. (F) Expression of p16 and GFP in mouse CPCs. Prior to immunocytochemical analysis of cells, CPCs were transduced with a p16-GFP reporter plasmid. (G) Expression of senescent protein p53 and heterochromatin marker HP1γ in 2N and 4N mouse cell lines.

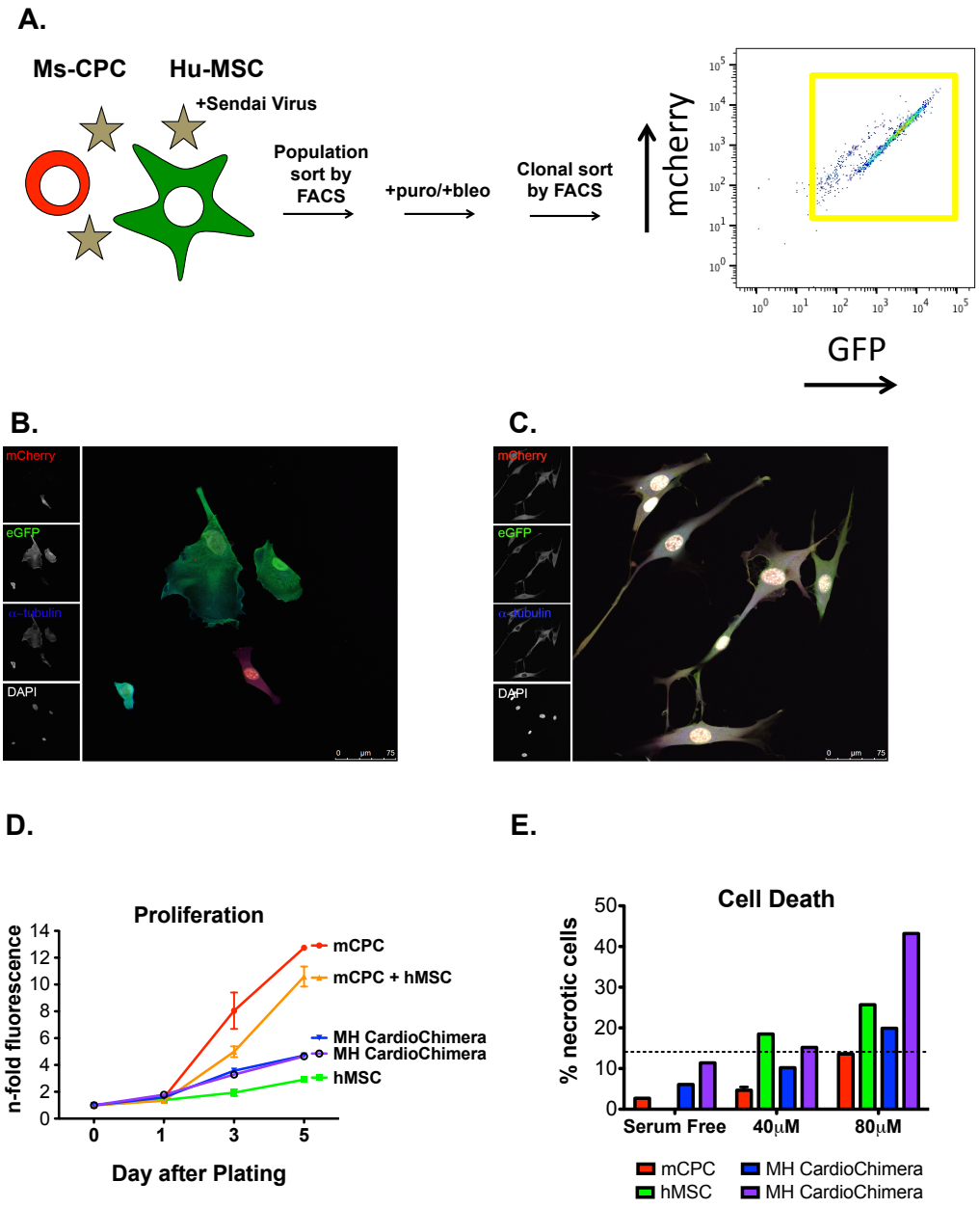

Figure 3.2: Phenotypic properties of cross-species CardioChimeras.
(A) Schematic representation of the fusion protocol to derive hybrids between mouse CPCs (Ms-CPC) and human (Hu-MSC). An initial population sort followed by a clonal sort selected for stable Mouse-Human CardioChimeras, which expressed mcherry and GFP from parental cell lines. (B) Non-fused mixed parental cell lines. Human MSCs express GFP and mouse CPCs express mcherry. (C) Representative Mouse-Human CardioChimera expresses both GFP and mcherry. (D) Proliferation of parental cells, individual or combined and two representative CardioChimeras based on fold change in fluorescence using a nucleic acid stain. (E) Cell death assay in parental cells compared to Mouse-Human CardioChimeras. Cell death was measured by percentage of TO-PRO-3 iodide positive cells. DAPI staining is used to visualize nuclei. Scale bar is 75μm.

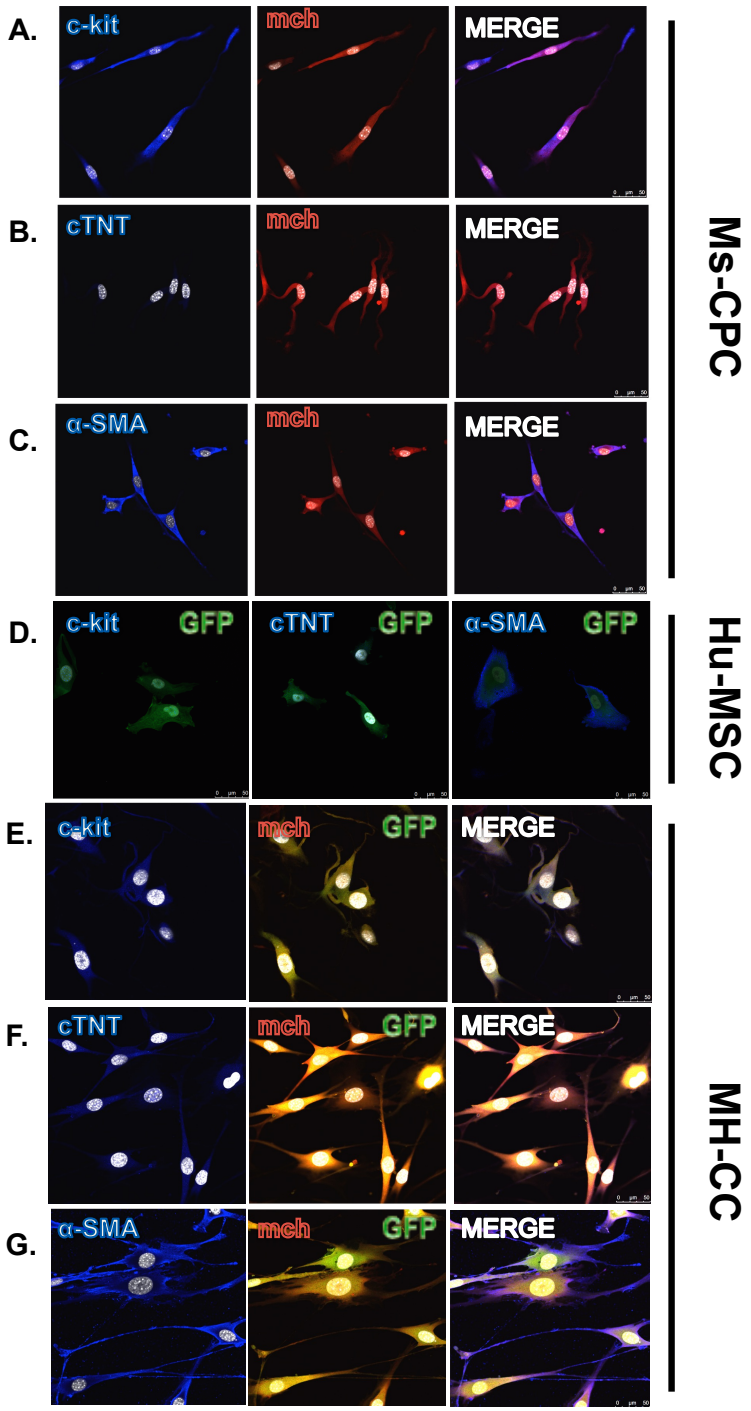

Figure 3.3: Mouse-Human CardioChimeras have increased expression of mature cardiomyogenic markers and reduced c-kit expression.
(A-C) Expression of (A) c-kit, (B) cTNT and (C) α-SMA in mouse CPCs, which co-express mcherry. (D) Expression of c-kit, cTNT and α-SMA in human MSCs, which co-express GFP. (E-G) Expression of (E) c-kit, (F) cTNT and (G) α-SMA in mouse-human CardioChimeras, which co-express mcherry and GFP. MERGED images are combination of left and center panels. Scale bar is 75μm.

Chapter 3 is presented in this dissertation as an extension of Chapter 2 to support the creation CardioChimeras between human derived stem cell lines. I would like to acknowledge Megan Monsanto for the isolation of fetal adult stem cells, Sarmistha Ganguly for her part in creating CardioChimeras between mouse and human adult stem cells and Michael McGregor for his studies identifying senescence markers in stem cells.

CONCLUSION OF THE DISSERTATION

The inability of cardiomyocytes to self-renew after myocardial damage has sparked extensive research into the underlying mechanisms that influence cardiomyocyte cell cycle entry and/or stimulation of endogenous stem cells to promote cardiac repair. Non-mammalian vertebrates such as the newt and the zebrafish display a remarkable ability to regenerate damaged hearts through cardiomyocyte de-differentiation and/or proliferation[165, 166]. The early postnatal mouse heart displays a similar ability to regenerate damaged heart regions, although this capacity is diminished a few days after birth[7]. Recently, there has been a surge of studies utilizing the neonatal mouse to understand the molecular and physiological factors that limit cardiomyocyte replacement observed in the adult heart[7, 167]. Coincident with decreased cardiomyocyte regeneration is an increase in the bi-nucleation of cardiomyocytes with age. Bi-nucleation occurs in 15% of cardiomyocytes identified in a toddler and is increased by 4-fold in young adults[168]. Additionally, robust neonatal heart regeneration is facilitated by a surge in hormones during adolescent years, the lack of a mature immune system and/or increased exposure to hypoxia, which are all physiological responses that stabilize or diminish with age[169-171]. Although cardiomyocytes show limited capacity for regeneration, adult resident cardiac stem cells show promise in the development of nascent cardiomyogenic structures[73]. Therefore, the theme of this dissertation is to investigate novel techniques such as genetic modification and cell fusion of adult stem cells to enhance stem cell cardioprotective abilities.

In the past decade, defining the optimal stem cell types for cardiac-based cellular therapy is becoming increasingly difficult, as there has been a rush in the

discovery of distinct stem cells. One strategy to enhance stem cell function and phenotypic youthfulness is by analysis of proteins that confer survival and cardiomyogenic commitment. Chapter 1 of this dissertation focused on defining proteins that promote differentiation of cardiac progenitor cells (CPCs). Regulation of calcium is required for proper cardiomyocyte contractility, but the role of Calcium Calmodulin Kinases (CaMKs) in stem cells derived from the myocardium has not been addressed. CaMKs contributes to cardiomyocyte development and growth, while nuclear-targeted CaMKs have been implicated in the regulation of gene transcription through HDAC signaling[83]. In adult myocytes, increases in cytosolic CaMKIIδ lead to decreased cardiomyocyte function, pathological hypertrophy and heart failure[172]. Conversely, nuclear CaMKIIδ (B isoform) increases cellular growth through activation of myocyte enhancing factor 2 (MEF2), contributes to cellular protection by regulation of transcription factor GATA4, and promotes cell lineage commitment[83, 87, 93]. In conclusion, this study identified a significant role of CaMKIIδB to promote cell specific lineage commitment and survival of CPCs, increasing the potential impact of these cells for cardiac therapy.

In Chapter 2 of this dissertation, we believe this study is highly significant and is the first report utilizing a novel application of cell fusion to create adult stem cell hybrids between cardiac progenitor and bone marrow derived mesenchymal stem cells (MSCs) for mitigation of myocardial injury. Moreover, we believe that this study increases our understanding of the positive impact of combinatorial cell delivery of CPCs with MSCs into the infarcted heart. Although

CPCs are valued for cardiomyogenic potential, the low persistence rates of MSCs prevent paracrine mediated endogenous reparations after damage. In this study we created CardioChimeras in order to ensure the long-term persistence of MSCs coupled with CPCs. CardioChimeras conferred significant improvements in anterior wall thickness and ejection fraction 18 weeks after adoptive transfer. Improvements in myocardial structure and function can be attributed to increased CardioChimera engraftment, which provides for stabilization of microvasculature and preserves cardiomyocyte size in the infarcted area not observed in CPC and MSC dual cell injected hearts. We believe that this report would be of interest to researchers in the field of stem cells as identification of novel strategies to enhance stem cell therapy continues to be an intense area of focus. Additionally, this study supports the application of cell fusion to create hybrid stem cell populations that combine optimal characteristics for directing cardiomyogenesis and protective paracrine secretion in a single cell type.

Application of CardioChimeras, a fused combinatorial cell delivery approach, provides for unique cell variability that is not unlike the inherent cell heterogeneity observed in tissue[173, 174]. In the bone marrow niche, hematopoietic stem cells undergo cellular fusion creating genetic variation without compromising mitotic ability or clonogenicity of stem cells[175]. Mosaic aneuploidy, or abnormal chromosome number, is observed in the inner cell mass and neural progenitor cells, a well known characteristic of stem cells that leads to somatic variation in several tissue types[128, 153]. Overall, these reports support the existence of chromosomal heterogeneity in stem cell populations, yet the

contribution of hybrids as a cell therapeutic geared towards cardiac tissue regeneration has only started to become of interest.

The heart and bone marrow are common sources of clinically relevant and heterogeneous adult stem cells. Therefore, It was no surprise that isolated cells from these tissues not only exhibit phenotypic variability but also chromosomal heterogeneity. Although, our studies could not identify the main mechanism of increased cellular ploidy in mouse CPCs relative to human CPCs, this topic is certainly a topic of several projects in the laboratory. The liver, which has a large number of tetraploid cells, much like what is observed in the heart, is further increased with telomere dysfunction leading to polyploidization[162]. Cardiomyocytes, which are primarily bi-nucleated tetraploid, have been reported to undergo a process of dedifferentiation a mechanism of cardiomyocyte remodeling[176]. Dedifferentiation of cardiomyocytes yields progenitor cells that re-express c-kit and are morphologically similar to progenitor cells with cardiomyogenic potential[177]. Although, cardiomyocyte dedifferentiation during homeostatic conditions is quite low, it is possible that this process promoted the residency of 4N CPCs derived from young adult mice. Furthermore, laboratory mice such as the FVB/NJ and C57/Bl6, which are subjected to long-term inbreeding exhibit unusually long telomeres (30-120kb), whereas the average human telomere length is 8-12kb[178]. Indicating that there can be certain issues with the use universal mouse strains that exhibit dysfunctions in the telomere/telomerase axis, which is known to contribute to altered DNA content.

From this point, the stem cell field should have better understanding of the cell biology of stem cells beyond focusing on presumed actions to mediate cardiac repair. Herein, two novel approaches are described that may improve the use of existing single cell or combinatorial delivery approaches through the use of 1) CaMKIIδB over expression in CPCs to promote cardiomyogenic commitment and survival and 2) CardioChimeras to compel communication between two chosen stem cell types resulting in a hybrid with blended phenotypic traits and genetic material derived from the individual parental cell lines. The field of cellular therapy will benefit from more “outside the box” thinking and approaches to more effectively take advantage of the unique traits of adult stem cells for the advancement of cardiac regeneration.

REFERENCES

1. Mozaffarian D, Benjamin EJ, Go AS, Arnett DK, Blaha MJ, Cushman M, de Ferranti S, Despres JP, Fullerton HJ, Howard VJ, Huffman MD, Judd SE, Kissela BM, Lackland DT, Lichtman JH, Lisabeth LD, Liu S, Mackey RH, Matchar DB, McGuire DK, Mohler ER, 3rd, Moy CS, Muntner P, Mussolino ME, Nasir K, Neumar RW, Nichol G, Palaniappan L, Pandey DK, Reeves MJ, Rodriguez CJ, Sorlie PD, Stein J, Towfighi A, Turan TN, Virani SS, Willey JZ, Woo D, Yeh RW, Turner MB, American Heart Association Statistics C, Stroke Statistics S. Heart disease and stroke statistics--2015 update: A report from the american heart association. *Circulation*. 2015;131:e29-322

2. Windecker S, Stortecky S, Stefanini GG, da Costa BR, Rutjes AW, Di Nisio M, Silletta MG, Maione A, Alfonso F, Clemmensen PM, Collet JP, Cremer J, Falk V, Filippatos G, Hamm C, Head S, Kappetein AP, Kastrati A, Knuuti J, Landmesser U, Laufer G, Neumann FJ, Richter D, Schauerte P, Sousa Uva M, Taggart DP, Torracca L, Valgimigli M, Wijns W, Witkowski A, Kolh P, Juni P. Revascularisation versus medical treatment in patients with stable coronary artery disease: Network meta-analysis. *BMJ*. 2014;348:g3859

3. Jessup M, Brozena S. Heart failure. *The New England journal of medicine*. 2003;348:2007-2018

4. Laflamme MA, Murry CE. Heart regeneration. *Nature*. 2011;473:326-335

5. Soonpaa MH, Field LJ. Assessment of cardiomyocyte DNA synthesis in normal and injured adult mouse hearts. *Am J Physiol*. 1997;272:H220-226

6. Soonpaa MH, Field LJ. Survey of studies examining mammalian cardiomyocyte DNA synthesis. *Circ Res*. 1998;83:15-26

7. Porrello ER, Mahmoud AI, Simpson E, Hill JA, Richardson JA, Olson EN, Sadek HA. Transient regenerative potential of the neonatal mouse heart. *Science*. 2011;331:1078-1080

8. Porrello ER, Mahmoud AI, Simpson E, Johnson BA, Grinsfelder D, Canseco D, Mammen PP, Rothermel BA, Olson EN, Sadek HA. Regulation of neonatal and adult mammalian heart regeneration by the mir-15 family. *Proceedings of the National Academy of Sciences of the United States of America*. 2013;110:187-192

9. Mahmoud AI, Kocabas F, Muralidhar SA, Kimura W, Koura AS, Thet S, Porrello ER, Sadek HA. Meis1 regulates postnatal cardiomyocyte cell cycle arrest. *Nature*. 2013;497:249-253

10. Bolli R, Chugh AR, D'Amario D, Loughran JH, Stoddard MF, Ikram S, Beache GM, Wagner SG, Leri A, Hosoda T, Sanada F, Elmore JB, Goichberg P, Cappetta D, Solankhi NK, Fahsah I, Rokosh DG, Slaughter MS, Kajstura J, Anversa P. Cardiac stem cells in patients with ischaemic cardiomyopathy (scipio): Initial results of a randomised phase 1 trial. *Lancet*. 2011;378:1847-1857

11. Rota M, Boni A, Urbanek K, Padin-Iruegas ME, Kajstura TJ, Fiore G, Kubo H, Sonnenblick EH, Musso E, Houser SR, Leri A, Sussman MA, Anversa P. Nuclear targeting of akt enhances ventricular function and myocyte contractility. *Circ Res*. 2005;97:1332-1341

12. Xiao G, Mao S, Baumgarten G, Serrano J, Jordan MC, Roos KP, Fishbein MC, MacLellan WR. Inducible activation of c-myc in adult myocardium in vivo provokes cardiac myocyte hypertrophy and reactivation of DNA synthesis. *Circ Res*. 2001;89:1122-1129

13. Zhong W, Mao S, Tobis S, Angelis E, Jordan MC, Roos KP, Fishbein MC, de Alboran IM, MacLellan WR. Hypertrophic growth in cardiac myocytes is mediated by myc through a cyclin d2-dependent pathway. *The EMBO journal*. 2006;25:3869-3879

14. Sanganalmath SK, Bolli R. Cell therapy for heart failure: A comprehensive overview of experimental and clinical studies, current challenges, and future directions. *Circ Res*. 2013;113:810-834

15. Isobe KI, Cheng Z, Nishio N, Suganya T, Tanaka Y, Ito S. Ipscs, aging and age-related diseases. *N Biotechnol*. 2014

16. de Almeida PE, Meyer EH, Kooreman NG, Diecke S, Dey D, Sanchez-Freire V, Hu S, Ebert A, Odegaard J, Mordwinkin NM, Brouwer TP, Lo D, Montoro DT, Longaker MT, Negrin RS, Wu JC. Transplanted terminally differentiated induced pluripotent stem cells are accepted by immune mechanisms similar to self-tolerance. *Nat Commun*. 2014;5:3903

17. Burridge PW, Thompson S, Millrod MA, Weinberg S, Yuan X, Peters A, Mahairaki V, Koliatsos VE, Tung L, Zambidis ET. A universal system for highly efficient cardiac differentiation of human induced pluripotent stem cells that eliminates interline variability. *PLoS One*. 2011;6:e18293

18. Xu C, Police S, Rao N, Carpenter MK. Characterization and enrichment of cardiomyocytes derived from human embryonic stem cells. *Circ Res*. 2002;91:501-508

19. Chong JJ, Yang X, Don CW, Minami E, Liu YW, Weyers JJ, Mahoney WM, Van Biber B, Palpant NJ, Gantz JA, Fugate JA, Muskheli V, Gough GM, Vogel KW, Astley CA, Hotchkiss CE, Baldessari A, Pabon L, Reinecke H, Gill EA, Nelson V, Kiem HP, Laflamme MA, Murry CE. Human embryonic-stem-cell-derived cardiomyocytes regenerate non-human primate hearts. *Nature*. 2014

20. Yang X, Rodriguez M, Pabon L, Fischer KA, Reinecke H, Regnier M, Sniadecki NJ, Ruohola-Baker H, Murry CE. Tri-iodo-l-thyronine promotes the maturation of human cardiomyocytes-derived from induced pluripotent stem cells. *Journal of molecular and cellular cardiology*. 2014;72:296-304

21. Shiba Y, Fernandes S, Zhu WZ, Filice D, Muskheli V, Kim J, Palpant NJ, Gantz J, Moyes KW, Reinecke H, Van Biber B, Dardas T, Mignone JL, Izawa A, Hanna R, Viswanathan M, Gold JD, Kotlikoff MI, Sarvazyan N, Kay MW, Murry CE, Laflamme MA. Human es-cell-derived cardiomyocytes electrically couple and suppress arrhythmias in injured hearts. *Nature*. 2012;489:322-325

22. Lundy SD, Gantz JA, Pagan CM, Filice D, Laflamme MA. Pluripotent stem cell derived cardiomyocytes for cardiac repair. *Current treatment options in cardiovascular medicine*. 2014;16:319

23. Shiba Y, Filice D, Fernandes S, Minami E, Dupras SK, Biber BV, Trinh P, Hirota Y, Gold JD, Viswanathan M, Laflamme MA. Electrical integration of human embryonic stem cell-derived cardiomyocytes in a guinea pig chronic infarct model. *Journal of cardiovascular pharmacology and therapeutics*. 2014;19:368-381

24. Anderson ME, Goldhaber J, Houser SR, Puceat M, Sussman MA. Embryonic stem cell-derived cardiac myocytes are not ready for human trials. *Circ Res*. 2014;115:335-338

25. Losordo DW, Henry TD, Davidson C, Sup Lee J, Costa MA, Bass T, Mendelsohn F, Fortuin FD, Pepine CJ, Traverse JH, Amrani D, Ewenstein BM, Riedel N, Story K, Barker K, Povsic TJ, Harrington RA, Schatz RA. Intramyocardial, autologous cd34+ cell therapy for refractory angina. *Circ Res*. 2011;109:428-436

26. Wang S, Cui J, Peng W, Lu M. Intracoronary autologous cd34+ stem cell therapy for intractable angina. *Cardiology*. 2010;117:140-147

27. Chugh AR, Beache GM, Loughran JH, Mewton N, Elmore JB, Kajstura J, Pappas P, Tatooles A, Stoddard MF, Lima JA, Slaughter MS, Anversa P, Bolli R. Administration of cardiac stem cells in patients with ischemic cardiomyopathy: The scipio trial: Surgical aspects and interim analysis of myocardial function and viability by magnetic resonance. *Circulation*. 2012;126:S54-64

28. Hare JM, Fishman JE, Gerstenblith G, DiFede Velazquez DL, Zambrano JP, Suncion VY, Tracy M, Ghersin E, Johnston PV, Brinker JA, Breton E, Davis-Sproul J, Schulman IH, Byrnes J, Mendizabal AM, Lowery MH, Rouy D, Altman P, Wong Po Foo C, Ruiz P, Amador A, Da Silva J, McNiece IK, Heldman AW. Comparison of allogeneic vs autologous bone marrow-derived mesenchymal stem cells delivered by transendocardial injection in patients with ischemic cardiomyopathy: The poseidon randomized trial. *JAMA*. 2012;308:2369-2379

29. Trachtenberg B, Velazquez DL, Williams AR, McNiece I, Fishman J, Nguyen K, Rouy D, Altman P, Schwarz R, Mendizabal A, Oskouei B, Byrnes J, Soto V, Tracy M, Zambrano JP, Heldman AW, Hare JM. Rationale and design of the transendocardial injection of autologous human cells (bone marrow or mesenchymal) in chronic ischemic left ventricular dysfunction and heart failure secondary to myocardial infarction (tac-hft) trial: A randomized, double-blind, placebo-controlled study of safety and efficacy. *Am Heart J*. 2011;161:487-493

30. Fisher SA, Brunskill SJ, Doree C, Mathur A, Taggart DP, Martin-Rendon E. Stem cell therapy for chronic ischaemic heart disease and congestive heart failure. *Cochrane Database Syst Rev*. 2014;4:CD007888

31. Bartunek J, Behfar A, Dolatabadi D, Vanderheyden M, Ostojic M, Dens J, El Nakadi B, Banovic M, Beleslin B, Vrolix M, Legrand V, Vrints C, Vanoverschelde JL, Crespo-Diaz R, Homsy C, Tendera M, Waldman S, Wijns W, Terzic A. Cardiopoietic stem cell therapy in heart failure: The c-cure (cardiopoietic stem cell therapy in heart failure) multicenter randomized trial with lineage-specified biologics. *J Am Coll Cardiol*. 2013;61:2329-2338

32. Hare JM, Fishman JE, Gerstenblith G, DiFede Velazquez DL, Zambrano JP, Suncion VY, Tracy M, Ghersin E, Johnston PV, Brinker JA, Breton E, Davis-Sproul J, Schulman IH, Byrnes J, Mendizabal AM, Lowery MH, Rouy D, Altman P, Wong Po Foo C, Ruiz P, Amador A, Da Silva J, McNiece IK, Heldman AW, George R, Lardo A. Comparison of allogeneic vs autologous bone marrow-derived mesenchymal stem cells delivered by transendocardial injection in patients with ischemic cardiomyopathy: The poseidon randomized trial. *JAMA*. 2012;308:2369-2379

33. Lee WY, Wei HJ, Wang JJ, Lin KJ, Lin WW, Chen DY, Huang CC, Lee TY, Ma HY, Hwang SM, Chang Y, Sung HW. Vascularization and restoration of heart function in rat myocardial infarction using transplantation of human cbmsc/huvec core-shell bodies. *Biomaterials*. 2012;33:2127-2136

34. Pittenger MF, Mackay AM, Beck SC, Jaiswal RK, Douglas R, Mosca JD, Moorman MA, Simonetti DW, Craig S, Marshak DR. Multilineage potential of adult human mesenchymal stem cells. *Science*. 1999;284:143-147

35. Wang W, Itaka K, Ohba S, Nishiyama N, Chung UI, Yamasaki Y, Kataoka K. 3d spheroid culture system on micropatterned substrates for improved differentiation efficiency of multipotent mesenchymal stem cells. *Biomaterials*. 2009;30:2705-2715

36. Ramkisoensing AA, de Vries AA, Atsma DE, Schalij MJ, Pijnappels DA. Interaction between myofibroblasts and stem cells in the fibrotic heart: Balancing between deterioration and regeneration. *Cardiovasc Res*. 2014;102:224-231

37. Nowbar AN, Mielewczik M, Karavassilis M, Dehbi HM, Shun-Shin MJ, Jones S, Howard JP, Cole GD, Francis DP. Discrepancies in autologous bone marrow stem cell trials and enhancement of ejection fraction (damascene): Weighted regression and meta-analysis. *BMJ*. 2014;348:g2688

38. Hansson EM, Lindsay ME, Chien KR. Regeneration next: Toward heart stem cell therapeutics. *Cell Stem Cell*. 2009;5:364-377

39. Segers VF, Lee RT. Stem-cell therapy for cardiac disease. *Nature*. 2008;451:937-942

40. Tallini YN, Greene KS, Craven M, Spealman A, Breitbach M, Smith J, Fisher PJ, Steffey M, Hesse M, Doran RM, Woods A, Singh B, Yen A, Fleischmann BK, Kotlikoff MI. C-kit expression identifies cardiovascular precursors in the neonatal heart. *Proceedings of the National Academy of Sciences of the United States of America*. 2009;106:1808-1813

41. van Berlo JH, Kanisicak O, Maillet M, Vagnozzi RJ, Karch J, Lin SC, Middleton RC, Marban E, Molkentin JD. C-kit cells minimally contribute cardiomyocytes to the heart. *Nature*. 2014

42. Fransioli J, Bailey B, Gude NA, Cottage CT, Muraski JA, Emmanuel G, Wu W, Alvarez R, Rubio M, Ottolenghi S, Schaefer E, Sussman MA. Evolution of the c-kit-positive cell response to pathological challenge in the myocardium. *Stem Cells*. 2008;26:1315-1324

43. Ellison GM, Vicinanza C, Smith AJ, Aquila I, Leone A, Waring CD, Henning BJ, Stirparo GG, Papait R, Scarfo M, Agosti V, Viglietto G, Condorelli G, Indolfi C, Ottolenghi S, Torella D, Nadal-Ginard B. Adult c-kit(pos) cardiac stem cells are necessary and sufficient for functional cardiac regeneration and repair. *Cell*. 2013;154:827-842

44. Frangogiannis NG. The immune system and the remodeling infarcted heart: Cell biological insights and therapeutic opportunities. *J Cardiovasc Pharmacol*. 2013;63:185-195

45. Hilgendorf I, Gerhardt LM, Tan TC, Winter C, Holderried TA, Chousterman BG, Iwamoto Y, Liao R, Zirlik A, Scherer-Crosbie M, Hedrick CC, Libby P, Nahrendorf M, Weissleder R, Swirski FK. Ly-6chigh monocytes depend on nr4a1 to balance both inflammatory and reparative phases in the infarcted myocardium. *Circ Res*. 2014;114:1611-1622

46. Hong KU, Li QH, Guo Y, Patton NS, Moktar A, Bhatnagar A, Bolli R. A highly sensitive and accurate method to quantify absolute numbers of c-kit+ cardiac stem cells following transplantation in mice. *Basic Res Cardiol*. 2013;108:346

47. Hong KU, Guo Y, Li QH, Cao P, Al-Maqtari T, Vajravelu BN, Du J, Book MJ, Zhu X, Nong Y, Bhatnagar A, Bolli R. C-kit+ cardiac stem cells alleviate post-myocardial infarction left ventricular dysfunction despite poor engraftment and negligible retention in the recipient heart. *PLoS One*. 2014;9:e96725

48. Fischer KM, Cottage CT, Wu W, Din S, Gude NA, Avitabile D, Quijada P, Collins BL, Fransioli J, Sussman MA. Enhancement of myocardial regeneration through genetic engineering of cardiac progenitor cells expressing pim-1 kinase. *Circulation*. 2009;120:2077-2087

49. Mohsin S, Khan M, Toko H, Bailey B, Cottage CT, Wallach K, Nag D, Lee A, Siddiqi S, Lan F, Fischer KM, Gude N, Quijada P, Avitabile D, Truffa S, Collins B, Dembitsky W, Wu JC, Sussman MA. Human cardiac progenitor cells engineered with pim-i kinase enhance myocardial repair. *J Am Coll Cardiol*. 2012;60:1278-1287

50. Cottage CT, Bailey B, Fischer KM, Avitable D, Collins B, Tuck S, Quijada P, Gude N, Alvarez R, Muraski J, Sussman MA. Cardiac progenitor cell cycling stimulated by pim-1 kinase. *Circ Res*. 2010;106:891-901

51. Muraski JA, Rota M, Misao Y, Fransioli J, Cottage C, Gude N, Esposito G, Delucchi F, Arcarese M, Alvarez R, Siddiqi S, Emmanuel GN, Wu W, Fischer K, Martindale JJ, Glembotski CC, Leri A, Kajstura J, Magnuson N, Berns A, Beretta RM, Houser SR, Schaefer EM, Anversa P, Sussman MA.

Pim-1 regulates cardiomyocyte survival downstream of akt. *Nat Med*. 2007;13:1467-1475

52. Balsam LB, Wagers AJ, Christensen JL, Kofidis T, Weissman IL, Robbins RC. Haematopoietic stem cells adopt mature haematopoietic fates in ischaemic myocardium. *Nature*. 2004;428:668-673

53. Quijada P, Toko H, Fischer KM, Bailey B, Reilly P, Hunt KD, Gude NA, Avitabile D, Sussman MA. Preservation of myocardial structure is enhanced by pim-1 engineering of bone marrow cells. *Circ Res*. 2012;111:77-86

54. Cottage CT, Neidig L, Sundararaman B, Din S, Joyo AY, Bailey B, Gude N, Hariharan N, Sussman MA. Increased mitotic rate coincident with transient telomere lengthening resulting from pim-1 overexpression in cardiac progenitor cells. *Stem Cells*. 2012;30:2512-2522

55. Mohsin S, Khan M, Nguyen J, Alkatib M, Siddiqi S, Hariharan N, Wallach K, Monsanto M, Gude N, Dembitsky W, Sussman MA. Rejuvenation of human cardiac progenitor cells with pim-1 kinase. *Circ Res*. 2013;113:1169-1179

56. Siddiqi S, Sussman MA. Cell and gene therapy for severe heart failure patients: The time and place for pim-1 kinase. *Expert Rev Cardiovasc Ther*. 2013;11:949-957

57. Siddiqi S, Gude N, Hosoda T, Muraski J, Rubio M, Emmanuel G, Fransioli J, Vitale S, Parolin C, D'Amario D, Schaefer E, Kajstura J, Leri A, Anversa P, Sussman MA. Myocardial induction of nucleostemin in response to postnatal growth and pathological challenge. *Circ Res*. 2008;103:89-97

58. Hariharan N, Sussman MA. Stressing on the nucleolus in cardiovascular disease. *Biochim Biophys Acta*. 2013;1842:798-801

59. Acquistapace A, Bru T, Lesault PF, Figeac F, Coudert AE, le Coz O, Christov C, Baudin X, Auber F, Yiou R, Dubois-Rande JL, Rodriguez AM. Human mesenchymal stem cells reprogram adult cardiomyocytes toward a progenitor-like state through partial cell fusion and mitochondria transfer. *Stem Cells*. 2011;29:812-824

60. Islam MQ, Panduri V, Islam K. Generation of somatic cell hybrids for the production of biologically active factors that stimulate proliferation of other cells. *Cell Prolif*. 2007;40:91-105

61. Islam MQ, Ringe J, Reichmann E, Migotti R, Sittinger M, da SML, Nardi NB, Magnusson P, Islam K. Functional characterization of cell hybrids

generated by induced fusion of primary porcine mesenchymal stem cells with an immortal murine cell line. *Cell Tissue Res*. 2006;326:123-137

62. Quintana-Bustamante O, Grueso E, Garcia-Escudero R, Arza E, Alvarez-Barrientos A, Fabregat I, Garcia-Bravo M, Meza NW, Segovia JC. Cell fusion reprogramming leads to a specific hepatic expression pattern during mouse bone marrow derived hepatocyte formation in vivo. *PLoS One*. 2012;7:e33945

63. Alvarez-Dolado M, Pardal R, Garcia-Verdugo JM, Fike JR, Lee HO, Pfeffer K, Lois C, Morrison SJ, Alvarez-Buylla A. Fusion of bone-marrow-derived cells with purkinje neurons, cardiomyocytes and hepatocytes. *Nature*. 2003;425:968-973

64. Takei S, Yamamoto M, Cui L, Yue F, Johkura K, Ogiwara N, Iinuma H, Okinaga K, Sasaki K. Phenotype-specific cells with proliferative potential are produced by polyethylene glycol-induced fusion of mouse embryonic stem cells with fetal cardiomyocytes. *Cell Transplant*. 2005;14:701-708

65. Anversa P, Rota M, Urbanek K, Hosoda T, Sonnenblick EH, Leri A, Kajstura J, Bolli R. Myocardial aging--a stem cell problem. *Basic Res Cardiol*. 2005;100:482-493

66. Fujita J, Itabashi Y, Seki T, Tohyama S, Tamura Y, Sano M, Fukuda K. Myocardial cell sheet therapy and cardiac function. *Am J Physiol Heart Circ Physiol*. 2012;303:H1169-1182

67. Cheng K, Blusztajn A, Shen D, Li TS, Sun B, Galang G, Zarembinski TI, Prestwich GD, Marban E, Smith RR, Marban L. Functional performance of human cardiosphere-derived cells delivered in an in situ polymerizable hyaluronan-gelatin hydrogel. *Biomaterials*. 2012;33:5317-5324

68. Beohar N, Rapp J, Pandya S, Losordo DW. Rebuilding the damaged heart: The potential of cytokines and growth factors in the treatment of ischemic heart disease. *J Am Coll Cardiol*. 2011;56:1287-1297

69. Mohsin S, Khan M, Toko H, Bailey B, Cottage CT, Wallach K, Nag D, Lee A, Siddiqi S, Lan F, Fischer KM, Gude N, Quijada P, Avitabile D, Truffa S, Collins B, Dembitsky W, Wu JC, Sussman MA. Human cardiac progenitor cells engineered with pim-i kinase enhance myocardial repair. *J Am Coll Cardiol*. 2012

70. Orlic D, Kajstura J, Chimenti S, Limana F, Jakoniuk I, Quaini F, Nadal-Ginard B, Bodine DM, Leri A, Anversa P. Mobilized bone marrow cells repair the infarcted heart, improving function and survival. *Proc Natl Acad Sci U S A*. 2001;98:10344-10349

71. Rota M, Padin-Iruegas ME, Misao Y, De Angelis A, Maestroni S, Ferreira-Martins J, Fiumana E, Rastaldo R, Arcarese ML, Mitchell TS, Boni A, Bolli R, Urbanek K, Hosoda T, Anversa P, Leri A, Kajstura J. Local activation or implantation of cardiac progenitor cells rescues scarred infarcted myocardium improving cardiac function. *Circ Res*. 2008;103:107-116

72. Zaruba MM, Soonpaa M, Reuter S, Field LJ. Cardiomyogenic potential of c-kit(+)-expressing cells derived from neonatal and adult mouse hearts. *Circulation*. 2010;121:1992-2000

73. van Berlo JH, Kanisicak O, Maillet M, Vagnozzi RJ, Karch J, Lin SC, Middleton RC, Marban E, Molkentin JD. C-kit+ cells minimally contribute cardiomyocytes to the heart. *Nature*. 2014;509:337-341

74. Leri A, Kajstura J, Anversa P. Role of cardiac stem cells in cardiac pathophysiology: A paradigm shift in human myocardial biology. *Circ Res*. 2011;109:941-961

75. Volkers M, Rohde D, Goodman C, Most P. S100a1: A regulator of striated muscle sarcoplasmic reticulum ca2+ handling, sarcomeric, and mitochondrial function. *J Biomed Biotechnol*.2010:178614

76. Hook SS, Means AR. Ca(2+)/cam-dependent kinases: From activation to function. *Annu Rev Pharmacol Toxicol*. 2001;41:471-505

77. Luczak ED, Anderson ME. Camkii oxidative activation and the pathogenesis of cardiac disease. *Journal of molecular and cellular cardiology*. 2014;73:112-116

78. Mishra S, Ling H, Grimm M, Zhang T, Bers DM, Brown JH. Cardiac hypertrophy and heart failure development through gq and cam kinase ii signaling. *J Cardiovasc Pharmacol*. 2010;56:598-603

79. Sossalla S, Fluschnik N, Schotola H, Ort KR, Neef S, Schulte T, Wittkopper K, Renner A, Schmitto JD, Gummert J, El-Armouche A, Hasenfuss G, Maier LS. Inhibition of elevated ca2+/calmodulin-dependent protein kinase ii improves contractility in human failing myocardium. *Circ Res*. 2010;107:1150-1161

80. Fischer TH, Eiringhaus J, Dybkova N, Forster A, Herting J, Kleinwachter A, Ljubojevic S, Schmitto JD, Streckfuss-Bomeke K, Renner A, Gummert J, Hasenfuss G, Maier LS, Sossalla S. Ca(2+) /calmodulin-dependent protein kinase ii equally induces sarcoplasmic reticulum ca(2+) leak in human ischaemic and dilated cardiomyopathy. *European journal of heart failure*. 2014;16:1292-1300

81. Awad S, Al-Haffar KM, Marashly Q, Quijada P, Kunhi M, Al-Yacoub N, Wade FS, Mohammed SF, Al-Dayel F, Sutherland G, Assiri A, Sussman M, Bers D, Al-Habeeb W, Poizat C. Control of histone h3 phosphorylation by camkii in response to hemodynamic cardiac stress. *The Journal of pathology*. 2014

82. Srinivasan M, Edman CF, Schulman H. Alternative splicing introduces a nuclear localization signal that targets multifunctional cam kinase to the nucleus. *The Journal of cell biology*. 1994;126:839-852

83. Zhang T, Kohlhaas M, Backs J, Mishra S, Phillips W, Dybkova N, Chang S, Ling H, Bers DM, Maier LS, Olson EN, Brown JH. Camkiidelta isoforms differentially affect calcium handling but similarly regulate hdac/mef2 transcriptional responses. *J Biol Chem*. 2007;282:35078-35087

84. Little GH, Bai Y, Williams T, Poizat C. Nuclear calcium/calmodulin-dependent protein kinase iidelta preferentially transmits signals to histone deacetylase 4 in cardiac cells. *J Biol Chem*. 2007;282:7219-7231

85. Backs J, Song K, Bezprozvannaya S, Chang S, Olson EN. Cam kinase ii selectively signals to histone deacetylase 4 during cardiomyocyte hypertrophy. *The Journal of clinical investigation*. 2006;116:1853-1864

86. Peng W, Zhang Y, Zheng M, Cheng H, Zhu W, Cao CM, Xiao RP. Cardioprotection by camkii-deltab is mediated by phosphorylation of heat shock factor 1 and subsequent expression of inducible heat shock protein 70. *Circ Res*. 2010;106:102-110

87. Little GH, Saw A, Bai Y, Dow J, Marjoram P, Simkhovich B, Leeka J, Kedes L, Kloner RA, Poizat C. Critical role of nuclear calcium/calmodulin-dependent protein kinase iideltab in cardiomyocyte survival in cardiomyopathy. *J Biol Chem*. 2009;284:24857-24868

88. Ling H, Gray CB, Zambon AC, Grimm M, Gu Y, Dalton N, Purcell NH, Peterson K, Brown JH. Ca2+/calmodulin-dependent protein kinase ii delta mediates myocardial ischemia/reperfusion injury through nuclear factor-kappab. *Circ Res*. 2013;112:935-944

89. Li H, Li W, Gupta AK, Mohler PJ, Anderson ME, Grumbach IM. Calmodulin kinase ii is required for angiotensin ii-mediated vascular smooth muscle hypertrophy. *Am J Physiol Heart Circ Physiol*. 2009;298:H688-698

90. Scott JA, Xie L, Li H, Li W, He JB, Sanders PN, Carter AB, Backs J, Anderson ME, Grumbach IM. The multifunctional ca2+/calmodulin-dependent kinase ii regulates vascular smooth muscle migration through

matrix metalloproteinase 9. *Am J Physiol Heart Circ Physiol*. 2012;302:H1953-1964

91. Hoch B, Wobus AM, Krause EG, Karczewski P. Delta-ca(2+)/calmodulin-dependent protein kinase ii expression pattern in adult mouse heart and cardiogenic differentiation of embryonic stem cells. *Journal of cellular biochemistry*. 2000;79:293-300

92. Sun G, Fu C, Shen C, Shi Y. Histone deacetylases in neural stem cells and induced pluripotent stem cells. *J Biomed Biotechnol*.2011:835968

93. Clocchiatti A, Florean C, Brancolini C. Class iia hdacs: From important roles in differentiation to possible implications in tumourigenesis. *J Cell Mol Med*.15:1833-1846

94. Zhang LX, DeNicola M, Qin X, Du J, Ma J, Tina Zhao Y, Zhuang S, Liu PY, Wei L, Qin G, Tang Y, Zhao TC. Specific inhibition of hdac4 in cardiac progenitor cells enhances myocardial repairs. *American journal of physiology. Cell physiology*. 2014;307:C358-372

95. Bailey B, Izarra A, Alvarez R, Fischer KM, Cottage CT, Quijada P, Diez-Juan A, Sussman MA. Cardiac stem cell genetic engineering using the alphamhc promoter. *Regenerative medicine*. 2009;4:823-833

96. Khan M, Mohsin S, Avitabile D, Siddiqi S, Nguyen J, Wallach K, Quijada P, McGregor M, Gude N, Alvarez R, Tilley DG, Koch WJ, Sussman MA. Beta-adrenergic regulation of cardiac progenitor cell death versus survival and proliferation. *Circ Res*. 2013;112:476-486

97. Ferreira-Martins J, Ogorek B, Cappetta D, Matsuda A, Signore S, D'Amario D, Kostyla J, Steadman E, Ide-Iwata N, Sanada F, Iaffaldano G, Ottolenghi S, Hosoda T, Leri A, Kajstura J, Anversa P, Rota M. Cardiomyogenesis in the developing heart is regulated by c-kit-positive cardiac stem cells. *Circ Res*. 2012;110:701-715

98. Ferreira-Martins J, Rondon-Clavo C, Tugal D, Korn JA, Rizzi R, Padin-Iruegas ME, Ottolenghi S, De Angelis A, Urbanek K, Ide-Iwata N, D'Amario D, Hosoda T, Leri A, Kajstura J, Anversa P, Rota M. Spontaneous calcium oscillations regulate human cardiac progenitor cell growth. *Circ Res*. 2009;105:764-774

99. Ellison GM, Torella D, Karakikes I, Purushothaman S, Curcio A, Gasparri C, Indolfi C, Cable NT, Goldspink DF, Nadal-Ginard B. Acute beta-adrenergic overload produces myocyte damage through calcium leakage from the ryanodine receptor 2 but spares cardiac stem cells. *J Biol Chem*. 2007;282:11397-11409

100. Gomez AM, Ruiz-Hurtado G, Benitah JP, Dominguez-Rodriguez A. Ca(2+) fluxes involvement in gene expression during cardiac hypertrophy. *Current vascular pharmacology*. 2013;11:497-506

101. Clocchiatti A, Florean C, Brancolini C. Class iia hdacs: From important roles in differentiation to possible implications in tumourigenesis. *J Cell Mol Med*. 2011;15:1833-1846

102. Harrison BC, Huynh K, Lundgaard GL, Helmke SM, Perryman MB, McKinsey TA. Protein kinase c-related kinase targets nuclear localization signals in a subset of class iia histone deacetylases. *FEBS letters*. 2010;584:1103-1110

103. Lee S, Park JR, Seo MS, Roh KH, Park SB, Hwang JW, Sun B, Seo K, Lee YS, Kang SK, Jung JW, Kang KS. Histone deacetylase inhibitors decrease proliferation potential and multilineage differentiation capability of human mesenchymal stem cells. *Cell Prolif*. 2009;42:711-720

104. Zhu W, Woo AY, Yang D, Cheng H, Crow MT, Xiao RP. Activation of camkiideltac is a common intermediate of diverse death stimuli-induced heart muscle cell apoptosis. *J Biol Chem*. 2007;282:10833-10839

105. Leri A, Kajstura J, Anversa P. Cardiac stem cells and mechanisms of myocardial regeneration. *Physiological reviews*. 2005;85:1373-1416

106. Wang Y, Chen X, Cao W, Shi Y. Plasticity of mesenchymal stem cells in immunomodulation: Pathological and therapeutic implications. *Nature immunology*. 2014;15:1009-1016

107. Hatzistergos KE, Quevedo H, Oskouei BN, Hu Q, Feigenbaum GS, Margitich IS, Mazhari R, Boyle AJ, Zambrano JP, Rodriguez JE, Dulce R, Pattany PM, Valdes D, Revilla C, Heldman AW, McNiece I, Hare JM. Bone marrow mesenchymal stem cells stimulate cardiac stem cell proliferation and differentiation. *Circ Res*. 2010;107:913-922

108. Williams AR, Hatzistergos KE, Addicott B, McCall F, Carvalho D, Suncion V, Morales AR, Da Silva J, Sussman MA, Heldman AW, Hare JM. Enhanced effect of combining human cardiac stem cells and bone marrow mesenchymal stem cells to reduce infarct size and to restore cardiac function after myocardial infarction. *Circulation*. 2013;127:213-223

109. Johansson CB, Youssef S, Koleckar K, Holbrook C, Doyonnas R, Corbel SY, Steinman L, Rossi FM, Blau HM. Extensive fusion of haematopoietic cells with purkinje neurons in response to chronic inflammation. *Nature cell biology*. 2008;10:575-583

110. Yang WJ, Li SH, Weisel RD, Liu SM, Li RK. Cell fusion contributes to the rescue of apoptotic cardiomyocytes by bone marrow cells. *J Cell Mol Med*. 2012;16:3085-3095

111. Soza-Ried J, Fisher AG. Reprogramming somatic cells towards pluripotency by cellular fusion. *Curr Opin Genet Dev*. 2012;22:459-465

112. Tsubouchi T, Soza-Ried J, Brown K, Piccolo FM, Cantone I, Landeira D, Bagci H, Hochegger H, Merkenschlager M, Fisher AG. DNA synthesis is required for reprogramming mediated by stem cell fusion. *Cell*. 2013;152:873-883

113. Islam MQ, Meirelles Lda S, Nardi NB, Magnusson P, Islam K. Polyethylene glycol-mediated fusion between primary mouse mesenchymal stem cells and mouse fibroblasts generates hybrid cells with increased proliferation and altered differentiation. *Stem Cells Dev*. 2006;15:905-919

114. Konstandin MH, Toko H, Gastelum GM, Quijada P, De La Torre A, Quintana M, Collins B, Din S, Avitabile D, Volkers M, Gude N, Fassler R, Sussman MA. Fibronectin is essential for reparative cardiac progenitor cell response after myocardial infarction. *Circ Res*. 2013;113:115-125

115. Hariharan N, Quijada P, Mohsin S, Joyo A, Samse K, Monsanto M, De La Torre A, Avitabile D, Ormachea L, McGregor MJ, Tsai EJ, Sussman MA. Nucleostemin rejuvenates cardiac progenitor cells and antagonizes myocardial aging. *J Am Coll Cardiol*. 2015;65:133-147

116. Tsujita Y, Muraski J, Shiraishi I, Kato T, Kajstura J, Anversa P, Sussman MA. Nuclear targeting of akt antagonizes aspects of cardiomyocyte hypertrophy. *Proceedings of the National Academy of Sciences of the United States of America*. 2006;103:11946-11951

117. Muraski JA, Fischer KM, Wu W, Cottage CT, Quijada P, Mason M, Din S, Gude N, Alvarez R, Jr., Rota M, Kajstura J, Wang Z, Schaefer E, Chen X, MacDonnel S, Magnuson N, Houser SR, Anversa P, Sussman MA. Pim-1 kinase antagonizes aspects of myocardial hypertrophy and compensation to pathological pressure overload. *Proceedings of the National Academy of Sciences of the United States of America*. 2008;105:13889-13894

118. Gao E, Lei YH, Shang X, Huang ZM, Zuo L, Boucher M, Fan Q, Chuprun JK, Ma XL, Koch WJ. A novel and efficient model of coronary artery ligation and myocardial infarction in the mouse. *Circ Res*. 2010;107:1445-1453

119. Davani S, Marandin A, Mersin N, Royer B, Kantelip B, Herve P, Etievent JP, Kantelip JP. Mesenchymal progenitor cells differentiate into an endothelial phenotype, enhance vascular density, and improve heart function in a rat cellular cardiomyoplasty model. *Circulation*. 2003;108 Suppl 1:II253-258

120. Zaruba MM, Franz WM. Role of the sdf-1-cxcr4 axis in stem cell-based therapies for ischemic cardiomyopathy. *Expert opinion on biological therapy*. 2010;10:321-335

121. Zacchigna S, Giacca M. Extra- and intracellular factors regulating cardiomyocyte proliferation in postnatal life. *Cardiovasc Res*. 2014;102:312-320

122. Fontes JA, Rose NR, Cihakova D. The varying faces of il-6: From cardiac protection to cardiac failure. *Cytokine*. 2015

123. Endo J, Sano M, Fujita J, Hayashida K, Yuasa S, Aoyama N, Takehara Y, Kato O, Makino S, Ogawa S, Fukuda K. Bone marrow derived cells are involved in the pathogenesis of cardiac hypertrophy in response to pressure overload. *Circulation*. 2007;116:1176-1184

124. Wu JM, Hsueh YC, Ch'ang HJ, Luo CY, Wu LW, Nakauchi H, Hsieh PC. Circulating cells contribute to cardiomyocyte regeneration after injury. *Circ Res*. 2015;116:633-641

125. Pajcini KV, Pomerantz JH, Alkan O, Doyonnas R, Blau HM. Myoblasts and macrophages share molecular components that contribute to cell-cell fusion. *The Journal of cell biology*. 2008;180:1005-1019

126. Hochreiter-Hufford AE, Lee CS, Kinchen JM, Sokolowski JD, Arandjelovic S, Call JA, Klibanov AL, Yan Z, Mandell JW, Ravichandran KS. Phosphatidylserine receptor bai1 and apoptotic cells as new promoters of myoblast fusion. *Nature*. 2013;497:263-267

127. Estrada JC, Torres Y, Benguria A, Dopazo A, Roche E, Carrera-Quintanar L, Perez RA, Enriquez JA, Torres R, Ramirez JC, Samper E, Bernad A. Human mesenchymal stem cell-replicative senescence and oxidative stress are closely linked to aneuploidy. *Cell death & disease*. 2013;4:e691

128. Peterson SE, Westra JW, Rehen SK, Young H, Bushman DM, Paczkowski CM, Yung YC, Lynch CL, Tran HT, Nickey KS, Wang YC, Laurent LC, Loring JF, Carpenter MK, Chun J. Normal human pluripotent stem cell lines exhibit pervasive mosaic aneuploidy. *PLoS One*. 2011;6:e23018

129. Boheler KR, Joodi RN, Qiao H, Juhasz O, Urick AL, Chuppa SL, Gundry RL, Wersto RP, Zhou R. Embryonic stem cell-derived cardiomyocyte heterogeneity and the isolation of immature and committed cells for cardiac remodeling and regeneration. *Stem cells international*. 2011;2011:214203

130. Pavlath GK, Blau HM. Expression of muscle genes in heterokaryons depends on gene dosage. *The Journal of cell biology*. 1986;102:124-130

131. Foshay KM, Looney TJ, Chari S, Mao FF, Lee JH, Zhang L, Fernandes CJ, Baker SW, Clift KL, Gaetz J, Di CG, Xiang AP, Lahn BT. Embryonic stem cells induce pluripotency in somatic cell fusion through biphasic reprogramming. *Mol Cell*. 2012;46:159-170

132. Dong F, Harvey J, Finan A, Weber K, Agarwal U, Penn MS. Myocardial cxcr4 expression is required for mesenchymal stem cell mediated repair following acute myocardial infarction. *Circulation*. 2012;126:314-324

133. Taghavi S, Sharp TE, 3rd, Duran JM, Makarewich CA, Berretta RM, Starosta T, Kubo H, Barbe M, Houser SR. Autologous c-kit+ mesenchymal stem cell injections provide superior therapeutic benefit as compared to c-kit+ cardiac-derived stem cells in a feline model of isoproterenol-induced cardiomyopathy. *Clinical and translational science*. 2015

134. Poynter JA, Herrmann JL, Manukyan MC, Wang Y, Abarbanell AM, Weil BR, Brewster BD, Meldrum DR. Intracoronary mesenchymal stem cells promote postischemic myocardial functional recovery, decrease inflammation, and reduce apoptosis via a signal transducer and activator of transcription 3 mechanism. *Journal of the American College of Surgeons*. 2011;213:253-260

135. Usunier B, Benderitter M, Tamarat R, Chapel A. Management of fibrosis: The mesenchymal stromal cells breakthrough. *Stem cells international*. 2014;2014:340257

136. Islam MQ, Islam K, Sharp CA. Epigenetic reprogramming of nonreplicating somatic cells for long-term proliferation by temporary cell-cell contact. *Stem Cells Dev*. 2007;16:253-268

137. Makkar RR, Smith RR, Cheng K, Malliaras K, Thomson LE, Berman D, Czer LS, Marban L, Mendizabal A, Johnston PV, Russell SD, Schuleri KH, Lardo AC, Gerstenblith G, Marban E. Intracoronary cardiosphere-derived cells for heart regeneration after myocardial infarction (caduceus): A prospective, randomised phase 1 trial. *Lancet*. 2012;379:895-904

138. Quijada P, Sussman MA. Making it stick: Chasing the optimal stem cells for cardiac regeneration. *Expert review of cardiovascular therapy*. 2014;12:1275-1288

139. Chong JJ, Yang X, Don CW, Minami E, Liu YW, Weyers JJ, Mahoney WM, Van Biber B, Cook SM, Palpant NJ, Gantz JA, Fugate JA, Muskheli V, Gough GM, Vogel KW, Astley CA, Hotchkiss CE, Baldessari A, Pabon L, Reinecke H, Gill EA, Nelson V, Kiem HP, Laflamme MA, Murry CE. Human embryonic-stem-cell-derived cardiomyocytes regenerate non-human primate hearts. *Nature*. 2014;510:273-277

140. Tat PA, Sumer H, Pralong D, Verma PJ. The efficiency of cell fusion-based reprogramming is affected by the somatic cell type and the in vitro age of somatic cells. *Cell Reprogram*. 2011;13:331-344

141. Sousa BR, Parreira RC, Fonseca EA, Amaya MJ, Tonelli FM, Lacerda SM, Lalwani P, Santos AK, Gomes KN, Ulrich H, Kihara AH, Resende RR. Human adult stem cells from diverse origins: An overview from multiparametric immunophenotyping to clinical applications. *Cytometry A*. 2014;85:43-77

142. Lopez-Otin C, Blasco MA, Partridge L, Serrano M, Kroemer G. The hallmarks of aging. *Cell*. 2013;153:1194-1217

143. Tumpel S, Rudolph KL. The role of telomere shortening in somatic stem cells and tissue aging: Lessons from telomerase model systems. *Ann N Y Acad Sci*. 2012;1266:28-39

144. D'Amario D, Leone AM, Iaconelli A, Luciani N, Gaudino M, Kannappan R, Manchi M, Severino A, Shin SH, Graziani F, Biasillo G, Macchione A, Smaldone C, De Maria GL, Cellini C, Siracusano A, Ottaviani L, Massetti M, Goichberg P, Leri A, Anversa P, Crea F. Growth properties of cardiac stem cells are a novel biomarker of patients' outcome after coronary bypass surgery. *Circulation*. 2014;129:157-172

145. Kajstura J, Bai Y, Cappetta D, Kim J, Arranto C, Sanada F, D'Amario D, Matsuda A, Bardelli S, Ferreira-Martins J, Hosoda T, Leri A, Rota M, Loscalzo J, Anversa P. Tracking chromatid segregation to identify human cardiac stem cells that regenerate extensively the infarcted myocardium. *Circ Res*. 2012;111:894-906

146. Sanada F, Kim J, Czarna A, Chan NY, Signore S, Ogorek B, Isobe K, Wybieralska E, Borghetti G, Pesapane A, Sorrentino A, Mangano E, Cappetta D, Mangiaracina C, Ricciardi M, Cimini M, Ifedigbo E, Perrella MA, Goichberg P, Choi AM, Kajstura J, Hosoda T, Rota M, Anversa P, Leri A. C-kit-positive cardiac stem cells nested in hypoxic niches are

activated by stem cell factor reversing the aging myopathy. *Circ Res*. 2013;114:41-55

147. D'Amario D, Cabral-Da-Silva MC, Zheng H, Fiorini C, Goichberg P, Steadman E, Ferreira-Martins J, Sanada F, Piccoli M, Cappetta D, D'Alessandro DA, Michler RE, Hosoda T, Anastasia L, Rota M, Leri A, Anversa P, Kajstura J. Insulin-like growth factor-1 receptor identifies a pool of human cardiac stem cells with superior therapeutic potential for myocardial regeneration. *Circ Res*. 2011;108:1467-1481

148. Brady JJ, Li M, Suthram S, Jiang H, Wong WH, Blau HM. Early role for il-6 signalling during generation of induced pluripotent stem cells revealed by heterokaryon rna-seq. *Nature cell biology*. 2013;15:1244-1252

149. Chong JJ, Chandrakanthan V, Xaymardan M, Asli NS, Li J, Ahmed I, Heffernan C, Menon MK, Scarlett CJ, Rashidianfar A, Biben C, Zoellner H, Colvin EK, Pimanda JE, Biankin AV, Zhou B, Pu WT, Prall OW, Harvey RP. Adult cardiac-resident msc-like stem cells with a proepicardial origin. *Cell Stem Cell*. 2011;9:527-540

150. Chong JJ, Reinecke H, Iwata M, Torok-Storb B, Stempien-Otero A, Murry CE. Progenitor cells identified by pdgfr-alpha expression in the developing and diseased human heart. *Stem Cells Dev*. 2013;22:1932-1943

151. Andreassen PR, Lohez OD, Lacroix FB, Margolis RL. Tetraploid state induces p53-dependent arrest of nontransformed mammalian cells in g1. *Molecular biology of the cell*. 2001;12:1315-1328

152. Ravid O, Shoshani O, Sela M, Weinstock A, Sadan TW, Gur E, Zipori D, Shani N. Relative genomic stability of adipose tissue derived mesenchymal stem cells: Analysis of ploidy, h19 long non-coding rna and p53 activity. *Stem cell research & therapy*. 2014;5:139

153. Peterson SE, Westra JW, Paczkowski CM, Chun J. Chromosomal mosaicism in neural stem cells. *Methods in molecular biology*. 2008;438:197-204

154. Margolis RL, Lohez OD, Andreassen PR. G1 tetraploidy checkpoint and the suppression of tumorigenesis. *Journal of cellular biochemistry*. 2003;88:673-683

155. Yamanaka S, Blau HM. Nuclear reprogramming to a pluripotent state by three approaches. *Nature*. 2010;465:704-712

156. Yanai G, Hayashi T, Zhi Q, Yang KC, Shirouzu Y, Shimabukuro T, Hiura A, Inoue K, Sumi S. Electrofusion of mesenchymal stem cells and islet cells for diabetes therapy: A rat model. *PLoS One*. 2013;8:e64499

157. Panopoulos A, Pacios-Bras C, Choi J, Yenjerla M, Sussman MA, Fotedar R, Margolis RL. Failure of cell cleavage induces senescence in tetraploid primary cells. *Molecular biology of the cell*. 2014;25:3105-3118

158. Laugesen A, Helin K. Chromatin repressive complexes in stem cells, development, and cancer. *Cell Stem Cell*. 2014;14:735-751

159. Lee HW, Blasco MA, Gottlieb GJ, Horner JW, 2nd, Greider CW, DePinho RA. Essential role of mouse telomerase in highly proliferative organs. *Nature*. 1998;392:569-574

160. Horii T, Yamamoto M, Morita S, Kimura M, Nagao Y, Hatada I. P53 suppresses tetraploid development in mice. *Scientific reports*. 2015;5:8907

161. Anderson CA, Roberts S, Zhang H, Kelly CM, Kendall A, Lee C, Gerstenberger J, Koenig AB, Kabeche R, Gladfelter AS. Ploidy variation in multinucleate cells changes under stress. *Molecular biology of the cell*. 2015;26:1129-1140

162. Beier F, Martinez P, Blasco MA. Chronic replicative stress induced by ccl4 in trf1 knockout mice recapitulates the origin of large liver cell changes. *Journal of hepatology*. 2015

163. Opiela J, Samiec M, Bochenek M, Lipinski D, Romanek J, Wilczek P. DNA aneuploidy in porcine bone marrow-derived mesenchymal stem cells undergoing osteogenic and adipogenic in vitro differentiation. *Cellular reprogramming*. 2013;15:425-434

164. Ben-David U, Arad G, Weissbein U, Mandefro B, Maimon A, Golan-Lev T, Narwani K, Clark AT, Andrews PW, Benvenisty N, Carlos Biancotti J. Aneuploidy induces profound changes in gene expression, proliferation and tumorigenicity of human pluripotent stem cells. *Nat Commun*. 2014;5:4825

165. Jopling C, Sleep E, Raya M, Marti M, Raya A, Izpisua Belmonte JC. Zebrafish heart regeneration occurs by cardiomyocyte dedifferentiation and proliferation. *Nature*. 2010;464:606-609

166. Simon HG, Odelberg S. Assessing cardiomyocyte proliferative capacity in the newt heart and primary culture. *Methods in molecular biology*. 2015;1290:227-240

167. Tian Y, Liu Y, Wang T, Zhou N, Kong J, Chen L, Snitow M, Morley M, Li D, Petrenko N, Zhou S, Lu M, Gao E, Koch WJ, Stewart KM, Morrisey EE. A microrna-hippo pathway that promotes cardiomyocyte proliferation and cardiac regeneration in mice. *Science translational medicine*. 2015;7:279ra238

168. Walsh S, Ponten A, Fleischmann BK, Jovinge S. Cardiomyocyte cell cycle control and growth estimation in vivo--an analysis based on cardiomyocyte nuclei. *Cardiovasc Res*. 2010;86:365-373

169. Aurora AB, Porrello ER, Tan W, Mahmoud AI, Hill JA, Bassel-Duby R, Sadek HA, Olson EN. Macrophages are required for neonatal heart regeneration. *The Journal of clinical investigation*. 2014;124:1382-1392

170. Puente BN, Kimura W, Muralidhar SA, Moon J, Amatruda JF, Phelps KL, Grinsfelder D, Rothermel BA, Chen R, Garcia JA, Santos CX, Thet S, Mori E, Kinter MT, Rindler PM, Zacchigna S, Mukherjee S, Chen DJ, Mahmoud AI, Giacca M, Rabinovitch PS, Aroumougame A, Shah AM, Szweda LI, Sadek HA. The oxygen-rich postnatal environment induces cardiomyocyte cell-cycle arrest through DNA damage response. *Cell*. 2014;157:565-579

171. Naqvi N, Li M, Calvert JW, Tejada T, Lambert JP, Wu J, Kesteven SH, Holman SR, Matsuda T, Lovelock JD, Howard WW, Iismaa SE, Chan AY, Crawford BH, Wagner MB, Martin DI, Lefer DJ, Graham RM, Husain A. A proliferative burst during preadolescence establishes the final cardiomyocyte number. *Cell*. 2014;157:795-807

172. Mishra S, Ling H, Grimm M, Zhang T, Bers DM, Brown JH. Cardiac hypertrophy and heart failure development through gq and cam kinase ii signaling. *J Cardiovasc Pharmacol*.56:598-603

173. Altschuler SJ, Wu LF. Cellular heterogeneity: Do differences make a difference? *Cell*. 2010;141:559-563

174. Dey D, Han L, Bauer M, Sanada F, Oikonomopoulos A, Hosoda T, Unno K, De Almeida P, Leri A, Wu JC. Dissecting the molecular relationship among various cardiogenic progenitor cells. *Circ Res*. 2013;112:1253-1262

175. Skinner AM, Grompe M, Kurre P. Intra-hematopoietic cell fusion as a source of somatic variation in the hematopoietic system. *J Cell Sci*. 2012;125:2837-2843

176. Szibor M, Poling J, Warnecke H, Kubin T, Braun T. Remodeling and dedifferentiation of adult cardiomyocytes during disease and regeneration. *Cellular and molecular life sciences : CMLS*. 2014;71:1907-1916

177. Malliaras K, Ibrahim A, Tseliou E, Liu W, Sun B, Middleton RC, Seinfeld J, Wang L, Sharifi BG, Marban E. Stimulation of endogenous cardioblasts by exogenous cell therapy after myocardial infarction. *EMBO molecular medicine*. 2014;6:760-777

178. Manning EL, Crossland J, Dewey MJ, Van Zant G. Influences of inbreeding and genetics on telomere length in mice. *Mammalian genome : official journal of the International Mammalian Genome Society*. 2002;13:234-238